SOME COMPRESSIBILITY EFFECTS IN CAVITATION BUBBLE DYNAMICS

Thesis by
Arthur John Rudolph Schneider

In Partial Fulfillment of the Requirements
For the Degree of
Doctor of Philosophy

California Institute of Technology
Pasadena, California
1949

ACKNOWLEDGMENT

The writer wishes to express his thanks to Drs. R. T. Knapp and M. S. Plesset of the Hydrodynamics Laboratory, whose pioneering research work on cavitation phenomena first initiated this study, and whose leadership, guidance, and criticism were very important in the completion of this thesis. The remarkable photographs secured by Dr. Knapp in the Water Tunnel showed unsuspected new details of the life history of an isolated cavitation bubble. The extensive theoretical studies being conducted by Dr. Plesset inspired this investigation into the effects of compressibility as an individual project which, it is hoped, will supplement the larger field of investigation.

Thanks are also due to Prof. A. Hollander, the writer's advisor, who offered continual encouragement and helpful criticism. His long time interests in hydraulic machinery greatly influenced the course of the writer's graduate studies.

Finally, the writer wishes to thank his wife, Jane, whose moral encouragement and perseverance with the chores of typing made this thesis possible.

ABSTRACT

1. Theories on the dynamics of cavitation are critically examined, and are found to need clarification.

2. The contents of a bubble formed from a submicroscopic nucleus are agreed to be almost entirely water vapor. This water vapor is shown to be unable to offer decisive resistance to inward flow during the finite portion of the collapse.

3. The effect of compressibility of the liquid is analyzed in detail. It is found to reduce velocities noticeably, but does not, in itself, eliminate the anomaly of an infinite collapse velocity as the bubble radius approaches zero. The pressures in the fluid surrounding the bubble are found to be markedly reduced by the assumption of compressibility.

4. Energy is found to be continually transported inward during the collapse period.

5. The mechanism of rebound of a compressible liquid is examined when the bubble collapse is arrested by an immovable barrier of finite radius. A shock wave is formed followed by a tension wave responsible for rupturing the liquid.

6. The shock wave is estimated to carry off 47% of available energy, and limit rebound to 81% of former size.

7. The maximum pressure in the outgoing shock wave is found to be incapable of damaging a metallic wall when the point of collapse is not on that boundary.

TABLE OF CONTENTS

PART	TITLE	PAGE
	Introduction	1
I.	The Beginning of the Problem	7
II.	Review of Previous Research Work of primarily Experimental Nature.	11
	2:1 Trend of Research after 1919.	11
	2:2 Nature of Cavitation Attack	11
	2:3 Test Apparatus	13
	2:4 Other Experimental Work	14
	2:5 Discussion of Results	24
	2:6 Recent Photographic Results	37
	2:7 Conclusions based on Experimental Data	39
III.	Previous Theoretical Studies	41
	3:1 Rayleigh-Cook Solution	41
	3:2 Ackeret	48
	3:3 Van Iterson, Bottomley, and Surface Tension	50
	3:4 Silver and Heat Conduction	51
	3:5 Herring Approximate Solution	54
	3:6 Oza Hemispherical Cavity	55
	3:7 Rightmire Bubble Mass	57
	3:8 Need for a Solution Valid at High Velocities and Pressures	59
IV.	The Interior of the Bubble	62
	4:1 Contents of the Bubble	62
	4:2 Latent Heat of Evaporation	64
	4:3 Effect of Finite Condensation Rate	68
	4:4 Shock Wave Phenomena in Vapor	70
	4:5 Conclusions	71
V.	Problems to be Investigated	73
	5:1 Collapse of the Bubble	73
	5:2 Rebound of the Bubble	75

PART		TITLE	PAGE
VI.	Compressible Flow and the Method of Calculation.		77
	6:1	Equation of State.	77
	6:2	Equations of Motion	81
	6:3	Dimensionless Variables for Calculation.	86
	6:4	Nature of the Solution	87
	6:5	Method of Calculation	89
VII.	Bubble Collapse		95
	7:1	Boundary Conditions	96
	7:2	Initial Conditions	99
	7:3	Symmetry	102
	7:4	The Solution	104
	7:5	Discussion of the Results	106
	7:6	Conclusions	115
VIII.	Impact and Radiated Shock Pressure		117
	8:1	Assumptions	119
	8:2	The Solution	122
	8:3	Conclusions	123
IX.	Fluid Motion during Rebound		125
	9:1	Boundary Conditions	127
	9:2	Initial Conditions	128
	9:3	Shock Wave Conditions	129
	9:4	The Solution	131
	9:5	Conclusions	143
X.	References		145

I INTRODUCTION

Cavitation is a phenomenon which has attracted a great deal of interest and attention during the last thirty-five years because of its important effects on hydraulic machinery, reduction of efficiency of torpedo propellers, and the increase in drag of high speed underwater missiles associated with cavitation. Its appearance reduces the efficiency of the machine and can cause severe damage.

The property of liquids responsible for these occurences is boiling, or the ability of the liquid to transform into vapor at localized regions. Thus when cavitation occurs, there are two phases of the liquid present similtaneously in a limited space. In the usual case, masses of bubbles form at one locality and collapse in another as the liquid moves through the system. This process is extremely complicated and not subject to very satisfactory analysis, though Ackeret (1)* has made a notable attempt.

The practical consequences of cavitation cannot be too strongly emphasized. The direct result of allowing severe cavitation can lead to rapid damage such as on the propellers of the French blue ribbon ship Normandie, which needed repair every fourth trip across the Atlantic.

---

* Numbers in parentheses refer to Bibliography.

A reduction in efficiency accompanies this damage although it is unusual for a machine to be operated for long periods of time in the low efficiency range for the sake of high output.

However, the price of avoiding cavitation is accepting a minimum limit to local pressure, or a maximum limit to velocity, depending upon the point of view. This means that a hydraulic machine must be larger and run at a lower speed to accomplish a given duty. Thus the price of the physical equipment plus the installation space required all increase, simply because the liquid insists on boiling if given the opportunity.

There is one well known application, however, where cavitation is encouraged for a specific purpose. Condensate pumps in steam power plants are so located that cavitation will occur at the impeller inlet whenever the water level drops to a predetermined level in the condenser. The pump thereby eliminates a difficult and expensive regulation, controls the amount of water in the condenser by cavitation, and runs at lower power consumption than if it were throttled on the high pressure outlet line. The fact that damage is quite tolerable is attributed to the low output head of such pumps.

As has been observed frequently, cavitation may occur in many forms and degrees of intensity. Thoma (2)

was aware that an index of cavitation was desirable and proposed the cavitation parameter σ. This parameter was written for use with pumps, but has the disadvantage that variations in parameter occur from pump to pump and the definitions are not standardized.

$$\sigma = \frac{P_s - P_v}{\Delta P}$$

where P_s suction pressure of pump

P_v vapor pressure of liquid corresponding to its temperature

ΔP pressure rise obtained from suction to discharge at the best efficiency point of pump

As written for the flow of liquid about a submerged body:

$$K = \frac{P_o - P_v}{\frac{1}{2} \rho V_o^2}$$

where P_v vapor pressure of the liquid at its temperature

P_o static pressure

V_o uniform flow velocity a distance from the body

ρ liquid density

Plesset (3) points out that three distinct regimes of flow are encountered which may be qualitatively correlated by the cavitation parameter K. The first regime, when K is large, is non-cavitating flow which consists of the liquid phase only. Compressibility effects are

negligible and the principles of analysis are well known. If K is made smaller a state of flow is attained in which a relatively small number of bubbles form next to the boundary of the submerged body. This is taken to be the second regime of flow, where the flow pattern established in non-cavitating flow is not appreciably disturbed by the presence of a few isolated bubbles.

As K is further reduced bubbles are formed in increasing numbers until they merge into a large bubble mass and eventually form a large single cavity. This latter state, which is regarded as Regime III, may be called Cavity Flow and involves a major change in the flow pattern from the non-cavitating regime. If K is reduced more, the cavity merely increases in size.

Most cavitation research, which has been concerned with flows which cause physical damage, has been performed in Regime II and extended into the transition to Regime III. Such descriptive terms as "incipient cavitation" and "pluming cavitation" have been applied to the observed phenomena.

The discussion to this point has been concerned mainly with steady flow of liquid relative to a single body. It is necessary, however, to point out that the word cavitation is very broad in general meaning and has been used to describe many different phenomena involving

two phase regions in liquid motion.

Some examples of various types of cavitation observed are listed below:

a. The cavity formed when a missile enters the surface of a body of water.

b. The cavities formed by the trailing vortices from propeller tips and hub.

c. The cavity formed about a high speed body in liquid when complete separation occurs.

d. The cavities formed at a vibrating boundary of a liquid mass.

e. Cavities formed at a rebound of a liquid impact against a surface.

The studies made in this paper are concerned with single isolated bubbles, and the vital role of compressibility in their life history. Hence the results can be applied only approximately to Regime II.

This work was engendered by the Hydrodynamics Laboratory at the California Institute of Technology, where the techniques of high speed photography developed and used in conjunction with the High Velocity Water Tunnel made possible the most detailed information yet available on the phenomenon of Cavitation. These data have inspired new theoretical work to extend knowledge of the life history of a bubble.

It was felt that a critical analysis of previous work on cavitation bubble dynamics would be a useful addition to cavitation literature in the English language. Nowotny (4) published a thorough but brief book in German on cavitation erosion, which has an excellent bibliography. The David Taylor Model Basin (5) gathered a thorough bibliography on the subject. However, no analytical study of previous work on bubble dynamics has been compiled. Therefore, the first portion of this thesis is devoted to a critical summary.

THE BUBBLE COLLAPSE PROBLEM

I. The Beginning of the Problem

A study initiated in England in 1915 by the Propeller Subcommittee of the Institute of Naval Architects because of the troubles encountered with warship propeller damage started research work on cavitation. The interest aroused by this phenomenon has not abated in the last few years since no details of the problem have been solved conclusively. On the contrary, several schools of thought have been formed, each presenting its individual theory.

The Propeller Subcommittee was commissioned to study the causes of severe pitting on the surface of propeller blades. The report (6) published by them stated that the cause of this pitting was the localized repeated hammering that resulted from the collapse of small cavities in water directly on the blade surfaces. This phenomenon was captioned cavitation, a name which has remained dominant in the literature.

An experiment was performed to substantiate the statements made in the report. A submerged hollow cone with its apex completely filled with water was lowered at a uniform velocity. Its downward motion was suddenly arrested by a mechanical stop, but the liquid inside was

restrained only by small pressure forces. The water therefore continued in its downward motion, separating from the inside surface of the cone at its apex, thus forming a cavity in this region. Due to the effect of the pressure gradient, the bubble grew to a maximum size and subsequently collapsed.

A metallic plate was retained over a small aperture at the cone apex where the inrushing water, closing the cavity, would strike it at a small diameter cross section. By this means, the experimenters were able to shear circular slugs out of plate. Calculations based upon the shear strength of the plate showed that pressures of the order of 300,000 psi had been exerted on the plate surface. By the fact that a finite surface had been presented to the water, they reasoned that the pressures would be much higher on an infinitesimal surface or region encountered in complete collapse. Hence pressures sufficient to damage most materials have been discovered.

An analytic solution to the problem was brought forth by S. S. Cook (6) and Lord Rayleigh (7) independently, proposing the following idealized problem. Suppose a spherical region of a liquid were suddenly annihilated. If the pressure at a large distance from the cavity were constant and greater than the pressure inside, then the cavity would close under the influence

of the pressure gradient. The solution which results when the fluid density is constant and when the pressure inside the bubble is constant has a singularity at the origin, $r = o$ and the velocity tends to infinity as the radius of the bubble wall becomes smaller.* It was noted that the velocity was independent of absolute bubble size before collapse.

Cook then proposed that an incompressible ball be inserted into the cavity and the instantaneous elastic pressure of contact be calculated, assuming the liquid to be compressible the moment contact commences. The pressures calculated approached infinity as the ball radius approached zero, since it was calculated on the basis of the foremention ed analysis.

Though this calculation was based upon a purely artificial hypothesis, the results were satisfying insofar as they showed that very high localized pressures are feasible in a liquid as a cavity collapses.

Infinite pressures were disturbing, however, because any physical phenomenon has a finite limit if only enough pertinent data can be included in the analysis. The pressure distribution equations as written by Rayleigh for the case of an incompressible fluid are not

*See Section 3:1 for discussion of this solution.

intuitively acceptable because the high spherical convergence near the origin causes high pressures which are felt instantaneously at infinity. This produces inordinately high pressures at large distances from the origin, while nevertheless properly satisfying the condition of constant pressure at $r = \infty$.

Furthermore, the pressures produced in the neighborhood of the bubble wall as it collapses led Rayleigh to state that his original assumption of incompressibility was violated when the bubble became fairly small. A calculation considering compressibility is to be desired, because the compression of the liquid requires energy, which is then subtracted from the total supply available, leaving less to form velocity.

II. Review of Previous Research Work of Primarily Experimental Nature

2:1. Trend of Research after 1919

The work of Parsons (6), Cook (6), and Lord Rayleigh (7) demonstrated quite forcibly, despite some drawbacks, that mechanical action due to closure of cavities in the liquid was responsible for severe damage to materials used in hydraulic equipment. Whereas many theoretical questions were still unanswered, the immediate practical problem in the years following was to find materials most suitable for use where cavitation was expected.

2:2. Nature of Cavitation Attack

Damage to materials was immediately divided into two categories: (1) Erosion due to mechanical action only. (2) Erosion due to a combination of chemical action plus mechanical removal of material.

It is clear that ordinary corrosion will proceed at an accelerated rate if some mechanical action is available to remove the products of chemical attack as soon as they are formed, and thus prevent attainment of a chemical equilibrium. This process is the exact opposite of corrosion of Aluminum in air, whose oxide forms a tightly adhering layer which excludes air from

further contact with the pure metal. Thus materials susceptible to corrosion are naturally excluded from application, since cavitation will surely accelerate the rate of damage. Recently Petracchi (8) has shown that reduction in attack can be obtained by use of cathodic protection methods.

To show that mechanical action alone is sufficient to cause severe damage, a large number and variety of tests have been performed where corrosion is infinitesimal and thus mechanical action must account for the damage. This type of evidence is found in almost every report, from the earliest investigations by Fottinger (9) on glass, down to the present day. In fact, some of the more modern tests of cavitation resistance are conducted with intense action in such a short time that corrosion does not find time to act.

In addition to these direct tests, microscopic examination of the structure of a specimen exposed to cavitation reveal the effects of mechanical action. Boetcher (10) reports a work hardening of the surface layer with the appearance of surface cracks typical of high pressure blows. Further, he remarks that the rough and pitted surface suggests the hammering or removal of tiny pieces of metal. Most investigators of metallic damage reach the same conclusions, according to Vater

(11). Mousson (12) bases many of his conclusions upon the mechanical impact of the liquid, and recognizes the strain hardenability of a material as an important factor.

2:3. Test Apparatus

The apparatus used for testing can be separated into two general classes: (1) Those seeking to reproduce cavitation in a form similar to its occurrence in a hydraulic machine; (2) Those seeking to produce an impact of liquid against a test specimen in order to study the effects on the specimen and modes of damage. The devices grouped under (2) were first evolved to allow a more rapid means of evaluating the erosion resistance of various materials.

a. Venturi and Water Tunnel Apparatus

The most natural step in studying cavitation is to reproduce it in the laboratory under conditions so controlled that actual effects can be simulated. The Venturi and/or Water Tunnel fulfill these requirements quite satisfactorily, the principal distinction between the two normally being whether cavitation is produced on the wall or whether it is produced on a body inserted at the test section.

The Venturi with glass walls was the first device to demonstrate forcibly that mechanical hammering was the primary cause of cavitation damage. These glass walls were found by Foettinger (9) to be etched in the region where the bubbles disappeared or collapsed. Since corrosion could certainly not account for the damage, blows of high intensity must have attacked the glass.

The Propeller Subcommittee of 1915 under Parsons and Cook (6) employed a Venturi Water Tunnel with glass walls to study cavitation. The specimen was in the form of a rod mounted in the center in such a way that the upstream end was located in the Venturi throat.

Foettinger (9), Schroeter (13), (14), (15), Ackeret (1), de Haller (16), Hunsaker (17), (18), and many others have also used this type of equipment in many varied forms.*

The principal disadvantage of a Water Tunnel or Venturi became apparent from the first. Parsons and Cook (6) report that the rate of damage is comparatively slow, even when the throat is cavitating quite heavily. This experience is borne out by subsequent investigators and was a great handicap in the work of rating materials

*A tabulation of investigators and a few notes on their equipment is included in Table I.

on their ability to resist damage. Studies were made by Hunsaker (17) (18) to determine the nozzle proportions producing the greatest damage while Schroeter (13) developed a nozzle-impingement combination which he claimed increased the rate of damage ten-fold. Nevertheless more rapid methods were sought.

Another disadvantage was that an individual bubble or bubble mass formed and collapsed so quickly in a water stream of high velocity that detailed studies of the mechanism were extremely difficult. This inhibited fundamental studies in favor of more direct practical results. However, a recent report by Knapp and Hollander (19) indicates that new resolution is available by means of photographic techniques offering frame speeds up to 30,000 per second.

b. Impact Wheel or Wasserschlag Tester

The Wasserschlag testing machine first used by Honegger (29), accelerated the resistance rating of various materials against erosion. The mechanical features are illustrated in Figure I. A wheel with arms is so located that, as the wheel rotates, these arms must pass through a small stream emitted from an adjacent orifice. Thus each time a rapidly moving arm strikes the pencil of water, a broadside impact against the side

of the stream is produced. Each arm mounts a small test specimen at the proper point to contact the water stream and be eroded by these impacts.

This type of tester was subsequently applied by a number of investigators, the most notable of whom were Ackeret and de Haller (21), Schwarz and Mantel (22) and Soderberg (23).*

In these machines the mechanism causing erosion is vastly different from that in the Venturi tube. Here a ready made, controllable impact is substituted for the dynamic impact arising from the closure of cavities produced somewhat upstream. The rate of erosion can be readily adjusted and reproducible test results are secured at a rate superior to that of the Venturi.

c. Vibrating Specimen Tester

In his 1935 Progress Report Hunsaker (18) includes some remarks about a new vibratory method of testing cavitation damage developed at M.I.T. In a subsequent paper Schumb, Peters, and Milligan (24) describe this equipment (Figure 2), the operation of which is based upon the magnetostriction property of nickel as applied by Gaines (25) to obtain a powerful source of

*A tabulation of investigators and a few notes on their equipment is included in Table II.

sound.*

The heart of the apparatus is a nickel tube, supported in the middle only, cut to such a length that its fundamental frequency of longtitudinal vibration is in the range desired. 6,000 to 8,500 cycles per second appear to be satisfactory to produce intense mechanical damage. The center portion of the nickel tube is surrounded by coils connected to an electrical oscillator capable of producing an alternating magnetic field of great intensity and of the required frequency. When the oscillator is tuned to the natural frequency of physical vibration of the nickel tube, the amplitude of motion at the free ends of the tube becomes remarkably extreme. Since this occurs in the condition of resonance, the power required to maintain this state is small.

One end of the nickel tube is then equipped with a device to mount various specimens to be tested, and this end is subsequently immersed in the test liquid.

In its simplest terms, this type of tester produces cavitation bubbles because the pressure gradients available in the liquid are not great enough to permit it to follow the specimen as it accelerates away from the mass of liquid. As in all sinusoidal motion, the specimen

*A tabulation of investigators is also shown on Table III.

is shortly decelerated and its direction reversed for the inward stroke. The liquid boundary, which has been accumulating velocity in an attempt to follow the specimen, now rapidly overtakes the piston and an abrupt collapse occurs directly on the surface. When the acceleration is inward, the liquid is pressed firmly against the specimen suppressing any tendency for the bubbles to reopen.

Rightmire (26) constructed a magnetostriction tester which placed the specimen at the bottom of a closed vessel containing the liquid, thereby obtaining a greater hydrostatic pressure over the specimen. The Edgerton photographic technique was applied, and fairly clear photographs were obtained of the repeating bubble pattern at different times in the cycle of specimen motion. The bubbles were reported to form once during a limited portion of the cycle, and remain closed the rest of the time. A theoretical derivation of collapse pressures based upon acoustic theory and an observed number of bubble sizes and locations was made.*

The magnetostriction vibrator was a great boon to the study of material damage and modes of damage. The equipment required is small and relatively inexpensive. Great intensities of collapse can be generated, and thus erosion proceeds at a rapid rate, facilitating wider

*See Section III for further discussion.

studies.

It is to be noted, however, that there are some striking differences between cavitation produced by a vibrator and that caused by localized low pressures in flow processes. Since no transverse flow is involved, the bubbles collapse on the spot where they were formed, furthermore, the bubble pattern is normally stationary; that is, a bubble will form and re-form at the same spot relative to the specimen, subjecting the same spot to repeated blows. In the Water Tunnel, individual bubble collapses are distributed at random over the collapse region.

There is some question regarding the effect of energy input from the oscillator to the mass of liquid surrounding the area where cavitation occurs. Rightmire (26) discusses this matter, as do Kornfeld and Suvarov (27) who observe a peculiar phenomenon called "dancing bubbles," which detach from the surface of the vibrating specimen and move erratically through the liquid. This apparently indicates a forced vibration of the body of the liquid, but its effect has not been explained satisfactorily.

2:4. Other Experimental Work

Some work has been done which does not fit in

the usual categories but which raises some interesting questions.

a. Surface Tension and Adhesion

In the process of examining the effects of surface tension and also the effect of oil in the water, Van Iterson (28) found that a bubble forms an angle of contact with an oily boundary surface distinctly different from the angle of contact with a clean surface. On a clean steel surface, the angle was measured to be $22\frac{1}{2}^{o}$, but when the surface was heavily greased with vaseline, the angle increased to 90^{o}, indicating much greater tenacity for the wall.

Van Iterson utilizes this fact to explain serious cavitation damage which was experienced by a pump which operated in oily water after testing satisfactorily in clean laboratory water. He suggests that a bubble which has a small angle of contact may be washed into the main current of flow and away from the boundary, whereas a bubble with a high angle of contact caused by greasy surfaces will continue to adhere tightly until it collapses directly on the wall. The second bubble is accused of perpetrating erosion damage, and it is to be noted that Stepanoff (29) agrees with this contention.

It seems possible that two lines of study could

lead to favorable results. (1) Coatings should be found which hold the least attraction for bubbles. (2) Methods of displacing the bubbles away from a boundary should be studied. Perhaps devices analogous to slots used in aircraft wings would be effective.

b. Precompression and Penetration of Materials

Poulter (30) performed some interesting experiments on the penetration of liquids into solids under unusually high pressures. If the molecules of the liquid were not too large, an actual infiltration apparently took place when pressures of 50,000 Atm. were applied for five minutes or longer.

When he allowed five minutes for the liquid to enter the solid (e.g. glass), and then suddenly released the pressure, the material was broken in pieces. If the time were extended to twenty minutes, sudden release caused instant shattering. On the other hand, if he reduced the pressure gradually, no effect was observed, the liquid apparently having time to diffuse out of the material. It was not clear whether he suggested that the high impact pressures in cavitation caused damage by a similar process, but these means appear unlikely in view of the short time intervals available during the collapse period.

The most interesting item he mentions, from the

point of view of immediate application, is a protective treatment which reduced erosion damage. He applied high pressure for some time to a specimen immersed in paraffin oil and submitted it to a vibratory erosion test. This successfully reduced erosion, but he mentions that the use of a "special material" producing a layer of adsorbed molecules on the surface was more effective. No further details are given, but an avenue of investigation is opened which should not be ignored.

c. Osborne (31) conducted tests in which he studied the pressure pulse emitted from single collapsing bubbles. He constructed a closed vessel with sylphon bellows attached which would increase the volume in the vessel when stretched by an external force. The stretched bellows exerted a pressure on the liquid when they were no longer restrained. Osborne allowed a small air bubble to form at the top of the vessel, which was filled with de-aerated water, and then expanded the bellows, which enlarged the pocket and evaporated water into it. At a given instant, he released the bellows, and recorded the pressure pulses striking a pick up in the liquid as the cavity collapsed.

Osborne noted a strong correlation between the peak pressure recorded and the ratio of initial volume of the bubble to the original air bubble. There is also an

audible method of distinguishing large ratios from small. Above a certain ratio, the air has a strong cushioning action, and the collapse is characterized by a "thud"; below, it has a distinct "clink". It is interesting to note that when experimenting at small air bubble sizes, several of Osborne's pyrex cover plates were broken, and he had to change to brass.

In addition he notes a periodicity, which he likens to the periodicity found in underwater explosions.

d. Shock Wave Cone

The cone type shock wave tester used by de Haller and Ackeret (21) consists of a chamber which is completely filled with liquid. The major portion is cylindrical to accomodate a piston; the other end tapers conically to a half that diameter. The piston is struck regular blows at the rate of 16 per second by an air hammer, and thereby produces a shock wave which travels to the other end, is intensified by the conical section and finally strikes a test specimen held tightly in place.

The authors calculate the intensity of this wave and then proceed to measure it by means of the crystal pick-up described briefly in Section II, 5, d. Values of about 6,000 psi are obtained under the same con-

ditions that damage the specimens severely. Criticism of these values has been made on the basis that cavitation occurred after the reflection of each shock wave from the specimen surface.*

2:5. Discussion of Results

a. Resistance of Metals to Damage

The most tangible direct results which have been obtained from the equipment previously described are the relative rating of materials according to their erosion resistance. Data are quite plentiful today on this subject, since many of the investigators quoted in the bibliography devoted considerable time to this study.

It is quite remarkable that the ratings conferred by the various tests agree as well as they do, but of course the validity of the Impact Wheel and Vibrating Specimen tests depend upon that experimental agreement. Those discrepancies which do exist are minor in nature, and are sometimes attributable to differences in the effect of corrosion or metallic crystal structure. Their primary purpose, excepting the steam turbine blade investigations of Soderberg (23), has been the acceleration of damage in order to produce comparative results

*See Poulter's (39) remarks in Section II, 5, d.

in the most efficient way.

There have been no precise correlations between erosion resistance and the physical properties of materials, but some definite trends have been observed. Resistance increases as the strength of the material increases, a trend to be expected. Schroeter (13) makes this observation as does Mousson (12) in stating that the primary variables are Tensile Strength, Yield Strength, and Fatigue Strength. Exceptions are due to the fact that other properties such as corrosion resistance, grain size, and strain hardenability are also quite important.

Boetcher (10) thinks that surface hardness is very important, and that a thin layer of very great hardness is preferable, and Mousson agrees. Soderberg (23) shows high resistance to pitting with very hard materials and indicates particularly good success with stellite coating, which is extremely hard. Of course general uniformity, and lack of cracks and soft constituents which can be readily removed are necessary to good erosion resistance. Ackeret and de Haller (21) observe the preliminary removal of graphite from gray cast iron before general attack begins.

Most investigations have been made with metallic materials, whose modulus of elasticity is very high compared to a substance like rubber. With the thought in

mind that the greater deformability of rubber would greatly reduce the stress induced by cavitation blows, such coatings have been proposed by Mousson.* They have performed satisfactorily for a short period of time, and then suddenly peeled and disintegrated. Postmortems revealed that the apparent cause of failure was the excessive heat generated in the layer. Thin layers, whose heat could be conducted away rapidly, were much longer lived than thick layers, so one would believe that the new rubbers with high thermal conductivity would be even better. A line of investigation likely to net some direct results appears possible here, together with Poulter's (30) suggestions on penetrating liquids which seal up "pores".

b. Intensity of Attack

In the usual case, erosion is mild as cavitation commences, and increases as the number and size of the bubbles increase. The rate of damage reaches a maximum, however, and further increase in bubble volume decreases the intensity of attack. When Regime III, Cavity Flow, is reached, damage is generally small.

It is a recognized fact that the addition of air

*See discussion on Poulter's paper (30).

will attenuate erosion damage provided some means are available to allow the air to form tiny but not submicroscopic bubbles. However, completely dissolved air does not reduce damage. Hunsaker (17) reported that, when he used a Venturi with a long throat to prolong the bubble incubation period, the consequent damage was less severe than with shorter throats. The apparent cause of this effect is the greater time available for diffusion of air to the interior of the bubble, which finally results in a greater cushioning on collapse.

Kerr (32), who used the vibratory method of testing, indicates a variation in damage caused in water depending upon the temperature, reaching a maximum at moderate temperatures of 30°C for Brass and 50°C for Steel. Mousson (12) found a general increase in rate up to 30°C. Kerr theorizes that at low temperatures the comparatively large air content of water softens the blows, while at higher temperatures the relatively high vapor pressure allows more vapor to form and cushion the blows.

Notably, there seems to be much less work on the damage associated with liquids other than fresh and salt water. Of interest is Poulter's experiment with absolute alcohol, which preserved the iron chips removed from the test specimen free of corrosion. Briggs, Johnson, and

Mason (33) study other liquids but are primarily interested in minimum allowable pressures before cavitation commences.

c. Pressure at which Cavitation Bubbles Form

There is widespread agreement that, in ordinary clean water, the development of cavitation bubbles to visible size occurs very close to the vapor pressure at the existing temperature. Ackeret (1) obtained especially nice pressure distributions in the Venturi section used and checked vapor pressure quite closely. Knapp and Hollander (19) check these pressures by extensive measurements on a model in the Water Tunnel, as does Rouse (34).

The new Venturi meters used at the Hydrodynamics Laboratory have an entrance contour which is very carefully designed according to the work of Tsien (35) to minimize the growth of the boundary layer and inhibit separation. The point at which cavitation occurs is very close to the liquid vapor pressure, and is remarkably reproducible.

In contrast to the care taken in more recent times, some Venturi test sections used in the past have rather drastic entrance profiles. In addition, some investigators such as Van Iterson (28) and Bottomley (36) apparently did not consider the nonuniformity of pressure from the boundary of the nozzle to the center line due

to curvature of the flow. Rouse (37) presents the equations nicely and shows, for steady flow, that the pressure gradient normal to the streamline is represented by the following equation:

$$\frac{\partial p}{\partial n} = -\rho \frac{v^2}{r}$$

where n - coordinate normal to the streamline positive toward center of curvature

v - fluid velocity at a point

r - radius of curvature of streamline

p - pressure at a point

If the liquid approaching the contraction has approximately constant energy across the pipe, then consideration of Bernoulli's equation for steady flow shows there will be a considerable pressure deficiency at a nozzle wall which is curved sharply inward, as compared to the pressure at the center of the nozzle. This conclusion is verified by a general theorem of perfect fluid flow, which states that extremes of velocity and pressure must always occur at the fluid boundary.

Van Iterson (28) and Bottomley (36) state that bubbles form at pressures of one-half an atmosphere and more, and therefore contain air. These conclusions are based on calculated values of the pressure at the throat. Unfortunately they do not show these calculations, but

from the magnitude of these values and the appearance of their nozzles, one may infer that the effect of flow curvature was neglected. Bottomley even ignores, without further explanation, pressures of the order of vapor pressures he measured near the wall where bubbles form. These anomalies reduce the value of their further conclusions discussed under Collapse Theories and the Interior of the Bubble.*

The conclusion that bubbles form at the liquid vapor pressure is based upon "normal" conditions of clean water saturated with air at atmospheric pressure. An important factor is the time that the liquid spends in the region of reduced pressure. Briggs, Johnson and Mason (33) find that when liquids are degassed, their natural cohesive pressure becomes effective, and they will stand the considerable negative acoustic pressure of several atmospheres. This is notably a short time process, and they show that greater tension can be obtained when the tension pulse time is less than twenty milliseconds.

On the other hand Hunsaker (17) tested bubble formation over an extended incubation period in a long throated Venturi, and found the pressure for incipient

*See Section 3:3

cavitation was somewhat increased for water saturated with air, due to air release. Thus tiny air bubbles acted as nuclei for the formation of a vapor bubble at pressures about twice vapor pressure.

Plesset (3) discusses the initial formation of the bubble, and points out that the present view is that it is born from a nucleus in the liquid consisting of air, vapor, or even solid matter. These nuclei are frequently submicroscopic in size, but the absence of such nuclei means that very large forces of surface tension amounting to about 10,000 Atm. must be overcome to start cavitation or boiling. Recently Harvey (38) as well as Pease and Blinks (39) have shown experimentally that water saturated with air also has high tensile strength, provided it is denucleated. However, according to Plesset and Pease, ordinary water presumably contains gas nuclei which are stabilized on tiny particles of solid matter. The low energy associated with the surfaces of the solid-gas-liquid system accounts for the ready cavitation of ordinary water at liquid vapor pressure.

Harvey and Pease both note that solids may be classed as either hydrophilic or hydrophobic. The latter have a low affinity for water, and will always serve as starting point for cavitation in the absence of gas nuclei. Greasy surfaces are notably hydrophobic.

d. Pressures Encountered at Collapse and the Mechanism of Damage

The greatest controversies in the investigation of cavitation center about this subject. The entire process of attack takes place in such short individual time intervals that only recently has there been an approach to observations which hold promise of showing many details of the mechanism. For this reason, many hypotheses used in analysis have not been subject to challenge, and hence a reconciliation of theories has not been possible.

At the inception of serious study of the subject, Cook (6) and Rayleigh (7) demonstrated by analytical methods that, within their assumptions, extremely high localized pressures were certain to occur in the liquid. Later theorists often disagreed with the validity of the assumptions, and each followed his individual hypothesis to a unique conclusion, some of which indicated moderate impact pressures of less than 30,000 psi. The conglomeration of collapse theories will be discussed in Section III.

Those investigators who used the Venturi testing apparatus have generally been satisfied with the inductive reasoning process which concludes that high localized pressures must exist because even the strongest,

hardest materials can be severely damaged. The physical destruction and its pitted appearance, plus the convincing arguments of Cook (6) and Rayleigh (7) have attracted a large number of adherents to this theory.

The results of the microscopic examinations made by Boetcher (10) and Mousson (12) suggest high pressures because of the metallurgical effects observed. Work hardening implies that considerable plastic strain has taken place requiring pressures appreciably greater than the elastic limit, of the order of 200,000 psi for hardened steel. Pictures of chips partially removed, showing extreme localized strains, are convincing, as is Cook's (6) cone test.

General agreement on the mechanism of attack was secured until de Haller (16) and later Ackeret and de Haller (21) calculated impact pressures on the Impact Wheel tester according to the well known acoustic one-dimensional equations. Their values varied according to the specimen's linear velocity, but calculated pressures of 14,000 psi to 18,000 psi produced considerable damage in the tests previously conducted by Schwartz and Mantel (20). Further investigations by Ackeret and de Haller showed that the threshold of appreciable damage occurred at 6,000 psi calculated value.

A piezo-electric pressure pick-up utilizing

pistons 0.8 - 2 mm in diameter to transmit force acting through a 1.5 mm hole to the crystal was applied by de Haller (16) to three different test devices: a Venturi, an Impact Wheel, and a special conical tester which was designed to evaluate the damaging effect of shock waves. The measured values for the threshold of damage showed pressures of comparatively low order, namely 4,000 to 10,000 psi.

These published results immediately raised a host of questions, because they were far below the endurance limits of the materials which had suffered attack. The conclusions drawn from the experiments by the authors presented three possible causes for the erosion:

1. A new mode of metallic attack causes damage.
2. The endurance limit to surface stresses is much lower in water.
3. Submicroscopic fissures and cracks allowed severe local pressure rises due to converging effect on the liquid while at the same time presenting stress concentrations in the metal near the surface.

This opinion on the magnitude of the pressure impact is also widely held among those investigators who have used the vibratory tester extensively. Rightmire (26) calculates pressures of approximately 5,000 psi when a

bubble group collapses against the moving specimen. Hunsaker (17), in a discussion of a paper by Poulter (30), contends that the maximum pressures of impact are of the same order. However, it is not clear what mechanism of erosion can cause the drastic pitting frequently observed, except the unmeasurable effect of tiny fissures, as contended by Gardner (40) in the case of erosion of turbine wheels by droplets of condensed steam.

Other investigators remain dubious as to the validity of these low pressure measurements and the assumptions on which the calculations were based. They point out that, even if the frequency response of the crystal pressure pick-up used by de Haller (16) is quite high, it can measure only the area average of forces exerted on the 1.5 mm piston. Since the area affected by an individual bubble collapse is necessarily infinitesimal, no indication of the local peak pressures is obtained. A correlation between the measured values and the microscopic pressures predicted by the one dimensional impact theory is not surprising, particularly in the cases of the Impact Wheel and the conical shock wave tester.

The proponents of the high pressure school of thought such as Cook (41), Beeching (42), and Poulter (30) contend that the larger effects mask a cavitation which occurs during the impact process, but which is very

difficult to observe. Poulter, in the author's closure to discussion on his paper (30), cites a striking experiment which sheds a new light on the cone shock wave test made by de Haller. The shock waves were produced by hammer blows in the fashion of the original experiment, and the erosion was reproduced. He then applied a static pressure of about 6,000 psi to the water in the device, which is equal to the calculated value of the shock wave pressure, and repeated the test. This time no erosion was discovered, even though the peak pressure should have risen to 12,000 psi. The explanation offered is that the superimposed pressure supressed cavitation occurring at the shock wave reflection. Cavity collapse was causing the damage, as Nowotny (4) also indicates may be the case.

Thus although the low pressure school has injected doubt about whether high pressures are necessary to cause damage, the burden of proof still lies with them, since only the fissure pressure intensification and stress concentration theory fits previous metallurgical data. It seems likely that high pressures which are ample to pit any material are created by the collapse of bubbles, although the impact of droplets with a metallic surface may cause damage through fissure concentration.

2:6. Recent Photographic Results

Knapp and Hollander (19) reported the preliminary results of photographic observation in the Water Tunnel at Caltech. By extending and improving the flashing lamp technique of Edgerton, who took some nice pictures of cavitation for Hunsaker (17) at 3,000 frames per second in 1935, clear pictures were obtained at frame speeds up to 30,000 per second.

The most interesting pictures were taken of cavitation in Regime II on a model with a 1.5 caliber ogive nose and a long cylindrical body. The bubbles formed were fairly good sized (about .28 in.max. diameter) and not crowded. They formed near the base of the nose, and then moved into a higher pressure field which was practically constant.

This pressure provided the driving force for collapse, which was recorded in numerous frames until the bubble disappeared. These data have been compared with the calculations of Cook (6) and Rayleigh (7) and show remarkable agreement. Plesset (3) calculated the growth and collapse curves numerically, taking into account the variations of pressure due to translation along the model and also surface tension, and obtained excellent agreement during most of the life history of a bubble.

Then there appeared a phase in the life of a bubble which was never before suspected. The collapsed bubble reappeared and grew to a diameter somewhat smaller than the original size. This action has been termed the rebound, and clearly demonstrates that the liquid must have an appreciable compressibility at the pressures experienced during collapse, or sufficient energy could not be stored to cause a rebound to go as high as 86% of the previous size.

This fact, together with the velocities measured from the slope of the radius-time curve shows that extremely high local pressures must exist. Even 30,000 pictures per second leaves an increase in the number of observed points to be desired during the very last stages of bubble collapse, when the slope of the radius-time curve approaches the vertical. However, the values measured are as high as 100 feet per second, and there is reason to believe that this velocity continues to increase as the radius contracts closer to zero. If the sudden impact is calculated by the simple water hammer equation, the pressure corresponding to 100 feet per second is approximately 6,500 psi, which is below the normal endurance limit of most materials.

These results are the beginning of study by a new powerful tool which offers a wonderful opportunity

for detailed observation of the life histories of bubbles under cavitating conditions.

2:7. Conclusions Based on Experimental Data

a. Damage of primarily mechanical nature is caused by cavitation, and therefore a material of high corrosion resistance may be severely attacked.

b. Damage occurs in areas where the cavities collapse, exerting a hammering effect on the walls. Probably bubbles which collapse a few diameters away from the wall do no damage.

c. Rate of attack is low for incipient cavitation, increases with the number of bubbles formed, and decreases as Regime III, Cavity Flow, is approached. However, by the time the latter regime is reached, the efficiency of a hydraulic machine is greatly reduced, or the drag of an immersed body is greatly increased.

d. Collapse of a vapor filled cavity can create a high localized pressure at the point of collapse which is sufficient to damage the strongest metallic materials.

e. Rate of damage can be reduced by injecting air bubbles into the liquid to act as large nuclei for vapor formation. A cushioning action at collapse is thought to explain this result as well as the reduction in noise produced.

f. In ordinary clean water, either air saturated at one atmosphere or air free, bubble formation commences very close to the vapor pressure of the liquid at the existing temperature. If small air bubbles already exist in the liquid or are given time enough to form by diffusion of dissolved air, the pressure corresponding to bubble growth is increased.

III. Previous Theoretical Studies

3:1. Rayleigh-Cook Solution

The classic work on bubble collapse was done by Cook (6), who presented a solution in 1917 for the velocity of the bubble wall, and by Lord Rayleigh (7), who solved the same problem more completely and elegantly. Considering a spherical bubble in a perfect, incompressible liquid of infinite extent, they chose the origin of a co-ordinate system at its center, and supposed the pressure at infinity to be constant. If, then, the pressure in the center of the bubble is zero, or at any rate constant, the velocity of the bubble wall is:

$$\dot{R}^2 = \frac{2(P_\infty - P_i)}{3\rho}\left(\frac{R_o^3}{R^3} - 1\right) \qquad (1)$$

where P_∞ pressure at $r = \infty$

P_i pressure inside the bubble

R Radius of the bubble wall

R_o Original radius of the Bubble

ρ Density of the liquid

The time integral of this equation may be found analytically only for the point of complete collapse, and is written, from the Gamma Function solution:

$$\tau = R_o\sqrt{\frac{\rho}{6(P_\infty - P_i)}}\;\frac{\Gamma(\frac{5}{6})\Gamma(\frac{1}{2})}{\Gamma(\frac{3}{4})} = 0.9147 R_o\sqrt{\frac{\rho}{P_\infty - P_i}} \qquad (2)$$

where τ period of collapse

The relationship for other times may be written in the form:

$$t = f\left(\frac{R}{R_o}\right) R_o \sqrt{\frac{3\rho}{2(P_\infty - P_i)}} \qquad (3)$$

Knapp and Hollander (19) present a table of the function $f\left(\frac{R}{R_o}\right)$, which is also included in Table IV.

Lord Rayleigh (17) calculated the pressure field surrounding the collapsing cavity by integrating Euler's equation for motion of a perfect fluid. When written for a constant pressure inside the cavity, the equation is:

$$\frac{P - P_\infty}{P_\infty - P_i} = \frac{1}{3}\frac{R}{r}\left[\frac{R_o^3}{R^3} - 4\right] - \frac{1}{3}\frac{R^4}{r^4}\left[\frac{R_o^3}{R^3} - 1\right] \qquad (4)$$

where r radius to a point

P pressure at radius r

The radius at which the maximum pressure occurs is r = 1.587 R and thus is seen to be in the neighborhood of the bubble wall.

It is to be noted that the velocity of the bubble wall described by Equation (1) approaches infinity as the radius ratio $\frac{R}{R_o}$ becomes small. This, of course, is physically impossible, and it has been suggested that several different phenomena might account for a finite

collapse speed. Compressibility of the liquid, finite rate of vapor condensation, and finite rate of heat conduction could be significant.*

Cook was interested in evaluating the pressure created by elastic impact when the bubble closed. Since this pressure is approximately proportional to the liquid velocity at the instant of impact, an infinite velocity means an infinite pressure.

When a cavity closes to zero radius one can visualize opposite sides of the bubble meeting "head on" and suffering what is analogous to striking an immovable wall because of the conditions of spherical symmetry. To avoid the essential singularity at the origin, Cook placed his immovable wall at a small finite radius and called it an incompressible ball. It is possible to imagine a complete collapse as the limiting case of collapse on an incompressible ball, as the radius of that ball approaches zero.

The pressures exerted on the ball by cavity collapse were enormous when the ratio to the original cavity size was 0.10 or less. This led many investigators to believe that pressures capable of severe damage to any material were possible even if the process were

*See Section IV for discussion.

limited by factors not considered in the analysis.

The pressures in the liquid field surrounding the cavity, which may be found by means of Equation (4), have many interesting features. The factor which is responsible for infinite velocities is also found here, and indicates that the pressure at r = 1.587 R and throughout a great part of the field become very large simultaneously.

Let us suppose that $\frac{R}{R_0} << 1$. Then we may write:

$$\frac{P - P_\infty}{P_\infty - P_i} \doteq \frac{1}{3}\left[\frac{R}{r} - \frac{R^4}{r^4}\right]\frac{R_0^3}{R^3}$$

If we further suppose we are interested in the pressure at a point where $r = n R_0$

$$\frac{P - P_\infty}{P_\infty - P_i} \doteq \frac{1}{3}\left[\frac{1}{n}\frac{R}{R_0}\right]\frac{R_0^3}{R^3} = \frac{1}{3}\frac{1}{n}\frac{R_0^2}{R^2}$$

Thus it is clear that no matter how large n be chosen, an infinite pressure will be felt the instant the bubble collapses. Such effects violate the finite speed of sound and indicate that compressibility must be considered. Rayleigh stated in his paper that the extremely high pressures existing in the liquid before collapse made the assumption of incompressibility untenable, and that a solution considering compressible of liquids qualities was needed.

Hollander has presented the results of Rayleigh's solution in a very complete form on log paper. These curves are presented in Figure 3.

For comparisons sake, Lord Rayleigh calculated the minimum diameter which a collapsing bubble filled with an insoluble permanent gas would reach, if isothermal compression were realized. It is clear that this size may be found by equating the external work done by the pressure at infinity, to the energy stored in compression of the gas. This bubble may be visualized as oscillating between a maximum and a minimum size given by the following relation:

$$\frac{P_\infty}{P_{i_{max}}} = 3 \ln\left(\frac{R_o}{R}\right)\left[\frac{R_o^3/R^3}{R_o^3/R^3 - 1}\right]$$

where R_o initial or maximum bubble radius

R smallest bubble radius

$P_{i_{max}}$ final pressure of gas

P_∞ pressure at r = OO

Pressures calculated by this equation are not nearly as large as pressures found by Cook. This type of analysis can be extended somewhat by considering the interior of the cavity to be filled with two components - water vapor and permanent gas. The pressures exerted by them may be assumed to be independent, but the temperature of each remains constant for isorthermal com-

pression.

Thus we may write:

$$P_i = P_v + P_g$$

where P_v vapor pressure of liquid

P_g gas pressure

We assume that when $R = R_o$

$$P_{i_o} = P_v + m P_v$$

where m gas proportion index

By varying m we may consider a whole family of cases between a bubble filled with pure vapor of infinite condensability and a bubble filled with a permanent gas.

Neglecting surface tension and equating energy of gas compression to work done by the pressure difference, one can neglect some secondary terms and obtain:

$$\ln \frac{R_o}{R} \doteq \frac{P_\infty - P_v}{3m P_v}\left[1 - \frac{R^3}{R_o^3}\right]$$

The maximum pressure is, of course,:

$$P_{i_{max}} = P_v\left(1 + m\frac{R_o^3}{R^3}\right) \doteq m P_v \left(\frac{R_o}{R}\right)^3$$

A plot of these results for particular values of m is shown in Figure 4, and it is to be noted that the index m is an extremely critical quantity. As it becomes

less than 0.50, final pressures rapidly become extremely large because of the "delay period" incorporated in the pressure function. This effect is illustrated by Figure 5, which shows the radius through which the bubble must contract before $P_i = P_\infty$.

The reason for this discussion is that current observations by Knapp and Hollander (19) and also Plesset (3) lead one to believe that the proportion of permanent gases inside the bubble is rather small.* Also one is inclined to believe that the water vapor inside the bubble does not deviate far from equilibrium pressure until interface velocities are of the order of 500 feet per second. For these reasons, a pressure versus R/R_o curve should tend to resemble one for $m \doteq .05$ where the final pressure was calculated to be 36,000 Atm. for adiabatic compression of the permanent gas portion (Figure 4).

This result means that moderate positive values of $P_\infty - P_i$ which exist during the early part of the collapse act through a large volume change since $V = \frac{4}{3}\pi R^3$. At smaller R, when $P_\infty - P_i$ is negative, only a small volume change is available, and, thus P_i must become enormous to absorb the kinetic energy in the field. The point where $P_i = P_\infty$, shown in Figure 5, also shows the surprisingly large ratio of volume traversed to volume

*Further discussion will be found in Section IV.

remaining, for two particular values of m.

It may be argued that the assumptions concerning the behavior of the bubble contents are not physically warranted, however, the calculations were made primarily for illustrative purposes to show the decisive effect of "delay" in pressure rise as a function of radius. If P_i remains less than P_∞ during a large portion of the contraction, $P_{i\,max}$ must be enormous to arrest the inward velocity.

3:2. Ackeret

Excellent experimental work was done by Ackeret (1) in the Water Tunnel at Gottingen, following Fottinger. Using a two dimensional Venturi of gradual profile, he measured pressures as a function of distance along the center line of a nozzle. At constant water velocity and varying system pressure, he found pressure distributions were similar to those calculated from Bernoulli's equation when the system pressure was sufficiently high. However, at low system pressures, he found that the vapor pressure of the saturated water was a lower limit to the minimum pressure in the throat.

At system pressures markedly lower than the critical, where the minimum pressure in the throat just equalled the vapor pressure of the liquid, the pressure distribution was altered due to the appearance of cavita-

tion. The presence of the cavities kept the pressure constant for an appreciable distance into the diffusor section of the Venturi, at which point a sudden pressure recovery occurred similtaneously with the disappearance of the bubbles. The lower the system pressure, the more severe the cavitation and the more abrupt the pressure rise.

Ackeret saw in this phenomenon a strong resemblance to compression shocks in the flow of gases through De Laval nozzles, and analyzed the gross effects on this basis. From the velocity of the liquid and the distance to the point where the bubbles disappeared, he estimated the time of collapse for the cavities to be of the order of 1/4000 of a second. He then reasoned that the time interval was so short that the gases contained in the bubbles would behave polytropically, and perhaps close to the adiabatic. He therefore criticized the work of Cook and Rayleigh, and calculated bubble collapse assuming various exponents in the polytropic process equation, $p = \rho^{n} \text{const.}$

His results predicted pressures on the order of 2700 times initial pressure and temperatures of 2300° K. These latter values of temperature excited some criticism of this work. Consideration in the section on the Interior of the Bubble (Section IV) indicates that heat conduction is more effective on water vapor than Ackeret

supposed, and that the pressure is much more likely to remain in the neighborhood of vapor pressure until the final stages of collapse.

3:3. Van Iterson, Bottomley and Surface Tension

As the result of erroneous deductions indicating that air bubbles were formed in cavitating water at pressures varying from 7 psia to 12.5 psia,* Van Iterson (31) (32) established the following hypotheses concerning bubble collapse:

a. The bubble is filled with air at a pressure approximately equal to the pressure in the stream.

b. If the bubble volume reduces, this air offers no resistance to resorption.

c. The net force tending to contract the bubble is due to surface tension.

He then equated the energy available from the reduction of bubble surface area to the kinetic energy in the liquid field, assuming the liquid to be incompressible. This results in the following equation for velocity:

$$\dot{R}^2 = \frac{2\sigma}{\rho} \quad \frac{R_o^2 - R^2}{R^3}$$

*See Section 2:5 c.

where σ = surface tension.

In this case, like Lord Rayleigh's, the velocity is seen to approach infinity as the bubble closes to zero radius. Thus all the difficulties attending Rayleigh's solution are repeated here by a factor which has heretofore been neglected.

The assumptions backing this analysis are open to challenge, as pointed out in Sections II, 5, c, and IV, on Experimental Work and the Interior of the Bubble, respectively. The great majority of experimenters disagree, and consider P_i approximately equal to vapor pressure during the major portion of collapse.

Bottomley (33) enthusiastically accepts these hypotheses concerning bubble collapse. He regards surface tension as exerting a pull on the liquid, causing it to follow and accelerate up to the velocity of sound, which he considers as the terminal velocity. These remarks have apparently been made without recourse to the methods and principles of non-steady compressible flow, which clearly indicate that the velocity of sound is not a barrier to higher velocities.*

3:4. Silver and Heat Conduction

Silver (54) developed a theory in which he de-

*Refer to Courant (47), Courant and Friedricks (48) and de Haller (49).

pends upon an approximation to the rate of heat removal during collapse to evaluate an overall average pressure difference acting on the liquid field during this period. He apparently assumed that the pressure and temperature rise in the cavity are not large, and applied the Clapeyron equation as if $\left(\frac{\partial P}{\partial T}\right)$ saturation were inversely proportional to the absolute temperature only.

He differentiated an expression for the differential work with respect to P in order to find the pressure which resulted in the maximum energy input. However, the element of radius that he took to be traversed to perform that work depended upon the amount of vapor condensed only, and not upon the motion of the fluid field. Furthermore, the meaning of the overall average pressure is not clear, since it is independent of both bubble wall velocity and radius.

He then stated that the maximum conceivable pressure would occur if all the energy released during collapse were stored in compression of the liquid which is condensed from the vapor originally contained in the cavity. This portion of the liquid surrounds the origin, and at the moment of complete collapse, is calculated to be of radius "b":

$$b = R_0 \left(\frac{V_\ell}{V_v}\right)^{\frac{1}{3}}$$

where v_ℓ specific volume of liquid at T

v_v specific volume of vapor at T

Since it is at a much higher pressure than the surrounding water, the liquid ball immediately expands, radiating an acoustic wave whose amplitude is computed according to the well known inverse law.* In particular, the amplitude is calculated as it passes the original radius of the bubble, R_o , since it is argued that this is closer than a boundary wall can be located without completely changing the purely radial flow pattern and perhaps modifying results seriously.

The pressures which he calculates at this radius are of the order of 20,000 psi, as given by the following equation:

$$P = \sqrt{k(P_\infty - P_i)\left(\frac{v_v}{v_\ell}\right)^{1/3}}\left\{1 + \frac{3\sigma}{(P_\infty - P_i)R_o}\left(1 - \left(\frac{v_\ell}{v_v}\right)^{2/3}\right)\right\}$$

where k bulk modulus of the liquid

Thus he contends that a bubble which collapses one radius away from a boundary wall will emit an acoustic wave of sufficient intensity to damage that wall. There are however, a number of questions which

*Lord Rayleigh (43) Theory of Sound.

must be answered before these values can be accepted.

a. How much energy is stored in compression of the liquid field? Lord Rayleigh (1) has shown that the pressures encountered in the surrounding field are certainly intense before collapse is completed, and require appreciable compression energy.

b. Can the entire energy of the liquid motion be stored in the immediate neighborhood of the origin the moment that collapse is completed? The finite velocity of sound means that only a portion of the kinetic energy of motion can be transformed to energy of compression at a given instant. Section VIII shows a detailed study of such a motion.

c. Is the inverse radiation law valid for the pressures encountered? Wartime studies of underwater explosions and their radiated shock waves show decided deviations from the acoustic law.*

Work in later sections demonstrates that these questions may be answered satisfactorily by use of the Method of Characteristics, and that the values computed by Silver for the radiating shock wave pressure are high by a factor of 5.

3:5. Herring Approximate Solution

*Cole (44), Underwater Explosions.

A solution which considers the effect of compressibility was presented by Herring (45), but is valid only to the first order of the ratio of collapse speed to the velocity of sound. The final effect on the velocity equation is to add a correction factor to the Rayleigh solution:

$$\dot{R}^2\left(1+\frac{4}{3}\frac{\dot{R}}{a_o}\right) = \frac{2(P_\infty - P_i)}{3\rho}\left[\frac{R_o^3}{R^3} - 1\right]$$

where a_o velocity of sound in liquid at atmospheric pressure

No equation covering the pressure and velocity distributions in the field was included.

Since interest in the effect of compressibility is focussed particularly on speeds equal to and greater than that of sound, the Herring solution is not of major interest for cavitation bubble collapse. The exact solution requires the solution of non-linear differential equations, which must necessarily be accomplished by numerical methods. The Method of Characteristics was developed to meet just such a need.

5:6. Oza Hemispherical Cavity

In 1945 Oza (46) presented a solution for the collapse of a hemispherical cavity seated on a plane surface. During collapse, he assumed that the bubble

took the shape of an oblate spheroid whose cross sectional shape was elliptical. The major axis of this ellipse was coincident with the plane surface, and did not contract. The minor axis was perpendicular to the surface and contracted under the influence of the pressure at infinity until the elliptical trace degenerated into a straight line at the moment of impact.

In observing bubbles in the vibratory apparatus by Rightmire's pictures, Oza found reduction of contact diameter to one-third the original diameter. This he estimated would increase his values by a factor of 9. The collapse is somewhat different in a water tunnel. Knapp and Hollander find complete collapse of a bubble on a model wall proceeding with not great deviation from hemispherical symmetry, and final collapse apparently occurs a small distance above the wall.

Oza showed that a velocity distribution at the bubble surface which was proportional to the square of the normal distance away from the surface of the wall would produce the elliptical shapes approximately. He then presented the equation below which purported to represent the kinetic energy in the entire liquid field, assuming incompressibility:

$$KE = \pi \rho a^3 U^2 \left\{ \frac{1}{5} - \frac{149}{225} + \frac{ab}{30} \left[\frac{8a^4 - 20a^2b^2 + 15b^4}{b(a^2-b^2)^{5/2}} \left(\pi - 2\tan^{-1} \frac{b}{\sqrt{a^2-b^2}} \right) - \frac{2(5a^2-8b^2)}{(a^2-b^2)^2} \right] \right\}$$

where a radius of hemisphere and constant major axis

b minor axis of ellipsoid of revolution

U velocity of surface at minor axis or the "pole" of the oblate spheroid.

Apparently an error was made in the computation, for negative values of kinetic energy are calculated in the vicinity of $\frac{a}{b} = \frac{1}{4}$. This is, of course, physically impossible. Therefore the value of U computed at the time that $b = o$ or impact occurs on the wall cannot be considered valid.

3:7. Rightmire Bubble Mass

According to his unpublished thesis written in 1941, Rightmire (26) observed masses of bubbles forming and collapsing in the repeating pattern against the face of his vibrating specimen. Photographs taken by the flash technique enabled him to examine these bubble groups and analyze them into individual bubbles whose centers were located. Seventeen and more were identified in various cases.

He assumed that the motion observed was a forced vibration of the liquid induced by the moving specimen in the form of spherically radial motion about a set of sources which were the bubble centers observed experimentally. Therefore he took the amplitude of motion to

be inversely proportional to the radius from each source, and superimposed the motions to find the impact velocity. The net result was a calculated pressure of approximately 5,000 psi.

This study may be challenged on the question of the dependence of velocity upon radius in spherical motion. The sonic approximation depends basically on the assumption that the motion of the particles is small. In this case, the amplitude of the motion should be compared to the radial distance from the individual centers, which is appreciable for any collapse phenomenon.

In addition, the frequency of the motion was taken to be the same as the frequency of the vibrating specimen. This is true for elastic undamped systems in forced vibration, where each portion of the system executes its motion in phase with an exciter. However, the bubbles were observed to exist only in a minor portion of the cycle of specimen motion. Apparently the natural period of motion for the bubbles was considerably smaller than that of the forced vibration, since they appeared briefly, and were suppressed the remainder of the time. For these reasons, the small figure of 5,000 psi calculated is not satisfying.

3:8. Need for a Solution Valid at High Velocities and Pressures

Lord Rayleigh (7) noted that, as a bubble collapsed, extremely high pressures were produced in the liquid surrounding the cavity. He felt that the pressures were sufficiently high to invalidate results when the bubble had shrunk to small radius ratios. Furthermore, the assumption of incompressibility immediately introduces the effect of infinite sound velocity. As was pointed out previously,* the effect of the high spherical convergence near the origin is felt simultaneously at great distances, which is not possible with real fluids.

If this effect is examined from the point of view of energy distribution, the result is equally distressing. Since compression of a liquid is always associated with potential energy, the large volume pressurized would certainly contain more energy than was available from the work of the pressure forces if the pressure distribution were assumed to be the same as calculated by incompressible theory. Thus compressibility must be admitted to determine the error associated with the incompressible solution.

---

*See Section 3:1.

Ever since the introduction of the De Laval nozzle, students of fluid mechanics have been imbued with the idea that supersonic speeds can be obtained only in converging-diverging nozzles. This statement is perfectly correct for the case of steady flow, where sonic velocity in the narrowest portion of the throat is the limiting factor.

Unsteady flow is, on the other hand, an entirely different case. The theory of one dimensional unsteady flow has been quite thoroughly studied,* although the methods are not popularly known. The problem first attracted attention in "Interior Ballistics", - - questions of the processes and flows that take place inside a gun barrel during firing. It is well known that the missiles fired often reach velocities higher than the velocity of sound in the medium immediately behind them.

Limiting velocities exist, in straight tubes, which may be visualized as the velocity the gas particles would take if all the thermal energy were converted into velocity in a single direction, and the gas density expanded to zero. It is to be noted, however, that these limiting velocities do not exist for converging flow.

---

*Courant (47), Courant and Friedricks (48) and de Haller (49).

Bottomley (36) states that the velocity of sound in water limits the collapse velocity possible in the closure of a cavity. The solution obtained in Section VII considering compressibility shows that such is not the case. If limiting velocities are to be found, they must be derived from the finite rate of thermodynamic processes at the interface between the interior of the bubble and the surrounding fluid.

Knapp and Hollander (19) show beautiful pictures of successive rebounds of a cavitation bubble which is acted upon by a pressure field which is nearly constant. It is quite clear that such a phenomonon must be associated with liquid compressibility, and any detailed study of it must consider non-steady compressible flow.

IV. The Interior of the Bubble

The most perplexing problem involved in bubble collapse theory is the interior of the bubble, and its effect on the surrounding liquid. The first question to be answered is whether the interior consists entirely of water vapor, and if not, how much air or other permanent gases are present.

Some further questions to be answered are the following: (a) How rapidly is heat removed from the cavity? (b) Are the gases compressed, and if so, adiabatically, isothermally, or polytropically? (c) Is the condensation rate of the water vapor rapid enough so the pressure deviates only a small amount from equilibrium? (d) The velocity of sound in the vapors is certainly about one-quarter or less of the velocity of sound in the liquid. What is the effect of the shock waves which necessarily form in front of the advancing wall of liquid?

4:1. Contents of the Bubble

It has been clearly established by Knapp and Hollander (19) and Plesset (4) that only water vapor can enter the cavity in appreciable quantities during the growth period. Since in their case this growth time is only about 0.002 seconds, it is difficult to imagine dissolved air diffusing more than a tiny distance.

Knapp calculated that the partial pressure of air in a bubble is only 0.0004 Atm., if the air is assumed to have been released from a spherical shell next to the bubble 0.001 inches thick. A normal air concentration of 2% by volume is assumed in the liquid since the water is saturated at atmospheric temperature and pressure. The resulting air pressure is only about 1% of the vapor pressure of water at 72°F.

Plesset (3) mentions that he has carried out an analytic solution of the diffusion problem in collaboration with P. S. Epstein, and found the rate to be so slow that it does not contribute appreciably to the air content of the bubble. These conclusions are corroborated by the fact that the pressure recorded when a cavity covers a pressure tap in the water tunnel corresponds closely to that expected from vapor alone.

Thus it is seen that the total air content of the bubble is nearly the same as the air content of the nucleus from which it developed. Under normal conditions this nucleus is small, and the air content is certainly small compared to the vapor arising from subsequent expansion. On the other hand, liquids which have been deliberately aerated presumably develop most of their bubbles from existing air bubbles much larger than an ordinary nucleus. Thus their air content is greater,

and a certain amount of cushioning is to be expected at collapse, accounting for the diminution of damage found experimentally.

Van Iterson contends that air offers no resistance to collapse, but the preponderance of investigators disagree. The considerations on which his conclusions are based have been shown to be doubtful.*

The air content to attenuate damage, judging from previous calculations,* would necessarily correspond to an air proportion index at least $m = 0.25$ where $P_{i_0} = P_v(1+m)$ Special cases do exist, however, when diffusion must account for the increased air content of bubbles; e.g. the long throuated Venturi tested by Hunsaker (17) which had an unusually long "incubation" period.

4:2. Latent Heat of Evaporation

When evaporation takes place, heat must be supplied to drive the liquid into the vapor state, the reverse being necessary when condensation occurs. In the case of cavitation, the main body of the fluid is the heat reservoir, from which heat is taken for evaporation, and to which heat is returned during condensation. As

---

*See Section 2:5, c.

*See Section 3:1.

Knapp and Hollander (19) explain graphically, this means that the temperature of the vapor must be somewhat less than that of the main stream after the bubble has grown. Likewise, the temperatures during the final stages of collapse must be higher than that of the main stream. It is vital to know the order of these temperature differences in order to evaluate the magnitude of deviations from equilibrium conditions.

Plesset (3), by considering the magnitude of thermal diffusivity, the time of collapse measured from experimental photographs, and the heat required to condense the vapor included in the cavity, arrived at a mean temperature rise of $\theta = 1.7^{\circ}F$ for the layer affected.

It seems possible that the local temperatures on the interface between the cavity and the surrounding liquid might be much higher, because of the extreme velocities encountered in the latter stages of collapse. With this in mind, the calculations shown below were made to find the order of magnitude of such peak temperatures. Methods similar to those of Plesset were utilized.

In a heat conduction problem, one of the commonest boundary conditions is that the temperature gradient at a stated point shall be great enough for a

certain rate of heat transfer to be realized. During bubble collapse the temperature gradient at the liquid-vapor interface must be large enough to conduct away the heat released by vapor condensation. The following expression is an approximation to the necessary value:

$$\nabla\theta = \frac{\rho_v \dot{R} L}{k}$$

where $\nabla\theta$ temperature gradient ^{o}F per foot

k conductivity of water

L latent heat of evaporation

ρ_v vapor density

$\dot{R}$ velocity ft/sec of bubble wall

Upon substitution of the proper values for water, this gradient is found to be $1.15 \times 10^4 \dot{R}$ degrees F per foot, which attains extremely large values at high velocities.

The thickness of the layer through which this tremendous gradient is expected to act may be estimated by means of the thermal diffusivity and the time remaining before collapse is completed.

$$\delta \doteq \sqrt{Dt}$$

where δ - thickness of the layer

D thermal diffusivity

t time remaining until complete collapse

Therefore, the order of the maximum temperature to be expected at the bubble wall is:

$$\theta_{max} = (\nabla\theta)\,\delta$$

where θ_{max} temperature rise at the interface, where maximum value must occur.

If the values for the case to be considered are substituted, the temperature is found to be quite modest, and agrees remarkably well with the computation made by Plesset (3).

τ = .001 seconds total collapse time from Knapp and Hollander (19)

$t = 17 \times 10^{-4}\,\tau$ remaining time for $\frac{R_o}{R} = 10$

$D = 1.75 \times 10^{-6}$ ft^2/sec thermal diffusivity

$\dot{R} = 480$ ft/sec

These data result in a value of $\theta_{max} = 9^{\circ}$F, as the maximum value, which compares very well with the 1.7°F mean temperature previously mentioned. Therefore it is justified to dispense with further consideration involving temperature rise.

It is to be noted that these calculations fully neglect the effect of convection which is in the complete heat flow equation written below, and will increase removal of heat when $\dot{R}$ is large.

$$\frac{\partial\theta}{\partial t} = D\nabla^2\theta - \vec{v}\cdot\nabla\theta$$

4:3. Effect of Finite Condensation Rate

Although it seems clear that thermal diffusivity is rapid enough to restrain temperatures to values of the same order as those in the body of liquid, condensation effects must be examined to find whether sufficient mass can be liquified to keep pressure rise low.

When a liquid and its vapor are in contact, there is a constant exchange of molecules from one state to the other. Equilibrium is the unique point when the mass transferred from the liquid to the vapor equals the mass deposited from the vapor into the liquid. This rate of mass exchange has been estimated from elementary kinetic theory, and is:

$$j = P_v \sqrt{\frac{M}{2\pi B T}}$$

where j mass rate of exchange per unit area

M Molar mass

B Gas constant

T Absolute temperature

Plesset (3) utilizes this value to estimate the collapse velocity at which pressure and temperature increases should cause appreciable deviation from equilibrium. It is clear that if the bubble wall advances into the vapor at a speed which is the same order as the

speed associated with the mass exchange rate, the local vapor pressure will have to double, roughly, in order to deposit sufficient vapor molecules into the liquid.

Assuming that the vapor equation of state is like a perfect gas, Plesset calculates that the bubble wall can advance at a velocity of 500 feet per second before pressures are expected to double because of condensation effects. The velocity equation is shown below with the data used in the calculation.

$$\dot{R} = \sqrt{\frac{BT}{2\pi M}} = 480 \text{ Ft/Sec.}$$

where $T = 532^{\circ}R$

However, the pressure increase arising from this source cannot act as a great deterrent to high collapse velocities, since it is naturally measured in terms of the vapor pressure of the liquid, which is only .027 Atm. at $72^{\circ}F$. By examining the results calculated from the hypothetical vapor-gas mixtures shown in Figures 4 and 5, it is clear that enormous pressures are required to stop inward accelerations. Values of $\frac{P_L}{P_V}$ of 100 are small compared to those shown, but are probably larger than pressures available from finite condensation rates until velocities in excess of 5,000 feet per second are reached.

4:4. Shock Wave Phenomena in Vapor

Study of unsteady compressible flow reveals that whenever a piston advances into a stationary tube of gas, a shock wave will form where the influence of the piston is first felt. When the surrounding liquid closes in on the vapor core at velocities greater than the velocity of sound in that vapor, shock wave of some intensity may be expected to form in front of the liquid wall.

The maximum pressure rise which is to be expected across this shock wave is equal to the stagnation pressure corresponding to the velocity of the in-rushing liquid wall. Actually, the pressure will be somewhat less due to entropy increase across the shock wave, and the fact that the liquid is absorbing the vapor at a finite rate. Therefore, the pressure rise is on the order of:

$$\Delta P = \frac{1}{2} \rho_v \dot{R}^2$$

where ΔP pressure rise across shock wave

At a collapse velocity of 5,000 feet per second, this pressure rise amounts to only 4 psi, because density is so small, which is surely negligible. If the density had previously been increased 100 fold, this pressure would still be small compared to the peak local pressure

in the liquid field.

4:5. Conclusion

The conclusions to which the foregoing studies lead are itemized below:

a. Under normal conditions of clean water and no aeration, the interior of the bubble consists of 99% liquid vapor.

b. Thermal diffusivity is so effective that temperature rise is not expected to increase the pressure against the bubble wall appreciably.

c. The finite rate of condensation will increase the pressure by a factor of about twice the vapor pressure at speeds of 500 feet per second, so that at very high speed say 5,000 feet per second, a pressure rise of the order of 20 P_v would be necessary to deposit enough mass in the liquid.

d. The shock wave produced in the vapor is entirely negligible.

e. The pressure rise effects listed are equal to the vapor pressure times functions of the velocity and are therefore small in magnitude until velocities on the order of 5,000 feet per second are reached.

f. If the inward velocity were reduced, the pressure rise effects depending on velocity would also

reduce, leaving only the accumulated compression of permanent gases. Accumulated compression of water vapor would tend to dissipa te rapidly.

g. By the time high velocities are reached, so much of the original bubble volume has been traversed that only astronomical pressures would suffice to halt the flow.

h. The above statements indicate that something akin to complete closure must occur. The extremely large velocities in the last stages of collapse must be arrested in a very short distance, resulting in an impact-like phenomenon.

i. The mechanism of halting the flow is not clear, but the local pressures are certainly extreme. Possibly other factors, such as asymmetries, become of primary importance in these final stages of collapse.

V. Problems to be Investigated

Since it is agreed that compressibility is of necessity important in flow of a liquid when high velocities and pressures are encountered, there are two particular phases of cavitation bubble motion where a detailed study of the fluid motion by means of the exact theory of unsteady compressible flow would be a contribution to present knowledge of its history.

5:1. Collapse of the Bubble

In view of the shortcomings of incompressible theory which have previously been pointed out, it would be valuable to analyze a collapse where the boundary conditions are identical with the Rayleigh Solution. It should be noted that, after the first part of the collapse, the pressure against the bubble interface is always negligible in comparison with the peak pressure at r equal 1.587 R, in the finite regime of motion. Therefore, constant vapor pressure is approximately the correct boundary condition for a pure vapor bubble during all but the arresting period of the collapse.

Data would be compared with the incompressible flow for some of the quantities listed below.

a. Velocity During Collapse.

Since compressibility would necessarily reduce pressure gradients and absorb some of the energy available from the work of pressure forces, bubble wall velocities would reduce. How great is this reduction? Does the velocity of sound limit collapse velocity? If not, does another, higher limit exist?

b. Pressure Distribution and Peak Pressures.

Compressibility undoubtedly is the cause for lower pressures in the liquid. Also, it has been shown that the pressures calculated at great distance from the origin by incompressible theory are necessarily in great error during the latter portion of collapse. How strongly are the intense pressures in the neighborhood of the origin felt farther out in the fluid field?

c. Energy Distribution.

It has been suggested that radiation of energy due to the high pressures near the bubble wall would reduce the velocity of contraction decisively. An evaluation of this radiation would be of importance to the development of an approximate theory.

5:2. Rebound of the Bubble.

Compressibility is undoubtedly responsible for the reversal of the inward velocities of collapse, but the sequence of events that takes place has not been studied in detail. One point is of interest; what role does the spherical divergence play in rebound?

a. Effect of Spherical Divergence.

In a straight pipe, rebound does not occur until the shock wave of compression reaches an open end, and the rarefaction wave reflected there returns to the impact surface. In the absence of friction forces the mass of liquid in the pipe between the rarefaction wave and the open end moves away from the impact surface at the same speed as before the sudden arrest. By the time this wave reaches the impact surface, all the velocities have been reversed. In the absence of an open end, however, no reversal can occur.

In the case of the spherical bubble in an infinite compressible liquid striking an immovable spherical barrier, no "open end" exists. If rebound can be analyzed, then, it must be directly dependent upon the spherical divergence for its existence.

b. Shock Wave.

A shock wave will be emitted by impact pressures, and will decrease in peak pressure as it radiates. How rapidly does this peak pressure reduce? Will it be capable of damage to metallic boundaries of the order of one radius, R_o, away from the point of collapse?

The shock wave appears to be a principal cause of the dissipation of energy in the rebound process. How much energy is radiated by this shock wave? What is the ratio between rebound size and original size, considering radiation to be the only form of energy loss?

c. Sequence of Events.

What general sequence of events takes place in the liquid during the rebound process? What is the cause of the difference in appearance between the original bubble and the rebound bubble?

VI. Compressible Flow and the Method of Calculation

When a study of unsteady fluid flow is contemplated, the assumption of compressibility must be carefully considered in the majority of cases. The exclusion of compressibility means the assumption of an infinite velocity of sound, i.e., a local perturbation is felt instantly throughout the fluid field.

Whereas there are many cases when the dimensions of the fluid volume are small compared to the velocity of sound X the time interval studied, such is not always true, and each case must be decided on its merits.

It is natural to assume comprssibility where extreme pressures are expected or local velocities may exceed that of sound. As the classic solutions clearly indicate, all three conditions are found in the latter stages of bubble collapse.

6:1. Equation of State

Since compressibility is to be included, a clear evaluation of it must be provided which will cover a wide range up to extremely high pressures, The state of all media can be described by a function relating the pressure, density, temperature, entropy, and internal energy. It is a known principle of thermodynamics that only two of these variables are independent.

In studying an idealized problem, heat conduction and viscosity may often be neglected, which is tantamount to assuming isentropic processes for each particle. This assumption will be made for the flow of water in bubble collapse, which means that the pressure may be given as a function of density alone. This relation is often known as the "Equation of State", and will be so called in the remainder of the paper, even though it differs from the strict thermodynamic definition.

An equation recommended for use with water by Courant and Friedrichs (47) (48), as well as Cole (44), and applied in the computations is stated below:

$$P + B = C\rho^{\gamma}$$

where P pressure of water

ρ density of water

B a constant equalling 3,000 Atm. for water

γ exponent equalling 7 for water

C a constant

This is called the modified Tait equation, and has been widely used for calculations of shock wave phenomena in water including pressures up to 50,000 Atm. It is particularly adapted to this use since the constants change very little when the entropy varies, and therefore the calculations are simplified. Kirkwood

and Brinkley (50) use it in studying underwater explosions, and Cole (44) offers a nice discussion of its merits.

Measurements have been made of the adiabatic properties of salt water by Bridgman and Gibson, as well as Penney and Dasgupta (51) who present the following values for the constants:

$B = 3010$ Atm.	$B = 2900$ Atm.
$\gamma = 7.15$	$\gamma = 7.47$

Results of these two equations agree within 2% up to 80,000 Atm. for salt water.

However, the simplicity of the original equation together with its wide previous acceptance for fresh water has led to its use in the following studies.

Some data on the adiabatic compressibility of water at one atmosphere, and on the isothermal compressibility of water at high pressures are available in Dorsey (52). The values of compressibility computed from Tait's equation are presented in Table IV and compared with experimental data at constant temperature. This agreement is regarded as satisfactory since the temperature rise is only 100°C when a pressure of 30,000 Atm. occurs through a shock wave.

The velocity of sound for water may be calculated as shown below:

$$a^2 = \left(\frac{\partial P}{\partial \rho}\right)_S = \frac{\gamma(P+B)}{\rho}$$

where a velocity of sound

For P equal one atmosphere, the velocity of sound is 4,790 feet per second, which agrees very well with measured velocities. It is to be noted that the velocity of sound is now a function of one variable only, since adiabatic processes have been specified throughout. This velocity is seen to increase with pressure, according to the following equation which is presented in Figures 6 and 7.

$$A = \frac{a}{a_o} = \left(\frac{P+B}{1+B}\right)^{3/7}$$

where A dimensionless velocity of sound

a_o velocity of sound at one Atm.

The energy per unit volume of water may easily be computed as a function of the pressure by integrating the equation for work done by the pressure forces.

$$e_p = \left(\frac{P+B}{1+B}\right)^{\frac{1}{7}} \int_0^P \left(\frac{B}{p+B}\right)^{\frac{1}{7}} \left(\frac{p}{p+B}\right) dp$$

This equation may be integrated by parts, but unfortunately, the two parts are so nearly equal that the accuracy is destroyed. Therefore, this equation was integrated by Simpson's Rule, and plotted in Figure 8 for the lower range of pressures to indicate the form of its

variation with pressure. As would be expected, the curve is nearly parabolic in shape.

6:2. Equations of Motion

The equations of fluid motion are well known, and are derived from the most basic physical laws. However, a few remarks will be included because of the comparative lack of popular knowledge on unsteady, compressible flow.*

The differential equations are derived on the basis of the four statements below:

a. Conservation of Mass

b. Newton's Law

c. The condition that changes of state are adiabatic.

d. Equation of State for the fluid

In the case of water, and probably most liquids, the equation of state is usually presented in a form for adiabatic compression. When the Eulerian form of expression, which examines the velocities at given points in the inertial co-ordinate system, is used, the following set of quasi-linear differential equations are

*Consult Courant and Friedrichs (48) for a complete discussion.

derived from the above tenets.

$$\frac{\partial \bar{v}}{\partial t} + \bar{v} \cdot \nabla \bar{v} + \frac{1}{\rho} \nabla P = 0$$

$$\frac{\partial \rho}{\partial t} + \nabla \cdot (\rho \bar{v}) = 0$$

$$P + B - C\rho^{\gamma} = 0$$

*

In general, these equations are very difficult to solve, but methods have been presented for particular simplified cases. Even then, it is unusual when a solution in terms of elementary functions can be found.

In particular, the mathematical theory has been worked out quite well for the case of one dimensional unsteady flow, where the fluid motion depends on one space co-ordinate, say x, and time only.** By use of the equation for the velocity of sound, the dependent variables may be reduced to two: velocity u and density ρ. The differential equations are hyperbolic in nature, and are therefore amenable to the method of characteristics. Facile numerical integration is possible in principle, if not in number of steps required or accuracy to be maintained. Closed analytical solutions can be found

---

*A bar over the letter v indicates a vector quantity.

**Courant and Friedrichs (48) offer a complete derivation. de Haller (49) shows a brief derivation.

only in rare cases.

At every point in the x, t plane the hyperbolic nature of the equations is responsible for the existence of certain directions with special properties.

Suppose that $x(\zeta)$ and $t(\zeta)$ represent a curve in the x, t plane, and therefore $\frac{\partial x}{\partial \zeta} / \frac{\partial t}{\partial \zeta}$ is the slope of that curve at a point. If a linear combination of the two differential equations of motions is made, it is possible to find parameters such that u and ρ will combine to derivatives in the same direction which is known as a "characteristic" direction. If that direction is the same as the slope of the curve, $\frac{\partial x}{\partial \zeta} / \frac{\partial t}{\partial \zeta}$, then two solutions for the characteristic direction are found;

$$\frac{\partial x}{\partial \zeta} = (u + a) \frac{\partial t}{\partial \zeta}$$

$$\frac{\partial x}{\partial \zeta} = (u - a) \frac{\partial t}{\partial \zeta}$$

These two equations specify different slopes for each point in the x, t plane and therefore they delineate two families of intersecting one parameter lines which form a network. It is now natural to designate new parameters α and β to indicate the positive and negative families of curves, in such a way that β is constant along a plus line and α is constant along a negative line. We now rewrite the above equations in the clarified form:

$$\frac{\partial x}{\partial \alpha} = (u + a) \frac{\partial t}{\partial \alpha}$$

$$\frac{\partial x}{\partial \beta} = (u - a) \frac{\partial t}{\partial \beta}$$

Two more equations are derived from the condition that characteristic directions exist, which hold along the charateristic directions only. Note that the equation dependent upon α holds along α characteristic lines only, and vice versa. Here they are written as applied to spherically symmetric flow.

$$\frac{\partial u}{\partial \alpha} + \frac{a}{\rho} \frac{\partial \rho}{\partial \alpha} + 2 \frac{au}{x} \frac{\partial t}{\partial \alpha} = 0$$

$$\frac{\partial u}{\partial \beta} - \frac{a}{\rho} \frac{\partial \rho}{\partial \beta} - 2 \frac{au}{x} \frac{\partial t}{\partial \beta} = 0$$

We now have four equations, associated in pairs, to describe the fluid motion. From the form of these equations, one may well change the conceptual relationship of the quantities. α and β are very logically regarded as curvilinear co-ordinates while u, ρ, x, and t are considered to be the dependent variables.

Observation of the first pair of equations shows that they have a beautifully clear physical significance: the slope of the characteristic lines represent the speed at which a perturbation is propagated through the fluid relative to the inertial co-ordinate x. Thus the term

u + a shows the "absolute" velocity of a wave proceeding in the direction of increasing x co-ordinate, while u - a is the velocity in the opposite direction.

As yet, one more step remains to present the second set of equations in a form most suitable for application. This may be accomplished by use of the Riemann Invariants, which reduce the equations, in the u, a plane, to straight lines modified by a divergence term.

$$\frac{\partial u}{\partial \alpha} + \frac{2}{\gamma - 1} \frac{\partial a}{\partial \alpha} + \frac{2au}{x} \frac{\partial t}{\partial \alpha} = 0$$

$$\frac{\partial u}{\partial \beta} - \frac{2}{\gamma - 1} \frac{\partial a}{\partial \beta} - \frac{2au}{x} \frac{\partial t}{\partial \beta} = 0$$

It should be noted that equation of state of the exponential form, which includes the Tait equation, has been assumed to evaluate the Riemann Invariants.

These equations dictate the formation of a second network in the u, a plane. Each characteristic line in the x, t (space-time) plane has a corresponding line in the u, a (velocity-velocity of sound) plane, dictated by the corresponding equation in the second set.

A complete solution may then be represented by the networks in the two aforementioned planes, which are often known as the Plane of Wave Propagation and Plane of State, respectively. It is to be noted that the

solution thus obtained is exact insofar as the original assumptions are met and the calculations are sufficiently accurate.

6:3. Dimensionless Variables for Calculation

In order to present the solution to a problem of fluid motion in the most general form, it is desirable that as many of the variables as possible be measured in terms of physical units pertinent to the problem. This procedure has the merit that it not only presents the data in a form of clear physical significance, but that the range of variables come within convenient numerical range.

These variables are defined below with brief notes as to their physical significance of one unit.

$Z = \frac{a_o t}{R_o}$ Time required for a sound wave to travel from the origin to the original bubble radius when the liquid is at atmospheric pressure.

$X = \frac{r}{R_o}$ Radius of co-ordinate system. Original bubble radius at 1.

$U = \frac{u}{a_o}$ Velocity in terms of velocity of sound at one atmosphere. (Not a Mach number)

$A = \frac{a}{a_o}$ Velocity of sound in terms of velocity of sound at one atmosphere.

$Q = \frac{R}{R_o}$ Radius of Bubble Wall in terms of original bubble radius.

$\dot{Q} = \frac{\partial Q}{\partial Z}$ Velocity of Bubble Wall in terms of sound at

$= \frac{\dot{R}}{a_o}$ one atmosphere.

6:4. Nature of the Solution

The type of problem most amenable to the use of the Characteristics Method of calculation is known as an initial value problem; namely, given the condition of the fluid at a certain set of corresponding points in the x, t and u, a planes, plus the boundary conditions, calculate the subsequent history of the fluid motion.

The nature of compressible unsteady flow is clearly presented by two concepts. The first is the "Range of Influence," which is the region in the x, t plane subsequent to a particular point 1 and included between the plus (+) and minus (-) characteristic lines which pass through that point. An illustration is shown in Figure 9.

The disturbance caused by pressure and velocity at the point in question obviously cannot be propagated through the fluid at a speed greater than the local speed of sound. Thus the region outside the triangle bounded on two sides by the plus and minus characteristic lines cannot be affected by conditions at point 1. This is often expressed by saying, "the point n cannot

know about conditions at point 1."

In a similar fashion, the "Domain of Dependence" is the original data (initial conditions) whose values affect the velocity and pressure at the point of interest, say Point 2. By the same reasoning as previously applied, this data must be included between the plus (+) and minus (-) characteristic lines passing through point 2 as illustrated.

Clearly, as time elapses, more and more original data affects the values at a particular point in the field. Conversely, a finite set of initial points can supply a solution for only a limited portion of the motion. These facts have their beneficial asspects, since the influence of a given point of initial data on a point in the field is "diluted" strongly as the network is developed. For this reason, isolated errors do not invalidate more than a small region of a solution.

In general, the characteristic lines in either the x, t plane or the u, a plane are not known at the start of the solution, but must be laid out and calculated from the slopes as the solution progresses.

It should be noted that the existence of such Domains of Dependence and Ranges of Influence is inherent in the nature of wave propogation. In equilibrium states and subsonic steady flow, however, all the points

of the medium are interconnected, and the equations are elliptic.

6:5. Method of Calculation

Four Equations have been obtained to describe the motion of the compressible fluid by means of a network in two planes, the x, t and the u, a, which will be known henceforth in their dimensionless nomenclature as X, Z and U, A planes respectively.

For convenience in calculation, the normal co-ordinates α, β are dropped, the equations then being written as finite difference equations. This is permissible because only one independent variable appears per equation. However, a designation must be retained to indicate which line is being considered. One convention which has been widely adopted names the wave proceeding in the direction of increasing X co-ordinate a plus (+) wave, and the wave proceeding in the direction of decreasing X co-ordinate a minus (-).

The equations as used, then, are written in the following form using the notation described:

$$\left(\frac{dX}{dZ}\right)_+ = U + A \qquad \Delta A_+ = -3\Delta U_+ - \frac{6AU}{X}\Delta Z_+$$

$$\left(\frac{dX}{dZ}\right)_- = U - A \qquad \Delta A_- = 3\Delta U_- - \frac{6AU}{X}\Delta Z_-$$

It is seen that the slopes in the X, Z plane are determined by U + A or U - A. Each line is designated by a number or letter, and the intersections are thus named according to the lines passing through them. By convention, the plus (+) line is always mentioned first and thus the point B, 7 is the intersection of plus characteristic line B with minus characteristic line 7.*

Each point in the X, Z plane has a corresponding point in the U, A plane which indicates the velocity and velocity of sound at that point. Both the plus and minus designation as well as the nomenclature for intersections are carried over to the U, A plane for clarity. To find the velocity and sound velocity at a particular intersection on the X, Z plane, it is only necessary to look up the same intersection on the U, A plane. It is to be noted that a point on the U, A plane representing velocity and sound velocity may correspond to several points in the X, Z plane, but the converse is physically impossible.

The calculations are performed point by point through the portions of the field which are of interest,

*Figure showing a collapse solution illustrates the principle.

starting from selected data at $Z = 0$. The process is iterative at each point, but fortunately converges quite rapidly. The graphical nature of the work and the iteration make the computation self-checking. As the history of the flow is unfolded a pattern is created in the network of lines drawn in the X, Z and U, A planes, and any irregularity of more than minor importance stands out immediately. Furthermore, the nature of the Region of Influence indicates that the effect of an isolated mistake is soon diluted and is covered by the correct values within the Domain of Dependence.

To illustrate the method of calculation, let us suppose that the points (1, 7), (2, 7) and (2, 8), as shown in Figure 10, are known, and that we wish to calculate the values of U, A, X, and Z at a new point known as (1, 8). The sequence of steps found most satisfactory is given below:

a. Estimate the values of U, A at point (1, 8) from the U, A plane. Once the pattern is partially developed the calculator can become remarkably accurate in his predictions.

b. Calculate mean values of U, A between each of the known points (1, 7), (2, 8) and the new point (1, 8) using estimated values at the new point.

c. Calculate mean $\left(\frac{dX}{dZ}\right)_+ = U + A$ from point

(1, 7) to new point (1, 8). This is the estimated average slope of the plus (+) characteristic. By use of a drafting machine draw this slope on the X, Z diagram.

d. Calculate mean $\left(\frac{dX}{dZ}\right)_{-}$ = U-A from point (2, 8) to new point (1, 8). This is the estimated average slope of the minus (-) characteristic. By use of the drafting machine draw this slope on the X, Z diagram. The intersection of the two lines is the new point to a surprising accuracy.

e. After noting the values of X, Z at the new point (1, 8), calculate ΔZ_{+}, ΔZ_{-} and the mean values of X between each of the previous points and the new point.

f. Calculate $\delta A_{+} = \frac{6AU}{X}$ and $\delta A_{-} = \frac{6AU}{X}$ from their respective mean values and lay out as shown in the illustration.

g. Draw $\left(\frac{dA}{dU}\right)_{+} = -3$ and $\left(\frac{dA}{dU}\right)_{-} = 3$ from the points determined by δA_{+} and δA_{-}. The intersection of these two lines gives the calculated value of U and A.

h. Compare the calculated value of U and A with the estimated value, and repeat the entire process if agreement is not satisfactory. The diagrams should be checked for regularity of pattern.

A sample calculation sheet is included in the

appendix to show how the computations were carried forward. It was suggested that a purely numerical method of iterative calculation should be used, but this amounted to more work than the graphical means. The best time which could be made consistent with accuracy was fifteen minutes per point.

Attempts were also made to do the computation by means of the Differential Analyzer at UCLA or the IBM punched card machines at the Cōop Wind Tunnel. The former was not adapted to do the problem, except by complicated repetitive means which would have tied up the entire Analyzer and staff for at least a week. The latter was not investigated completely because the expense would have amounted to about $1,000.00.

The Analogue Computer staff examined the equations, and found it would be unable to accomplish the task. There were no suitable multipliers available nor could the high accuracy required be obtained.

Since all pressures in the computations appear as the dimensionless velocity of sound, A, the accuracy required is beyond anything except digital type computers. For example, when P = 100 Atmospheres, A = 1.0120. In all the numerical work, the velocity of sound was carried out to at least four digits after the decimal.

The accuracy of the results is dependent upon the interval chosen, as well as the accuracy with which the numerical and graphical work is carried out. To check the interval size required, duplicate calculations were occasionally made with half the usual interval. If the results checked well, no alterations were made. In the progress of the calculation it was found necessary to reduce the interval several times as velocities became great and spherical divergences ($\delta A's$) also became large. In some cases it was found that the interval was smaller than need be.

The temptation to use an interval larger than required for good accuracy was great, since the number of calculations required is proportional to the inverse square of the interval.

All numerical work was done on a desk calculating machine and all graphical work was done on two drafting tables simultaneously. The lines were laid out to a large scale with the aid of drafting machines. Angles were thereby drawn to an accuracy of plus or minus 5 minutes. Since very large scales were used, and the intervals were kept quite small, it is estimated that most calculations are good to four significant figures. In regions of rapid change, this may be reduced to three significant figures.

VIII. Bubble Collapse

A solution was planned for the bubble case where the boundary conditions on the fluid motion were identical with the Rayleigh solution. The pressure inside the cavity is considered to be constant and equal to the vapor pressure of water.

Considerable effort was expended in the attempt to find an approximate means of integrating the equations of motion. A numerical solution was deemed satisfactory, provided it involved appreciably less computation than the Characteristics Method, while retaining sufficient accuracy at high velocities. No solution was found which would meet these requirements.

It is to be noted that the approximations made in most high velocity theories are not applicable here. This was brought out forcibly when the exact solution was computed. Velocities exceeded Mach number 1.0 while pressures attained enormous values on the order of 15,000 Atm. in the region studied. This resulted in density increases of about 30% and dimensionless velocities of sound equalling 1.9. For these reasons, the velocity of sound could not be assumed approximately constant, nor could the density.

Furthermore, it was not possible to make any approximations concerning the velocity distribution, be-

cause the term in the continuity equation which expresses the rate of change of the density became relatively quite important. A plot of the velocity distributions obtained is shown in Figure 13, and it is seen that the deviation from the inverse square law for incompressible liquids is considerable. A large portion of each distribution curve is exponential, but the exponent is variable during collapse and no approximation of this nature was found useful.

The clever approximate method of solution for the propagation of a shock wave in water worked out by Kirkwood and Bethe (53) was not adaptable because the conditions were too different. In their case, it was possible to consider the effect of waves moving in one direction only, the result of the other waves being approximated by shock jump conditions only.

For these reasons, it was concluded that the only satisfactory solution would have to be exact, particularly since special interest lay in the region where velocities are equal to that of sound and tremendous pressures are encountered.

7:1. Boundary Conditions

It was decided that the boundary conditions should be identical with the Rayleigh solution with con-

stant internal pressure. Aside from the desirability of direct comparison between an incompressible and a compressible theory, this choice can be defended on the basis of Section IV on the interior of the bubble.

In addition, surface tension was neglected. The resulting tension is equal to the vapor pressure of water at 72°F when the bubble has a radius of only 2.65×10^{-2} inches. This amounts to approximately $0.2R_o$ for the 0.14 inch radius bubbles observed by Knapp and Hollander (17). At approximately this size, the velocity becomes considerable, and thus the surface tension would tend to counteract any pressure increase in the vapor at the bubble wall due to finite condensability.

Admittedly, surface tension would apparently become important for bubbles whose maximum size were less than about 0.01 inches in radius, but here the total energy associated with a single collapse is comparatively small, about 1/2400 of the larger bubble. It will be shown later that the shock wave emitted from a collapse is not capable of doing material damage at distances greater than one bubble radius from the point of collapse. Thus, for a bubble of less than 0.01 inches radius, the range of damage would be severely limited and probably the presence of boundary layers would insulate the wall from shock.

The pressure at infinity was assumed to be constant. This does not agree with the data from the CIT Water Tunnel, but the differences are small enough to warrant error for the sake of maintaining a strict correspondence to the Rayleigh case.

This pressure remains as one of the independent parameters in the solution. However, it exerts no influence on the essential character of the solution obtained, lower values merely postponing high pressures and velocities of the liquid until smaller bubble radii are attained. Therefore, the selection of a particular value does not prejudice the nature of the result as long as $P_\infty - P_i > 0$ which is naturally required for collapse. The same remarks would apply to the selection of a value for P_v.

In order to correlate with data taken from the CIT Water Tunnel the following values were chosen:

P_∞ = .544 Atm. $\qquad A_\infty = 0.999937$

P_i = .027 Atm. $\qquad A_i = 0.999857$

Only the latter value is used in the characteristic portion of the solution, specifying the condition at the bubble wall. This boundary condition appears as a horizontal straight line in the U, A plane of state.

7:2. Initial Conditions

Since the Characteristic Line Method is normally applied to find the subsequent history of flow given the initial conditions, the logical place to start would be at the maximum bubble size. There is, however, the problem of completing a solution within a reasonable length of time.

In this solution involving wave propagation, a modified time scale suitable to the problem has been adopted, namely $Z=a_0 t/R_0$, one unit being the length of time required for a sound wave to travel the radius of the original bubble size. It is then easy to calculate the total Rayleigh collapse time in terms of Z:

$$\frac{\tau}{t} = \frac{0.915\, R_0 \sqrt{\frac{\rho}{P_\infty - P_i}}}{R_0 Z / a_0} \quad ; \quad a_0 = \sqrt{\frac{\gamma(1+B)}{\rho}}$$

$$\frac{\tau}{t} = 0.915 \sqrt{\frac{\gamma(1+B)}{P_\infty - P_i}} = 188$$

Thus the work involved would be at least equivalent to starting with initial data from $r = R_0$ out to $r = 188R_0$. The tremendous amount of work involved may be more readily appreciated if one calculates that the time remaining, according to the Rayleigh theory, after a bubble has passed $R/R_0 = 0.08$. This time is only

0.183 units of Z. Yet this point is the beginning of the region requiring precise examination with the exact theory.

For these reasons it was clear that the best results were to be achieved by employing the incompressible theory for the major portion of the collapse, the exact compressible theory being applied when velocities and pressures become appreciable with respect to compressibility effects. In this way more effort was expended examining the regions of particular interest.

The Rayleigh solution was then written in terms of the dimensionless variables to be employed throughout the analysis:

$$\dot{Q}^2 = \frac{2}{3}\,\frac{P_\infty - P_i}{\gamma(1+B)}\left[\frac{1}{Q^3} - 1\right]$$

$$\frac{P - P_\infty}{P_\infty - P_i} = \frac{1}{3}\,\frac{Q}{X}\left[\frac{1}{Q^3} - 4\right] - \frac{1}{3}\,\frac{Q^4}{X^4}\left[\frac{1}{Q^3} - 1\right]$$

where the variables used are defined in Sections V, 3, and Appendix 1.

The selection of a starting bubble size ratio, Q, for the compressible solution was made on the basis of the above equations for the boundary conditions selected. The radius chosen for the application of the compressible theory was $Q = 0.08$ where $\dot{Q} = 0.179$.

Since the velocity distribution in the flow field

is taken as proportional to the inverse square law up to this point, all other velocities are considerably smaller with respect to the velocity of sound. At this bubble size the maximum pressure is found in the surrounding field at $X = 1.587$ Q and was calculated to be 159 Atm. This corresponds to a dimensionless velocity of sound $A = 1.0223$ and a density ratio $\rho/\rho_0 = 1.0074$.

From these data it is clear that the error caused by the assumption of incompressibility is very small throughout the greatest part of the field. However, the error is magnified at the bubble surface due to the effect of convergence, and this point must be considered specifically.

The Herring (45) solution for bubble wall velocity is considered valid up to the value for $Q = 0.08$ which is $\dot{Q} = 0.165$. The difference between the Rayleigh value and this is not serious, since it applies only to the region immediately at the bubble wall, whereas the results of a Characteristic Line solution depend upon the accuracy of the initial data throughout the entire Domain of Dependence. In this particular solution, the Domain affecting the velocity of the bubble wall was found to extend to $X = 0.26$ or 3.25 bubble diameters into the surrounding field. In the ensuing solution, the Characteristic Line solution is seen to be nearly

tangent to the Herring solution where the two intersect, as shown in Figure 12.

The results in the range where pressures and velocities become extremely high is therefore not invalidated by what appears to be an 8% error in initial conditions because this error applies to only the worst point in an entire set of data. It is regretted, however, that the Herring solution is contained in a Wartime report not generally available, and that is concerned only with the bubble wall velocity, giving no pressure or velocity distributions. It does not appear in the Taylor Model Basin Bibliography report (5) on Cavitation published in 1947, which is usually complete.

Given the initial data at $Q = 0.080$ out to $X = 0.32$, the computations commenced by arbitrarily establishing $Z = 0$ to correspond. The values for U and A at selected points in the Domain of Dependence were then calculated and plotted in the U, A plane, this being then the $Z = 0$ locus. The computations were carried forward by the scheme explained in Section 6:5.

7:3. Symmetry

Complete spherical symmetry was assumed throughout the studies, although cavitation normally occurs in the neighborhood of a boundary. It would seem as if the

presence of a wall next to the bubble might cause considerable disruption of symmetry, but photographs of bubble histories taken in the Hydrodynamics Laboratory show remarkably little distortion from the spherical shape. Distortion does occur when contraction is nearly complete.

The assumption of symmetry is particularly important in the latter stages of collapse, when enormous pressures and pressure gradients are calculated to exist. The cause underlying these pressures is the dynamic condition whereby the liquid between the pressure maximum and the bubble wall is being accelerated at the expense of motion farther away from the origin. The net result is that a finite amount of momentum is being transferred to a smaller and smaller mass which moves at higher velocities.

In the Water Tunnel at Caltech, the cavitation bubbles observed photographically are formed directly on the surface of the model, and remain in contact through most of their life histories. Their general shape is spherical, down to the "latitude" at which the model surface is intersected. The usual angle of contact with the surface allows the bubble to be somewhat more than a hemisphere.

This extreme proximity of the model surface would

seem to be sufficient cause for disruptions in symmetry. Observation indicates that the asymmetries due to the presence of the model are unimportant, since the distortion which does occur in the last portion of collapse seems to be caused by an adverse pressure gradient in the direction of flow.

However, it is felt that the simplification of complete symmetry does not obscure any major effects, except possibly in the final stages of collapse, when the inward velocities are arrested. It is this region which is as yet unknown, and which seems destined to remain obscure for some time.

7:4. The Solution

The solution for the bubble collapse as it appears in the X, Z (wave propagation) plane is shown in Figure 11 which is folded in the pocket in the back. The Domain of Dependence for the ensuing compressible computations in shown along the axis at $Z = 0$, and was calculated out to $X=0.32$. It is to be noted that the bubble wall, which is designated by point 0, has already reached $Q = 0.080$. The subsequent history of its location is given by the boundary line which ascends from point 0.

The individual Characteristic lines are designated according to the number or letter associated with

the data point on the boundary from which the particular Characteristic line emerges. Plus Characteristic (1), for instance, commences at point (1) and runs upward to the right, indicating a wave moving in the plus X direction. Likewise, a minus line emerges from the same point (1) and runs upward toward the left, indicating a wave moving in the minus X direction.

The computations were made for the intersections of the characteristic lines, and each point is therefore designated by the number or letter associated with the two intersecting lines. The convention was established that the plus designation is always mentioned first in specifying a particular point. Thus point (4, 11) is the point where plus characteristic line (4) meets minus characteristic line (11).

The calculated values of U,A, X, and Z for each intersection are to be found in Table V arranged by means of the designating numbers, or letter and number. These points are grouped according to the plus characteristic on which they occur. Thus point (4, 11) is the eleventh point to be found in the fourth group.

The boundary condition of constant vapor pressure inside the bubble is applied when each minus characteristic line reaches the bubble wall. Here then, values can be calculated which serve as data for new plus

characteristic lines which subsequently propagate the conditions felt at this point out into the flow field. These lines are designated by letters to distinguish them from the lines which emerge from initial conditions. Therefore point (A, 1) is the point where minus characteristic line (1) meets the bubble wall and where the pressure must equal vapor pressure. All subsequent points on characteristic line (A) have been directly affected by the boundary condition at the bubble wall.

It will be noted that after $Q = 0.080$, the region of the flow field farther out than about $X = 0.26$ cannot affect the velocity of the bubble wall because the minus characteristic line (13) shown in Figure 11 emerging from $X = 0.26$ at $Z = 0$ does not reach the bubble wall before complete collapse occurs.

It will also be noted by the plus characteristic lines that in this latter stage of collapse the high pressures experienced in the neighborhood of the bubble wall cannot be propagated far out into the surrounding field before collapse is completed. This is also shown by the energy distribution curves to be discussed later.

7:5. Discussion of the Results

In general, the velocities and pressures calculated for the collapse of a bubble in a compressible

liquid are reduced from those calculated from the incompressible case, as would be expected intuitively. The reduction of pressures is very marked in the latter stages when pressures are on the order of 1/10 of those calculated from incompressibile theory.

The calculated velocities are also substantially reduced, though not as markedly as the pressures. It is of particular interest to note that the velocity of sound does not serve as a barrier to higher velocities and no upper limit is prescribed by the theory employed.

a. Velocities

The velocities calculated for the bubble wall are presented in Figure 12 as a function of the bubble wall radius, Q. The Rayleigh solution and the Herring solution are also shown, as well as the ratio of computed velocities.

The velocity at $Q = 0.08$ was assumed to be equal to that of the Rayleigh solution, compressible effects being taken into account from that point onward. The velocities computed considering compressibility are seen to deviate slowly but definitely downward from the incompressible. When $Q_{inc} = 1.00$, $Q_{comp} = 0.685$ or the incompressible velocity is 1.45 times as great as the compressible.

When $Q_{comp} = 1.00$ the incompressible value has increased 1.74. The velocity of sound does not deter the bubble wall from higher velocities. Observation of the curve shows that the tendency toward higher velocities as the radius is reduced is marked, and does not lessen much as supersonic velocities are reached.

The fact that sonic velocity does not limit the speed of a compressible fluid is well known.* It has been shown that a limiting speed, known as the escape velocity, does exist for a compressible fluid flowing in a straight pipe. However, in a converging section, the pressure and velocity of sound are increased by the narrowing cross section. While a portion of the fluid is pushed ahead at increasing velocities, the remainder is decelerated. In this way, momentum and energy are transferred to a smaller and smaller mass of fluid as the collapse progresses, and ever increasing velocities are therefore to be expected.

Examination of the Wave Propagation Plane (X, Z) Figure 11, shows that the minus characteristic lines are still able to reach the bubble wall after sonic velocity has been obtained. Therefore perturbations within a

---

* Courant and Friedrichs (48)

limited distance can be expected to drive the velocity higher.

It is also seen that, unlike the case of a straight tube, the plus characteristic lines are propagated outward in the field, even though some delay must occur when Mach number is greater than 1.00. The reason for this behavior is the fact that the velocity is an inverse function of the radius. As the perturbation travels away from the bubble wall along a plus characteristic line, it eventually reaches a region where the velocity of sound is higher than the inward velocity of flow. The slope of the characteristic direction then changes to positive, and the line moves away from the origin. Characteristic line (X) is a good example of this effect.

Extrapolation of the velocity versus bubble wall radius curve in Figure 12 leads to values of $\dot{Q} = 7$ at $Q = 0.001$, barring any extreme pressure increases against the bubble wall. Since this velocity is 33,500 feet per second, it is effectively infinite and the original assumptions must be invalidated. However, it is hard to see how the pressure inside the bubble could be effective, since the extrapolated value of the pressure maximum in the liquid, reaches 7×10^5 Atm. as may be seen from Figure 15.

The velocity distribution is calculated for the

liquid surrounding the bubble at several different times corresponding to different bubble wall positions. The curves are shown in Figure 13.

For an incompressible fluid, the velocity distribution may be calculated from the continuity equation alone, and is proportional to the inverse square of the radius. When the fluid is compressible, the continuity equation is no longer directly integrable due to the variable density. Therefore the deviations from the inverse square law are a measure of the importance of compressibility.

The velocity distributions in Figure 13 are plotted against radius on log-log paper, and the slope of the curve is thus equal to the exponent of X that the distribution follows. Calculated slopes as low as -1.34 are shown, which demonstrates considerable deviation from the incompressible value of -2. The trend illustrated indicates that even lower slopes would be found during the latter stages of the collapse.

b. Pressures

The same general character of pressure distribution is retained in the two cases, but pressures are much lower for the compressible liquid. Figure 14 presents the compressible and incompressible pressure distri-

butions plotted as P/P_{max}, for each case respectively. Each exhibits a strong pressure rise from the bubble wall back to a maximum point. It should be remembered, however, that the ratio of maximum pressures between incompressible and compressible solutions is 7.9 for the time selected.

It is also interesting to note that the location of the pressure peak is approximately the same in the two cases with respect to the bubble wall radius Q. The peak is sharper in proportion for the compressible case than it is for the incompressible.

After the point of peak pressure, the relative pressure for the compressible case decreases more rapidly than the incompressible, which gives the pressure peak its sharper appearance. The farther one moves out into the surrounding field the smaller the compressible relative pressure becomes with respect to the incompressible. This is to be expected from two physical interpretations: first, compressibility means that energy can be stored in the form of pressure, and only a small total amount is available; second, a finite rate of wave propagation means less pressure travels outward.

The relative magnitudes of the compressible and incompressible pressures are illustrated by Figure 15,

where the maximum pressures are plotted as a function of bubble wall radius for each case. The compressible peak pressure starts deviating markedly from the incompressible the moment Characteristic computations begin, and continues as a straight line on log-log paper. The slope of this line is 1.91 as compared to 3.00 for the incompressible pressure.

The ratios obtained between peak pressures become very large, reaching 9.6 at $Q = 0.010$, and continue to increase as the bubble collapses. Thus a marked diminution of pressures is predicted during the collapse period.

The general history of the pressure distribution in compressible flow is clearly illustrated by Figure 16, where the pressures in the surrounding field at several bubble wall positions are plotted as a function of radius X. After the peak pressure has passed, the pressure at a particular value of radius, X, is seen to continue increasing as the bubble collapses, but at a slower rate, eventually reaching a practically constant value. In the meantime, the maximum pressure point has continued inward to higher and higher pressures.

c. Energy Distribution

During the collapse period energy is continually being transported inward toward the origin, Figure 17

shows the sum of kinetic and potential (pressure) energy as a function of the dimensionless radius for several positions of the bubble wall during the latter stages of collapse.

If the energy within a particular radius X is examined, it is found to increase as the liquid flows across it. On the other hand, the size of the sphere which contains a certain amount of energy may be calculated by integrating from the bubble wall outward. The size of the sphere which contains 40% of the energy available from the work of pressure forces, $(P_\infty - P_i)\frac{4}{3}\pi R_0^3$ is shown in Figures 17 and 18. As the bubble decreases in size, its radius decreases rapidly until the bubble is very small. Then the decrease becomes less rapid, and apparently tends to the limit $X = 0.051$ as the bubble goes to zero.

Judging from the shape of the energy curves computed, this curve is typical of all constant energy plots. Since the mass of liquid near the bubble wall becomes very small, extreme velocities are to be expected.

In the region near the bubble wall, the pressure energy stored in the liquid is small compared to the kinetic energy. When $Q = 0.0074$ for instance, the pressure energy at the point of peak pressure is only 9.4% of the kinetic energy at the same point. The velocity decreases so rapidly with radius, however, that the proportion of pressure energy is 22% at $X = .0604$. Between $Q = 0.0074$

and $X = 0.0604$, 16% of the total is computed to be pressure energy.

The proportion of total energy stored in pressure form is much smaller earlier in the collapse. When $Q = 0.023$, only 4% of the energy is stored between the bubble wall and $X = 0.776$ is due to pressure. When $Q = 0.080$, the point where the compressible solution was started, the pressure energy stored out to $Z = 0.480$ was 2% of the total energy.

It must be recalled that the Rayleigh solution cannot be considered valid at large distances from the origin, where the pressure is much less than that computed from the incompressible theory. Therefore, the energy outside $X = 0.48$ was not computed.. Furthermore, the Domain of Dependence for the region near the bubble wall extends to only $X = 0.26$ when $Q = 0.080$ and the compressible theory is applied. Thus the energy far out in the field need not be considered.

The conclusion may therefore be drawn that energy of compression does not soak up a large proportion of the energy available, and therefore velocities are inhibited only to a moderate degree. In addition, energy is not radiated during the collapse period, but is transported inward. Any radiation of energy which takes place must therefore be the direct result of extreme pressures occurring when the inward motion is

arrested.

7:6. Conclusions

A summary of the results of the study of bubble collapse considering compressibility of the liquid is presented below:

a. Velocities are less than those predicted by incompressible theory but sonic velocity does not act as an upper limit.

b. No upper limit to velocities exists, outside of relativistic effects, unless pressures of higher order than the peak pressure in the liquid are applied against the bubble wall.

c. Pressures are much lower throughout the field than the incompressible theory predicts, particularly during the latter stages of collapse. However, the pressures become indefinitely large as the bubble radius approaches zero.

d. The maximum pressure in the liquid occurs at about the same radius as the incompressible solution, but the pressure decreases much more rapidly in proportion at larger radii.

e. The region affected by extreme pressures is comparatively small at the moment the bubble disappears.

f. No energy is radiated before collapse is

completed. On the contrary, energy is transported inward, and concentrated in the region immediately surrounding the bubble wall.

g. The proportion of pressure energy stored in the liquid remains small until an arresting process begins: i.e., until high pressures are applied to the bubble wall.

VIII. Impact and Radiated Shock Pressure

Cook (6) calculated the pressures which resulted when the collapsing bubble is allowed to strike an incompressible ball of finite radius surrounding the origin. The values were based on the velocities calculated from the incompressible theory, compressibility being admitted the instant the liquid impringed on the ball or impact surface.

This assumption was made because the velocities predicted by theory tended to infinity as the bubble wall radius approached zero. It has been shown that the same anomaly exists if the liquid is assumed to be compressible, like water.

Furthermore, it has been shown in the section on the interior of the bubble, that the pressures which can be developed against the bubble wall by thermodynamic processes cannot be large with respect to the peak pressure in the fluid during the finite portion of the collapse when the bubble is filled primarily with water vapor. Therefore, it has been concluded that the liquid motion must continue inward to a very small radius at high velocity. However, since the origin is the center of symmetry, the liquid must be stopped abruptly as it reaches $X = 0$, producing an impact-like phenomenon.

For these reasons, it has been deemed worth while

to examine the impact of the collapsing bubble against an incompressible ball, assuming the liquid to be compressible. The high pressures created instantaneously would propagate outward as a shock wave carrying considerable energy, the peak pressures dropping due to the spherical divergence.

It is of considerable practical interest to know whether a bubble which collapses at a finite distance from a fluid boundary can radiate a shock wave capable of damage to materials commonly used in hydraulic machinery. Stepanoff (29) states that a bubble collapsing in the stream can do no damage to a neighboring wall.

However, Silver (54)* has computed the peak pressure associated with an outward moving shock wave according to his assumptions, which include the law of acoustic radiation. He finds that the pressure realized when the shock wave passes the radius corresponding to the original size of the bubble is on the order of 20,000 psi, and therefore is capable of damage to cast materials.

One can, however, make calculations which are based on assumptions having more definite physical meaning, and which produce a peak pressure at the shock wave which is certainly an upper limit to those actually

*See discussion in Section 3:4.

encountered.

8:1. Assumptions

a. Compressibility is assumed throughout the collapse period, and therefore the velocities used for computation are somewhat lower than the incompressible case.

b. Impact occurs against an incompressible impact surface or ball, the pressure being a function of the bubble wall velocity only. It is higher than the pressure which would result if deceleration were to start at the same radius as the incompressible ball, zero velocity occuring at a slightly smaller radius, as by an arresting mechanism involving compression of the bubble core. This mechanism has the feature that only the layer of liquid at the bubble wall is affected at the instant of impact, the effect being propagated outward slightly faster than the local velocity of sound as explained in more detail in Section .

The principal difficulty encountered by this analysis is the selection of a suitable radius Q_i for the impact surface. For this reason Q_i will be kept as a parameter whose effect will be examined as it varies.

c. Impact pressures are calculated by the Characteristics Method using the adiabatic equation of

state for water. The pressure obtained, plotted as a function of velocity just before impact, are shown in Figure 19. The curve showing pressures computed by the acoustic theory is a straight line, and the Characteristics method solution is nearly parabolic in form, giving much higher pressures at high velocities. This is due to the fact that the adiabatic equation of state decreases the compressibility of water as the pressure increases. However, both curves agree at low velocities.

d. Shock wave radiation is computed by use of radiation theory developed for underwater explosions during the war. Acoustic radiation theory is valid at only small pressure increases and when particle motion is small. These conditions do not apply to the situation following impact, as Section IX shows.

On the other hand, the shock wave data computed for underwater explosions and shown in Figure 20 would seem to fit the case being studied rather well. In each instance, a strong pressure shock advances rapidly into a region of much lower pressure. In the underwater explosion, energy is being supplied to the liquid by pressure against the wall of the gas bubble created by the products of combusion. In the case of the cavitation bubble, energy is carried across the shock front because the liquid still unaffected by the impact of closure is moving inward as the shock wave advances. The net result

of both energy transfers is to produce a pressure-time curve at a constant value of X which has approximately exponential decay.

In Section IX a detailed study of the motion of the fluid after such an impact is computed by the Characteristics Method. The pressure-time curve for the impact surface is shown in Figure 25 plotted on semi-log paper, and it is seen to be very close to an exponential decay.

In the same section, the peak pressure at the shock wave is computed on the adiabatic theory and is plotted as a function of the radius x, in Figure 21. Also plotted in the same figure are the peak pressures as predicted by the propagation theories of Kirkwood and Bethe (53) plus Penney and Dasgupta used for underwater explosions. It is to be noted that the slope of each curve is less than minus 1, which is the acoustic value. The lower values of the Penney - Dasgupta and Kirkwood - Bethe curves can be attributed to the accumulative effect of the entropy change across the shock wave which they take into account.

Furthermore, Figure 20 shows that the explosion theories have been carried to pressures on the order of 50,000 Atm. where the entropy change would be expected to produce an appreciable loss. Cole (48) indicates that

the Penney-Dasgupta (51) solution is to be preferred in this region, since it is a step by step integration utilizing the Riemann Invariants.

8:2. The Solution.

Utilizing the assumptions mentioned, the pressures at impact against incompressible cores of various sizes were computed. These pressures became very large as the velocity of the bubble wall increased, and reached the astronomical figure of 268,000 Atm. when the impact velocity reached $2\ a_o$, as shown in Figure 19.

The peak pressure at the radiating shock wave was then computed as it passed the radius corresponding to the original size of the bubble, according to the propagation theories of Penney-Dasgupta (51) and Kirkwood-Bethe (53). The computed values are shown in Figure 22 plotted as a function of the radius of the impact surface Q_o. The magnitude of the pressures is seen to be of the order of 200 Atm. even when the impact radius becomes quite small. It is to be noted that the pressures are practically insensitive to the size of the incompressible core.

The data available did not permit the extension of the calculations to smaller impact surfaces, so the trends indicated on the curves cannot be verified.

However, it is certain that the energy dissipation at the shock wave becomes increasingly important at pressures in excess of 50,000 Atm. The Penney-Dasgupta relation which is to be preferred in this regime, according to Cole (49), results in a decrease in the shock pressure as the impact surface becomes smaller. However, energy considerations would indicate that an asymptotic value should be reached. It seems probable therefore, that the pressure peak would be less than 300 Atm. as the shock wave passes $r = R_o$. At greater distances, the pressure would, of course, be considerably smaller, varying approximately as $1/r$.

Since the arresting process at the center of the bubble was assumed to be impact against an immovable wall, the pressures computed thereby must be the highest conceivable. Therefore the actual pressure felt at $r = R_o$ as the result of bubble collapse, must be less than that computed in this section, and damage to metallic materials by the radiating shock wave is not possible.

8:3. Conclusions.

a. Pressures during the arresting of the collapse motion must be very high.

b. Spherical radiation of these peak pressures reduces their values more rapidly than the acoustic

radiation theory due to Lord Rayleigh.

c. The peak pressures created by collapse on an incompressible ball of finite radius are less than 300 Atm. when they pass $r = R_o$, even when the ball is assumed to be very small.

d. The pressures from an actual collapse must be smaller than those computed for an incompressible ball. Therefore, the shock wave radiated from a bubble collapsing in a stream at a distance of at least one bubble radius from a boundary cannot be expected to damage that boundary.

IX. Fluid Motion During Rebound

Knapp and Hollander (19) point out that the compressibility of liquid performs a vital role in the rebound phenomenon which they observed in the water tunnel. Whereas it is clearly shown that the reopening of a cavitation bubble which has collapsed is due to the temporary storage of kinetic energy in the form of pressure energy, the detailed mechanism of this action is of further interest.

It is true that there exists a fundamental difficulty concerning the events happening inside the cavity when the bubble apparently disappears. The processes which account for the arrest of the extreme velocities observed and speculated over in calculations are as yet unknown. The section covering the Interior of the Cavity showed that ordinary thermodynamic considerations would not produce an appreciable effect in what may be regarded as the observable or finite regime of the bubble collapse. These comments apply when the bubble considered did not develop from an air nucleus of appreciable size.

The discussion in the previous section emphasized that the inward motion is stopped so abruptly when the size ratio, Q, becomes infinitesimal, that it may be modelled after impact against an immovable spherical barrier. The pressures occuring at the point of complete

collapse are purely speculative, since the choice of a proper size for a model barrier is a matter of dispute. However, it was shown that the peak pressure in the outward moving shock wave resulting from the impact is relatively insensitive to the size impact surface assumed, if observed as it passes a given radius.

Likewise, the sequence of events in the fluid field may be studied by the use of a model with an immovable spherical barrier at the center. The character of the events is not essentially different for various core sizes. Although this device is admittedly artificial, its properties are strictly definable, in contrast to the microscopic, non-equilibrium processes which must take place in the actual core, and which are at the present time the subject of speculation.

Some striking similarities may be pointed out between complete collapse and rebound of a vapor bubble, and the rebound from an immovable sphere.

a. A pressure which is high compared to the peak pressures in the fluid field is produced by the abrupt halt of the velocity at the bubble surface.

b. The total inward moving momentum which must be halted and the total energy is nearly equal in each case.

c. No energy is radiated until the local pres-

sures rise due to the arresting mechanism.

d. The impact pressure is produced so rapidly that a pressure discontinuity or shock wave is formed which propagates outward. (Note the distinct "clink" associated with cavitation bubble collapse.)

e. The fluid outside the shock wave is not affected until a later time when the shock passes.

f. Energy is radiated to infinity by means of the shock wave, thus decreasing the energy available for reopening the bubble.

g. Outward radial velocity is created by the re-expansion of the compressed liquid.

h. The cavity reopens when the pressure drops to vapor pressure or lower.

For these reasons, detailed study of the unsteady spherical motion of a compressible fluid which collapses against an immovable barrier was undertaken in the hope that a better qualitative understanding of the events taking place in the liquid may be obtained. In addition, an estimate of the energy radiated by the shock wave was found, since this was expected to be the major mode of energy loss.

9:1. Boundary Conditions.

The major requirement to be placed on the size of

the sphere to be selected is that it be small enough to permit the pressure at infinity to perform most of the work available during complete collapse, and that the impact pressures be great enough to produce appreciable change in liquid density. However, the pressures should not be so high that the equation of state could be doubted or that losses across the shock wave would become large.

The size selected was 0.10 the original size of the bubble, R_o where the velocity caused by a pressure difference of one atmosphere is $\dot{Q} = 0.178$. It produces an impact pressure of 5140 Atm. which is within the scope of the equation of state, and also produces a density increase of 15%, which is appreciable.

The boundary conditions which are to be applied to the fluid after impact has occured are physically clear. The velocity of the liquid in contact with the immovable barrier must be equal to zero as long as a positive pressure exists at that surface. The question of the phenomena which occur when the contact pressure reaches vapor pressure will be deferred to a later section.

9:2. Initial Conditions.

The dimensionless time Z was chosen to be zero

at the instant the liquid contacted the immovable barrier. The velocities and pressures in the fluid field at this instant were computed from the Rayleigh equation considering the pressure difference between infinity and the bubble interior to be one Atmosphere. The highest pressure in the field was 157 Atm., which is small enough to warrant the neglect of compressibility effects. The bubble wall velocity was 0.178.

The values of velocity and pressure at selected points were then utilized to form the Domain of Dependence of a Characteristics Method Solution.

9:3. Shock Wave Conditions.

The sudden impact of the bubble wall moving at a velocity $\dot{Q} = 0.178$ produced an instantaneous pressure jump in the layer of liquid which was decelerated to zero velocity. In order to analyze the subsequent motion of the entire fluid field, the effect of the discontinuous pressure jump and its rate of propagation must be correctly analyzed. The theory underlying shock wave phenomena was worked out by Rankine and Hugoniot, and stems from three fundamental principles: Conservation of Mass, Momentum, and Energy.

Courant and Friedrichs (48) point out that the entropy changes in water are so small that the Conser-

vation of Energy is automatically satisfied approximately if the adiabatic equation of state is used. This simplifies the calculations, since changes in velocity and velocity of sound are then restricted to satisfy the Riemann equations in the plane of state (U,A).

In general, to completely specify conditions at a shock front, five quantities must be known: The pressure and velocity in front of the shock wave and behind it, plus the velocity of the shock itself. This requires the knowledge of previous history both behind and in front of the shock. The following procedure was found satisfactory in calculating the shock wave at each point in its trajectory:

a. Estimate the shock wave velocity. This can be done very accurately, since the velocity is nearly constant.

b. Calculate the conditions in front of the shock wave, where the minus characteristic intersects the estimated position of the shock wave, by means of the Characteristics Method.

c. Find a point (ϕ, η) on the back side of the shock wave such that the plus characteristic through it intersects the estimated shock wave position at the same point as the minus characteristic on the front side of the shock wave.

d. Calculate the conditions on the back side of the shock wave by means of the Characteristics Method, following the plus and minus characteristic lines determined in the plane of state (U, A).

e. Calculate the shock wave velocity from the Equation of Continuity across the shock.

f. Check the values obtained, and iterate if more accuracy is required.

9:4. The Solution.

The solution as obtained from the Characteristics Method is hown in Figure 23, which is found folded in the pocket at the back. This is the X, Z plane, or plane of propagation. The shock wave is seen emerging from the impact surface at Z=0 and proceeding upwards and to the right as it propagates outward at a velocity slightly higher than the velocity of sound in the undisturbed liquid. It is to be noted that the fluid outside the shock wave continues to move inward as if no impact had occured, until met by the shock.

Conditions behind the shock wave are entirely different from those just in front, except that the entropy is approximately the same. They may best be examined by means of Figure 24, where the velocity and pressure distributions between the impact surface and

shock wave are shown for several specific times after impact.

a. Velocities

The first thing to note is that the velocity is restrained to be zero on the impact surface as long as a positive pressure exists there. Second, the impact against the surface produces a pressure rise to 5140 Atm. and a density increase of 15%. Third, succeeding layers of liquid moving inward impinge against the already decelerated layers, according to the shock wave conditions.

The sum of all these effects are the velocity and pressure distributions shown. After the initial impact, the pressure immediately begins to decrease, causing a decrease in density. Since the velocity at the impact surface must be equal to zero, the particles a few layers out must acquire an outward velocity according to the rate of increase of liquid volume between the point considered and the stationary impact surface. Therefore it is easy to see that the velocity must vary from zero at the impact surface to a maximum outward value at the shock wave.

This general shape of the velocity distribution is maintained for the several times depicted in Figure 24. It may be noted that the particle (liquid) velocity at

the shock front is zero at the instant impact occurs, rises quickly to a maximum, and then reduced slowly, indicating that the rate of change of the entire volume inside the shock changes in the same way.

It should be re-emphasized that this velocity distribution is possible only because the term in the continuity equation which accounts for the rate of change of density is negative, and opposite in sign to the divergence of the velocity.

b. Pressures

The pressure at a given instant of time varies as a function of radius from a positive value at the impact surface to a larger value at the shock wave, where the incoming undisturbed particles are met. The peak pressure is seen to reduce very rapidly at first, and more slowly later, being an inverse function of the radius. This pressure is plotted on log paper in Figure 21 and compared with the shock wave pressures as predicted by the Kirkwood-Bethe (53) and Penney-Dasgupta (51) underwater explosion data. This agreement is seen to be reasonable enough to warrant its use in the examination of shock waves peak pressures radiated from tiny impact surfaces as studied in Section VIII.

The pressure at successive instants of time behind the shock wave is seen to reduce rapidly at first

and then more slowly. A plot of the pressure against the impact surface as a function of time in Figure 25 shows that the pressure decrease is nearly exponential during a large portion of the contact period. This is similar to the history of underwater explosions.

This particular curve shows a feature which has not been mentioned heretofore. The compression and subsequent re-expansion of the liquid during rebound phenomena must take a finite, though short, time. The outward radial velocities which have the momentum to reopen the bubble are developed through the action of the shock wave, the propagation of which requires time. In the example solved, the time interval until the pressure on the impact surface equalled vapor pressure amounted to Z 0.61. In terms of the bubble of 0.14 inches radius studied by Knapp and Hollander (19), this would amount to 1.5 micro-seconds or 3% of the time between film exposures taken at 20,000 per second.

This value is negligible but it is of importance to estimate its size for smaller impact surfaces, to find whether it can always be neglected. Dimensional analysis shows that this time should be on the order of:

$$t = \frac{r}{2a_0} = 1.4 \times 10^{-6} \text{ sec} \qquad @\ r = 0.10 \times 0.14 \text{ in.}$$

where $\frac{2}{r}$ the rate of spherical divergence

A_o velocity of sound in liquid at one atmosphere

thus it is clear that this time is negligible for smaller impact surfaces.

c. Tension Wave

At the time that the pressure is reduced to vapor pressure against the impact surface, the pressure and velocity distributions have the same general character as previously described: i.e., they vary from zero at the immovable barrier monotonically to a peak value at the shock wave. Therefore considerable outward momentum has been generated in a velocity distribution which is considerably different from the incompressible.

Turning now to a particle which is located on the immovable barrier, it has been restrained by the previous positive pressure to remain at rest. The greatest outward driving pressure which is now available is the vapor pressure of the liquid. However, in ordinary considerations, the liquid is considered to cavitate when vapor pressure is reached. If this were true, no pressure gradient could exist to accelerate this particle, and it would remain seated on the incompressible core.

A similar situation would be met with particles

between the barrier and the shock wave at later times. The positive value of the velocity divergence due to the monotonically increasing velocity as a function of X, means that the volume of this liquid must continually increase with time. Therefore vapor pressure would be reached first on the barrier and later at finite distances from the barrier. This effect is propagated at the speed of sound in the liquid. The locus of point dropping to vapor pressure is shown in the X, Z plane.

If the liquid cavitated at the vapor pressure of water, no accelerating pressure gradient could act upon each particle at the time that it reached vapor pressure and cavities formed. Therefore each would continue to translate at the same velocity as it had at the instant of local rupture. Because of the fact that the divergence of the particle velocity would still be positive in this two phase region, its density would continue to decrease, thereby increasing the volume of the vapor portion.

Kennard (55) has analyzed the dynamics of what he has called breaking fronts: i.e., the interface between an intimately mixed two phase region and a homogeneous compressible liquid. He found that such fronts could advance or recede only at velocities equal to or higher than the velocity of sound in the medium. If the

liquid cavitates at vapor pressure, such a breaking front will develop when the bubble reopens, and the "interior" region will consist of an intimately mixed two phase region in which each liquid particle will continue to translate outward at a constant velocity. This situation probably would continue until the outer regions of fluid are decelerated to a lower velocity, and many of the individual particles in the froth catch up with the slower moving solid liquid.

On the other hand, there is evidence to show that liquids can stand considerable tensions for short periods of time, depending principally on the state of denucleation. In steady state oscillation, Briggs and his associates (33) found that tensions of the order of 5 Atm. could be sustained. Harvey (38) estimated that tensions of the order of 100 Atm. had been achieved with his "leaky piston" experiments.

Supposing that the liquid can sustain a moderate tension, a pressure gradient is then available from the bubble wall outward to accelerate the particles which have been virtually stagnated against or near the impact surface. The tension due to divergence of the flow is felt first and most severely at the inner boundary of the liquid. Rupture then occurs at the surface of the immovable barrier, and the pressure against the vapor-

liquid interface rises immediately to the vapor pressure corresponding to the temperature of the liquid. A gradient therefore exists from the vapor pressure down into tension of the liquid, which can accelerate the particles in the neighborhood of the bubble wall, producing a velocity distribution like the incompressible case.

The tension wave mentioned originates at the barrier surface and propagates outward at the velocity of sound, the locus of points in the X, Z plane dropping to vapor pressure being the same as the case previously discussed, and shown by the dashed line in Figure 23. It is to be noted then that a maximum tension must exist somewhere between the point in the fluid which has just been reduced to vapor pressure, and the new bubble surface which is moving outward. If this maximum tension should happen to be strong enough to rupture the liquid at a nucleus or weak spot a small distance from the new cavity wall, a secondary cavity could begin to form.

It is seen, therefore, that the ability of the liquid to withstand tensions for short time pulses is very important in determining the mode of reopening. If the liquid has high rupture resistance, the bubble formed on rebound should be clearly defined. If the liquid has very low rupture resistance, the cavity should consist of a frothy, intimately mixed two phase region of vapor and

liquid particles.

It seems likely that, for the tension wave durations of about a few microseconds being considered, ordinary liquids would exhibit a considerable ability to sustain tension. However, it would likewise be expected that numerous nuclei of solid particles and gas pockets of submicroscopic size would also exist in the liquid around the bubble wall. These would be incapable of supporting tension, in contrast to the strength of the homogeneous liquid. Therefore numerous small secondary ruptures might be expected in addition to a primary opening.

These conclusions would seem to be verified by examination of the photographic bubble histories due to Knapp and Hollander (19). The original bubble is a cleanly defined near-sphere seated against the model surface and it collapses to a point apparently just clear of that surface. The reopening, which occurs almost instantaneously, is of quite different character. The new cavity is quite irregular, and at first looks opaque, like a cloud of tiny cavities. As it grows larger, it looks more like a cluster of merged bubbles, perhaps a dozen in number. This appearance is retained through its growth to maximum size and until the second collapse occurs.

The dynamics of such a system is, of course,

extremely complicated, but an estimate has been made of the maximum size in the next section by means of energy considerations.

d. Radiated Energy in Shock Wave

One process which is a source of energy dissipation is radiation. It has been shown that energy is transported inward as long as the pressure against the bubble surface remains at vapor pressure. However, when impact against an incompressible core produces an extreme pressure against the inner boundary of the liquid, radiation can be expected to occur.

It should be noted that the selection of a core equal to $0.10\ R_o$ means that 99.9% of the work available from the pressure at infinity during complete collapse has already been obtained. Therefore the energy of fluid motion will be considered the same as the complete collapse.

The fluid motion which occurred behind the shock wave formed by the impact against the immovable barrier was essentially one of pressure relief. The dropping pressure resulted in a volumetric expansion of the liquid, causing outward radial velocities to accumulate to a maximum just behind the shock wave.

The time history of the pressure against the

barrier was shown in Figure 25, where Z 0.61 is the time at which the pressure returned to the liquid vapor pressure. Therefore, the total impulse per unit area of the barrier, which is available to create outward momentum, has been developed. That is to say, the only external force on the liquid capable of producing the outward momentum necessary to reopen the bubble is the pressure acting at the barrier from $Z = 0$ to $Z = 0.61$. After this time, the impulse is in the opposite direction due to $P_\infty - P_V$ acting to retard outward momentum.

In other words, once the bubble has started to reopen, a redistribution of pressures between the bubble wall and infinity could not increase the outward momentum which is available to reopen the bubble. Therefore, it has been assumed that the energy which remains in the form of compression of the liquid is carried away by the shock wave, and the kinetic energy of the outward moving particles is devoted to the work of reopening the bubble.

The pressure energy per unit radius between the core at $X = 0.10$ and the shock wave at $X = 0.54$ has been plotted as a function of radius in Figure 26. Because the surface area of a shell at a given radius is proportional to X^2, in addition to the facts that the pressure increases as X increases, and energy per unit volume is approximately proportional to P^2, the energy

per unit radius appears similar to a fifth power curve. Thus most of the pressure energy associated with the shock wave is concentrated in a comparatively narrow band immediately behind it. The figure shows that only 10% of the pressure energy is found between $X = 0.10$ and $X = 0.39$, whereas the remaining 90% is between $X = 0.39$ and $X = 0.54$. It is difficult to imagine any mechanism which could capture this pressure energy and utilize it to reopen the bubble.

When the pressure energy associated with this outgoing shock wave is evaluated, it is found to be equal to 47% of the total energy available by the work of the pressure difference $P_\infty - P_v$ during collapse. The remaining 53% of the available energy is assumed to be devoted to reopening the cavity, complex though it may be. The equivalent spherical cavity would therefore be 81% of the diameter of the original bubble.

This value is seen to be of the same order as the relative rebound sizes taken from data published by Knapp and Hollander (19). In that case, the relative diameter was 86% for the first rebound and 78% for the second. Later rebounds were smaller, but one would expect the greater turbulence of collapse with a cluster-like cavity to result in greater losses from viscous forces. It should be noted that the measurement of the diameter of

an irregular cavity is difficult, requires considerable judgment, and therefore the percentage of reopening quoted is not strictly accurate.

9:5. Conclusions

a. Rebound can occur through the compressibility of the liquid alone, an immovable barrier acting as the agent for producing arrest of inward velocities.

b. Considerable outward velocities are produced by re-expansion of the liquid which is compressed by impact.

c. An outward moving shock wave is formed, carrying considerable energy away.

d. The outward moving shock is followed by a tension wave, which is responsible for the reopening of the cavity. The tension produced is the greatest at the inner boundary of the liquid until the cavity re-opens.

e. The tension wave is responsible for a varying degree of secondary rupture to the liquid at points near the center of the new primary cavity, These secondary ruptures are responsible for the fact that the rebound cavity is no longer a cleanly defined portion of a sphere.

f. The energy radiated by the shock wave is estimated to be 47% of the energy of collapse, which would allow the cavity to re-open to an equivalent diameter

81% of the original diameter before collapse.

g. Time during which the cavity is completely closed is found to be of the order of one microsecond or less.

References

(1) Ackeret, J. — Experimentelle und Theoretische Untersuchungen uber Hohlraumbildung im Wasser. E.T.H. Zurich (1930).

(2) Thoma, D. — Die Kavitation bei Wasser Turbinen. Hydraulische Probleme V.D.I. Verlag (1926).

(3) Plesset, M. — Dynamics of Cavitation Bubbles. Hydrodynamics Laboratory Publication No. 70., Calif. Inst. of Tech., Pasadena, Calif.

(4) Nowotny, H. — Werkstoffzerstorung durch Kavitation. V.D.I. Verlag Berlin (1942). Reprinted by J. W. Edwards, Ann Arbor, Michigan

(5) Raven, Feiler, & Jespersen. — An annotated Bibliography of Cavitation. David Taylor Model Basin Report No. R-81.

(6) Parsons and Cook. — Investigation into the Causes of Corrosion or Erosion of Propellers. Engineering Vol. 107 (1919) p. 515.

(7) Lord Rayleigh — The Pressure developed in a Liquid during the Collapse of a spherical Cavity. Philosophical Mag. Vol. 34. (1917) p. 34.

(8) Petracchi, G. — Intorno all'interpretazione del processo di corrosione per cavitazione. La metallurgia italiana, No. 1. (1949) p. 1.

(9) Fottinger, H. — Untersuchungen uber Kavitation und Korrosion bei Turbinen, Turbopumpen, und Propellern. Hydraulische Probleme, V.D.I. Verlag (1926).

(10) Boetcher, H. — Failure of Metals due to Cavitation under Experimental Conditions. Transactions ASME Vol. 58 (1936). p. 355.

(11) Vater, M. — Das Verhalten Metallischer Werkstoffe bei Beanspruchunge durch Flussigkeitschlage. Zeitschrift V,D.I. Vol. 81 (1937).

(12) Mousson, J. — Pitting Resistance of Metals under Cavitation Conditions. Transactions ASME Vol. 59 (1937) p. 399.

(13) Schroter, H. — Werkstoffe Zerstorung bei Kavitation. Zeitschrift V.D.I. Vol. 78 (1934) p. 349.

(14) Schroter, H. — Metallographische Untersuchung zur Frage der Kavitationszerstorung. Zeitschrift V.D.I. Vol. 78 (1934) p. 1161

(15) Schroter, H. — Versuche uber Werkstoff Anfressung durch Kavitation. Zeitschrift V.D.I. Vol. 80 (1936) p. 479.

(16) de Haller, P. — Untersuchungen uber die Kavitation hervorgerufenden Korrosion. Schweizerische Bauzeitung Bd. 101 (1933) p. 274.

(17) Hunsaker, J. — Cavitation Research. Mechanical Engineering Vol. 57(1935) p 211

(18) Hunsaker, J. — Progress Report on Cavitation. Transactions ASME Vol. 57 (1935) p. 423.

(19) Knapp, R. & Hollander, A. — Laboratory Investigations of the Mechanism of Cavitation. Transactions ASME Vol. 70 (1948) p 419

(20) Honegger, E. — Ueber Erosionsversuche. Brown Boveri Co, Mitteilungen Vol. 14 (1927) p. 95

(21) Ackeret, J. & de Haller, P. — Ueber die Zerstorung von Werkstoffen durch Tropfenschlag und Kavitation. Schweizer Bauzeitung. Vol. 108 (1936) p. 105.

(22)	Schwartz and Mantel.	Die Zerstorung metallischer Werkstoffen durch Wasserschlag. Korrosion und Metalschutz Vol. 13(1937). Zeitschrift V.D.I. Vol. 80 (1936) p. 863.
(23)	Soderberg, C.	Turbine Blade Erosion. Electric Journal Vol. 31 (1935) p. 533.
(24)	Schumb, Peters, & Milligan.	A New Method for Studying Cavitation Erosion. Metals and Alloys. Vol. 8. (1937) p. 126.
(25)	Gaines.	A Magnetostriction Oscillator producing Intense Audible Sound. Physics Vol. 3 (1932) p. 209.
(26)	Rightmire, B.	M.I.T. Engineering Department Thesis. (1941).
(27)	Kornfeld and Suvarov.	On the Destructive Action of Cavitation. Journal of Applied Physics, Vol 15 (1944) p. 495.
(28)	Van Iterson.	Cavitation et Tension Superficielle. Koniklijke Akad. van Wetenshappen te Amsterdam. Vol. 39 (1936), p. 138 & 330. Abstract. Engineering Vol. 142 (1936) p. 95.
(29)	Stepanoff, A.	Cavitation in Pumps. Transations ASME Vol 67 (1947) p. 539.
(30)	Poulter, T.	Mechanism of Cavitation Erosion. Transactions ASME Vol. 64(1942) p. A-31. Discussion p. A-192.
(31)	Osborne, M.	The Shock produced by a Collapsing Cavity in Water. Transactions ASME Vol. 69(1947) p. 253.
(32)	Kerr, S. L.	Determ nation of Relative Resistance to Cavitation Erosion by Vibratory Method. Transactions ASME Vol. 59 (1937) p. 373.
(33)	Briggs, Johnson & Mason.	Properties of Liquids at High Sound Pressures. Journal of Acoustic Society of America. Vol. 19 (1947) p. 664.

(34)	Rouse, H.	Cavitation and Pressure Distribution. State University of Iowa, Studies in Engineering. Bulletin 32.
(35)	Tsien, H.	On the Design of the Contraction Cone for a Wind Tunnel. Journal of Aeronautical Sciences. Vol 10 (1943) pp. 68-70.
(36)	Bottomley, W.	Erosion due to Incipient Cavitation. Institute of Engineers and Shipbuilders (1948) p. 297.
(37)	Rouse, H.	Fluid Mechanics for Hydraulic Engineers. Engineering Societies Monographs. McGraw-Hill Co. (1938) P. 47.
(38)	Harvey, McElroy & Whiteley.	On Cavity Formation in Water. Journal of Applied Physics, Vol. 18 (1947) p. 162
(39)	Pease & Blinks	Cavitation from Solid Surfaces in the Absence of Gas Nuclei. Journal of Physical and Colloidal Chemistry. Vol. 51 (1947) p. 556.
(40)	Gardner, O.	The Erosion of Steam Turbine Blades. Engineer, London. Vol. 153 p. 146, 174, and 202. (1932)
(41)	Cook, S.	Erosion by Water Hammer. Proceedings of the Royal Society, London. Vol. A 119 (1928) p. 481.
(42)	Beeching	Resistance to Cavitation Erosion. Institution of Engineers and Shipbuilders in Scotland. Vol. 85 (1941-42) p. 210
(43)	Lord Rayleigh	Theory of Sound. Dover Publications, New York (1945) Vol. II, p. 109.

(44)	Cole.	Underwater Explosions. Princeton, Press, (1948).
(45)	Herring, C.	Theory of Pulsations of the Gas Bubble Produced by an Underwater Explosion. NDRC Report C4-sr20-010, October 1941.
(46)	Oza, H.	On the Collapse of a Hemispherical Cavity seated on a Surface. Transactions ASME Vol. ~~67 (1945)~~ 69. 1947 p. A-39.
(47)	Courant, R. & others.	Shock Wave Manual. NYU Applied Mathematics Panel.
(48)	Courant, R. & Friedrichs, K.	Supersonic Flow and Shock Waves. Interscience Publishers, Knc. New York, (1948).
(49)	de Haller, P.	The Application of a Graphic Method to some Dynamic Problems in Gases. Sulzer Technical Review, No. 1. (1945).
(50)	Kirkwood and Brinkley.	Theory of Propagation of Shock Wave. Physical Review, Vol. 71 (1947)
(51)	Penney and Dasjupta	British Report RC-333. Mentioned in Cole(44) p. 43 & 140.
(52)	Dorsey	Properties of Ordinary Water Substance. Reinhold Publishing Co.
(53)	Kirkwood and Bethe.	Basic Propagation Theory. Wartime OSRK 588(1942).
(54)	Silver, P.	Theory of Stress due to Collapse of Vapor Bubbles in Water. Engineering, Vol (1942) p. 501.
(55)	Kennard.	Cavitation in an Elastic Liquid. Physical Review, Vol. 63, p. 172.

APPENDIX I

Definitions of the Symbols used.

SYMBOL	DEFINITION
a	Velocity of sound in the liquid.
a_o	Velocity of sound in the liquid at 1 Atm. pressure.
$A = a/a_o$	Dimensionless velocity of sound.
b	Radius of liquid sphere which is condensed from the vapor in the bubble.
B	Pressure constant in Tait's equation of state for water. Specifically defined in two equations as the Universal gas constant.
C	Constant in Tait's equation of state for Water.
D	Thermal diffusivity in water.
e	Specific energy due to pressure.
f	Symbol for a function.
j.	Rate of Mass transfer between liquid and vapor at equilibrium conditions.
m	Gas proportion index.
M	Molal mass of vapor
n	A number or an exponent.
P	Pressure, used according to subscript.
p	Pressure appearing as variable of integration.
$Q = R/R_o$	Dimensionless bubble wall position, radius.
R	Bubble wall position, radius.
r	radius coordinate.
R_o	Original or maximum size of the bubble.
t	Time.

SYMBOL	DEFINITION
T	Absolute temperature.
u	Velocity.
$U = u/a_o$	Dimensionless Velocity.
v	Specific volume.
V	Total volume.
x	Space or lineal dimension.
$X = r/R_o$	Dimensionless radius coordinate.
$Z = a_o t/R_o$	Dimensionless time.
α	Normal coordinate of plus characteristic.
β	Normal coordinate of minus characteristic.
γ	Exponent of Tait's equation of state for water.
δ	Thickness of liquid layer through which temperature gradient exists.
$\nabla\theta$	Temperature gradient (vector notation).
$\int$	A parameter.
θ	Temperature rise.
ξ	Shock wave position.
$\Xi = \xi/R_o$	Dimensionless shock wave position.
ρ	Density of the liquid.
ρ_v	Density of the vapor.
τ	Total time of collapse

Note: a dot ($\dot{}$) immediately above a symbol denotes differentiation with respect to time, either dimensional or dimensionless according to the particular case.

FIGURE 1

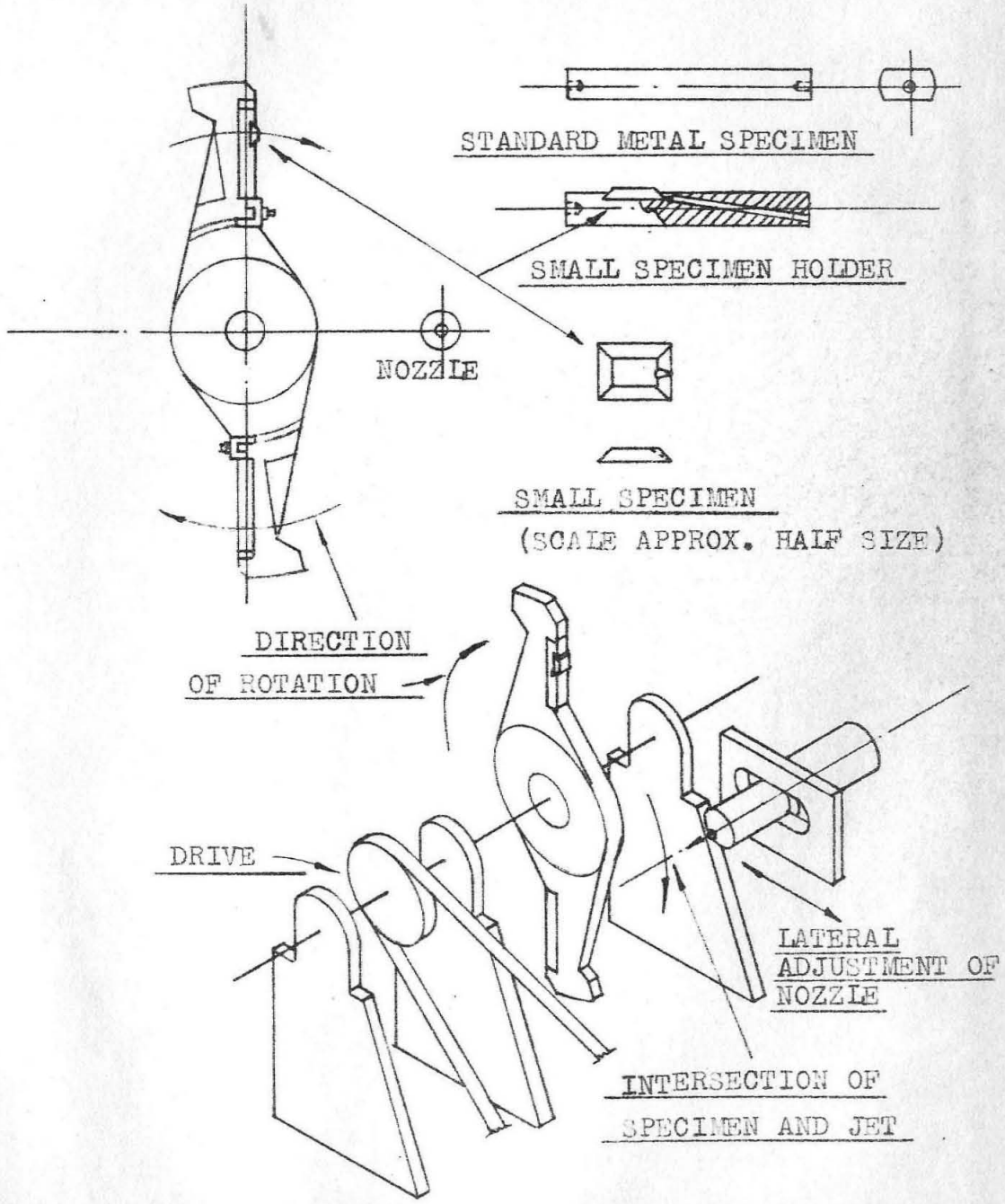

REPRODUCED FROM REFERENCE (22)

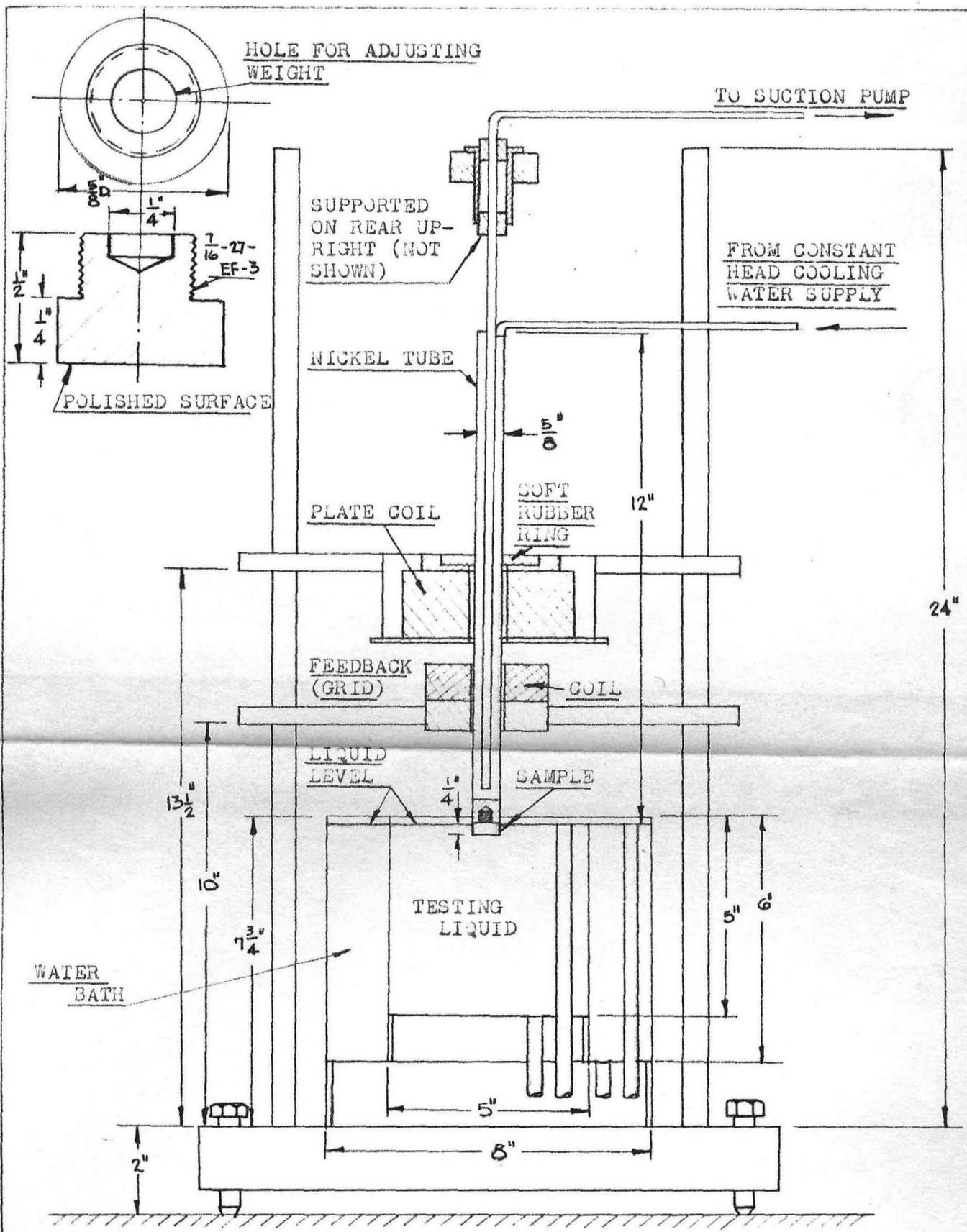

VIBRATORY-TYPE CAVITATION-TESTING APPARATUS

REPRODUCED FROM ASME TRANSACTIONS, VOL. 57
1937 PAGE 374

GJB 4-25-49

FIGURE 2

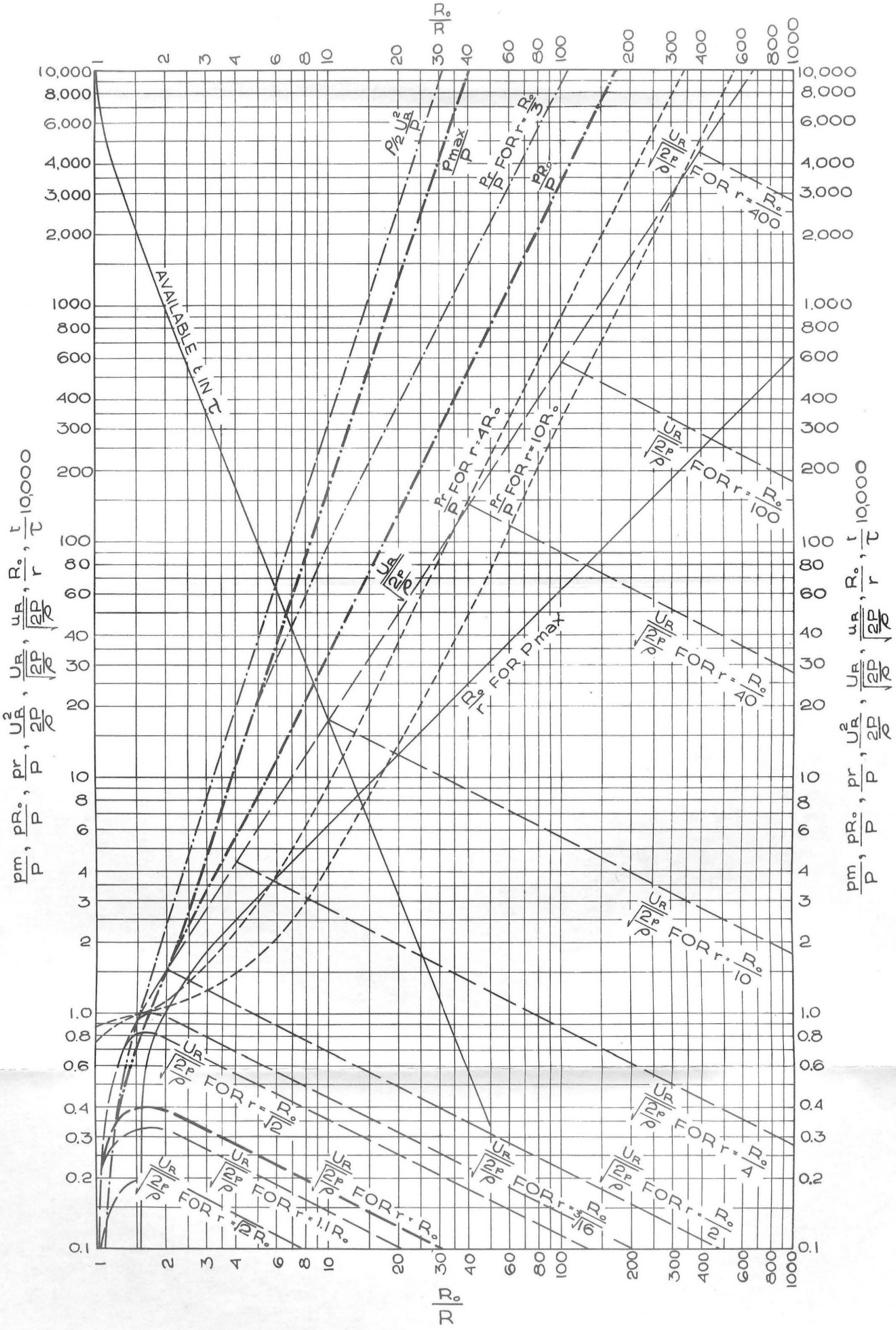
AVAILABLE t IN τ
P/2 U_R²/P
Pmax/P
Pr/P FOR r = R₀/3
PR₀/P
Pr/P FOR r = 4R₀
Pr/P FOR r = 10R₀
U_R/√2P/ρ
U_R/√2P/ρ FOR r = R₀/√2
U_R/√2P/ρ FOR r = 1.1R₀
U_R/√2P/ρ FOR r = √2R₀
U_R/√2P/ρ FOR r = R₀
U_R/√2P/ρ FOR r = 3/√16 R₀
U_R/√2P/ρ FOR r = 4/12 R₀
U_R/√2P/ρ FOR r = 4/10 R₀
U_R/√2P/ρ FOR r = 10/R₀
U_R/√2P/ρ FOR r = 400/R₀
R₀/r FOR Pmax
pm/P, pR₀/P, pr/P, U_R²/2P/ρ, R₀/r, t/τ 10,000
R₀/R

FIGURE 3.

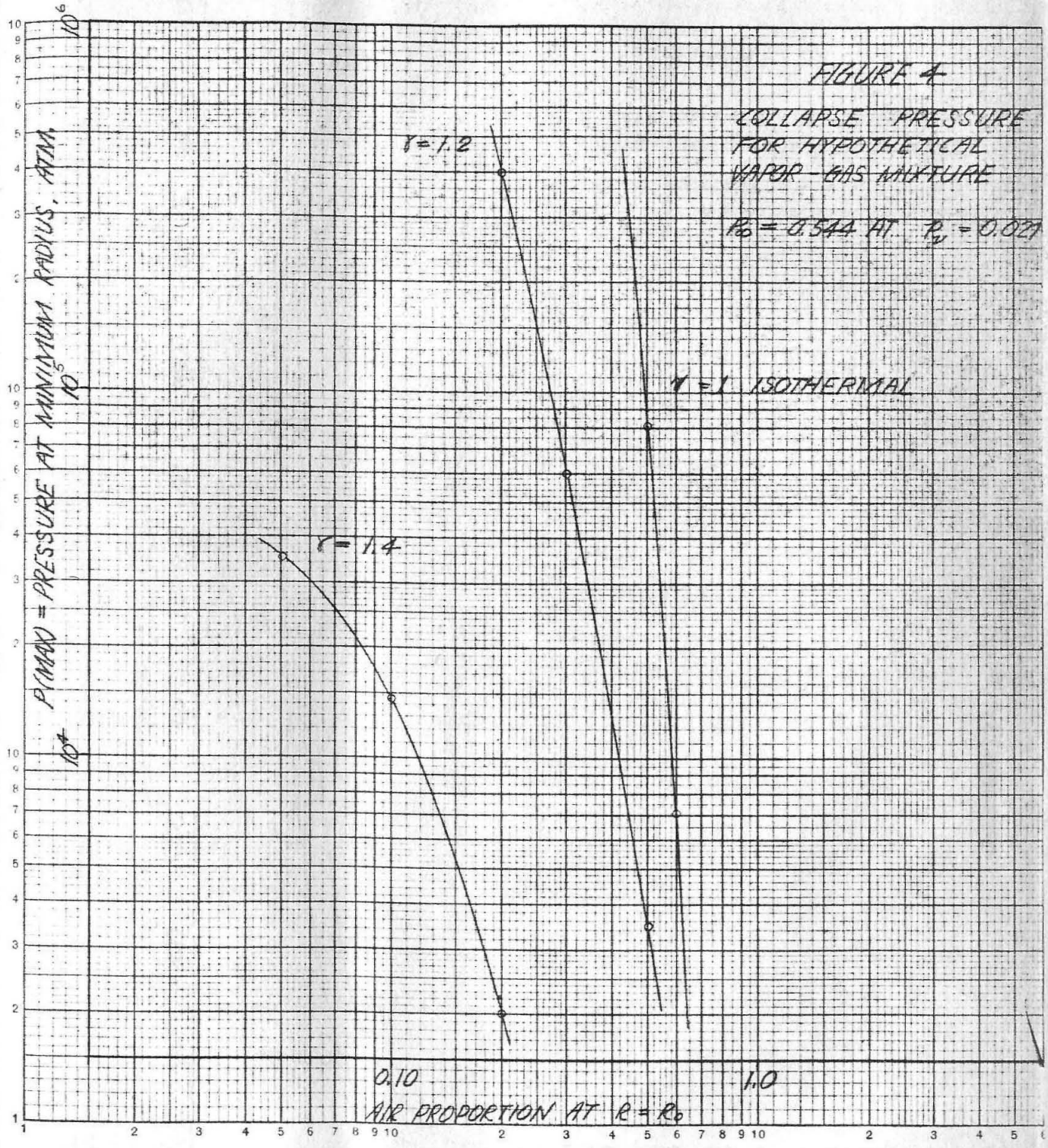
FIGURE 4
COLLAPSE PRESSURE FOR HYPOTHETICAL VAPOR-GAS MIXTURE
R_0 = 0.544 AT P_v = 0.021
γ = 1.2
γ = 1 ISOTHERMAL
γ = 1.4
P(MAX) = PRESSURE AT MINIMUM RADIUS, ATM
AIR PROPORTION AT R = R_0
0.10
1.0

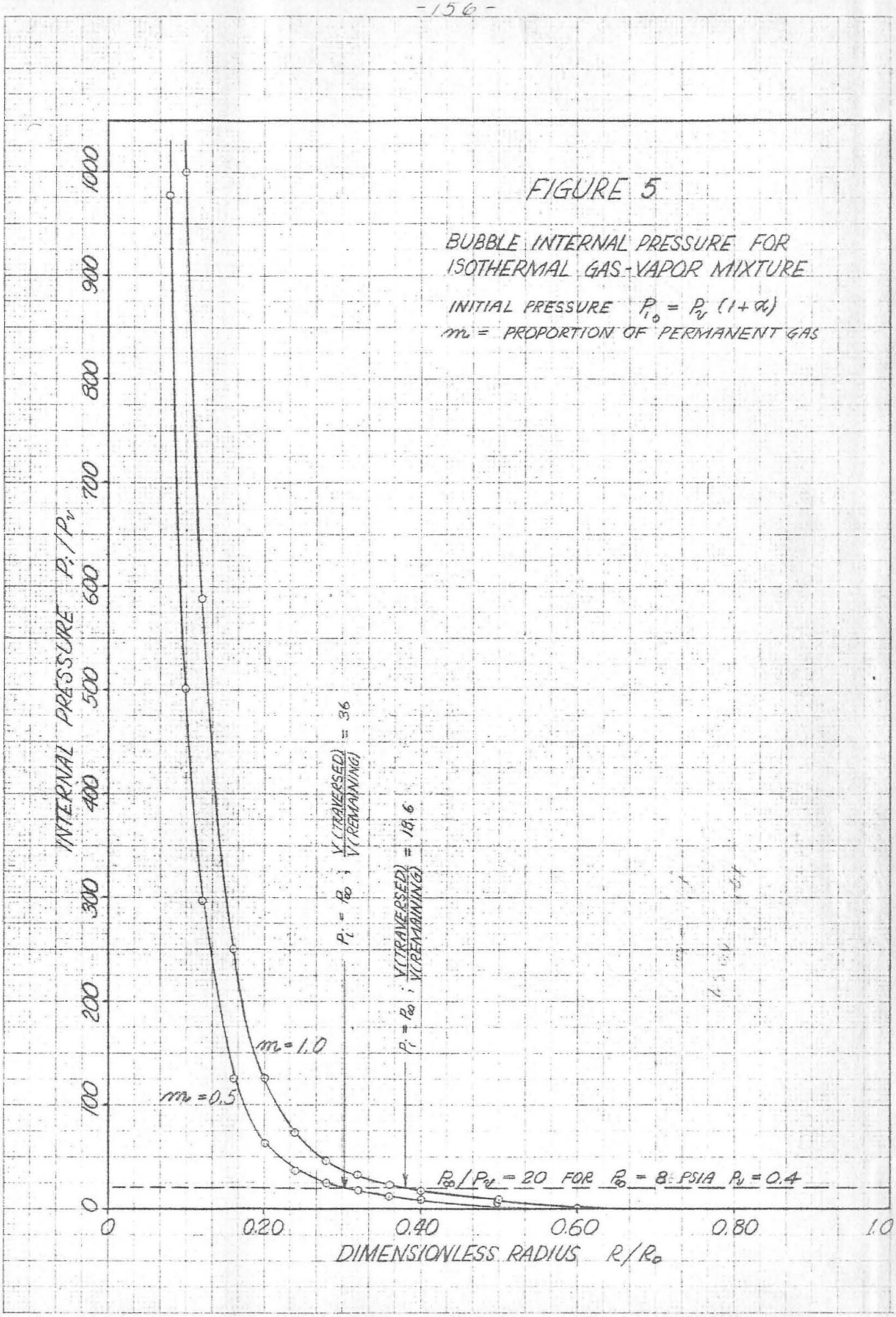
FIGURE 5
BUBBLE INTERNAL PRESSURE FOR ISOTHERMAL GAS-VAPOR MIXTURE
INITIAL PRESSURE $P_{i_0} = P_v (1+\alpha)$
m = PROPORTION OF PERMANENT GAS
INTERNAL PRESSURE P_i / P_v
DIMENSIONLESS RADIUS R/R_o
0
100
200
300
400
500
600
700
800
900
1000
0.20
0.40
0.60
0.80
1.0
$m = 1.0$
$m = 0.5$
$P_i = P_{i_0}$; $\frac{V(\text{TRAVERSED})}{V(\text{REMAINING})} = 36$
$P_i = P_{i_0}$; $\frac{V(\text{TRAVERSED})}{V(\text{REMAINING})} = 18.6$
$P_{i_0} / P_v = 20$ FOR $P_{i_0} = 8$ PSIA $P_v = 0.4$

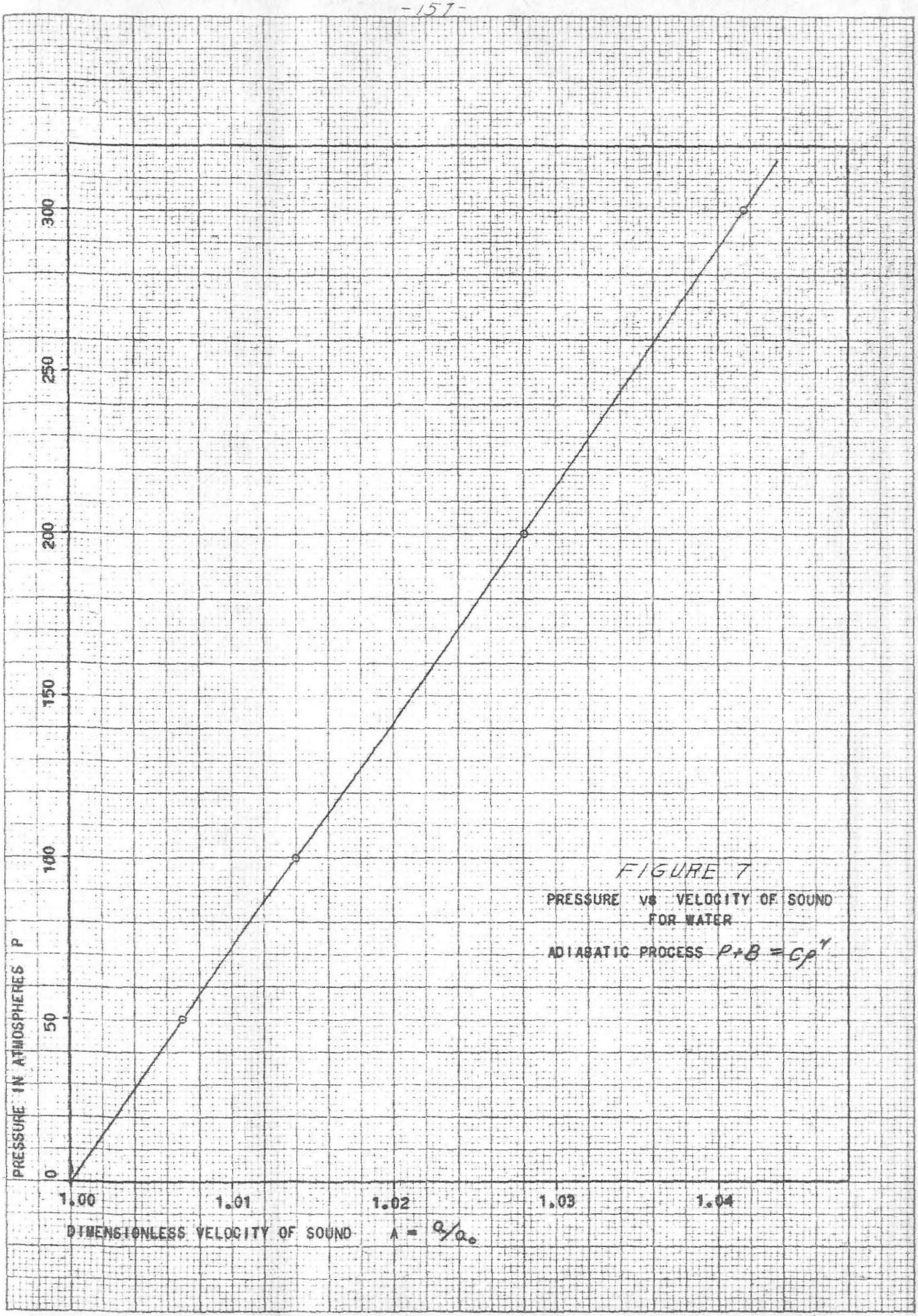

FIGURE 7

PRESSURE vs VELOCITY OF SOUND FOR WATER

ADIABATIC PROCESS $P+B = C\rho^{\gamma}$

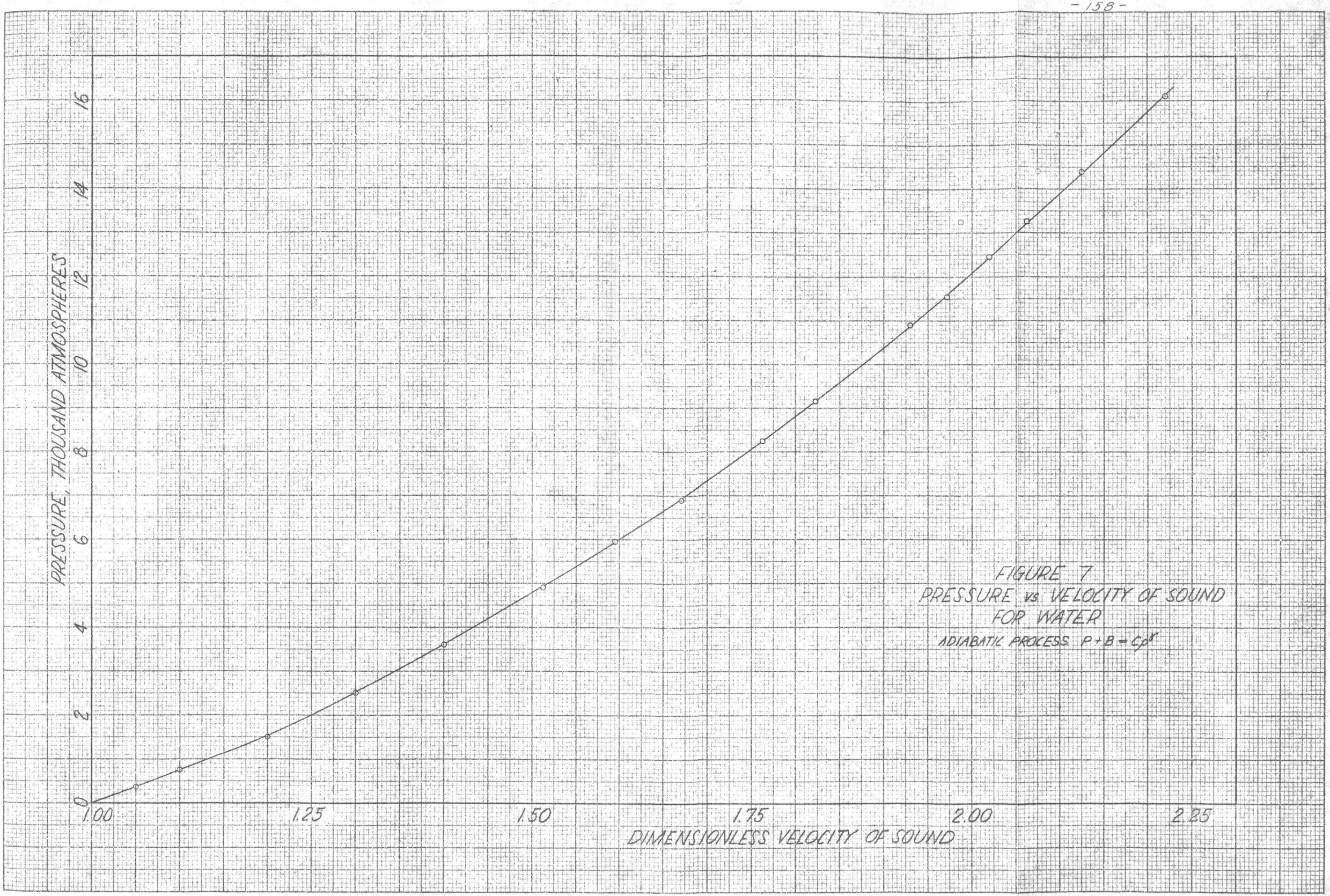

FIGURE 7
PRESSURE vs VELOCITY OF SOUND
FOR WATER
ADIABATIC PROCESS $P + B = Cp^{\gamma}$

FIGURE 8

ENERGY PER UNIT VOLUME vs PRESSURE
ADIABATIC PROCESS $P+B=C\rho^{\gamma}$

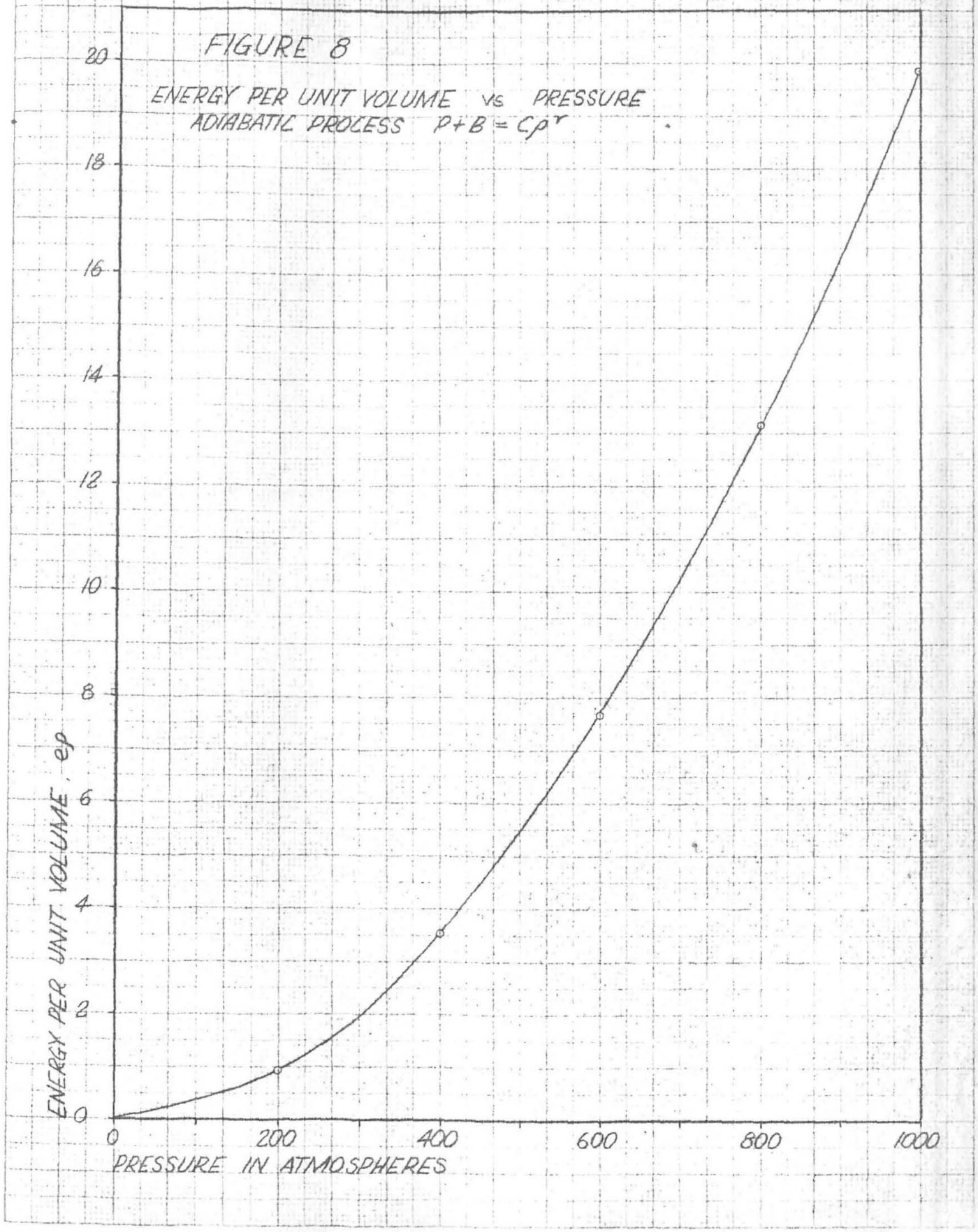

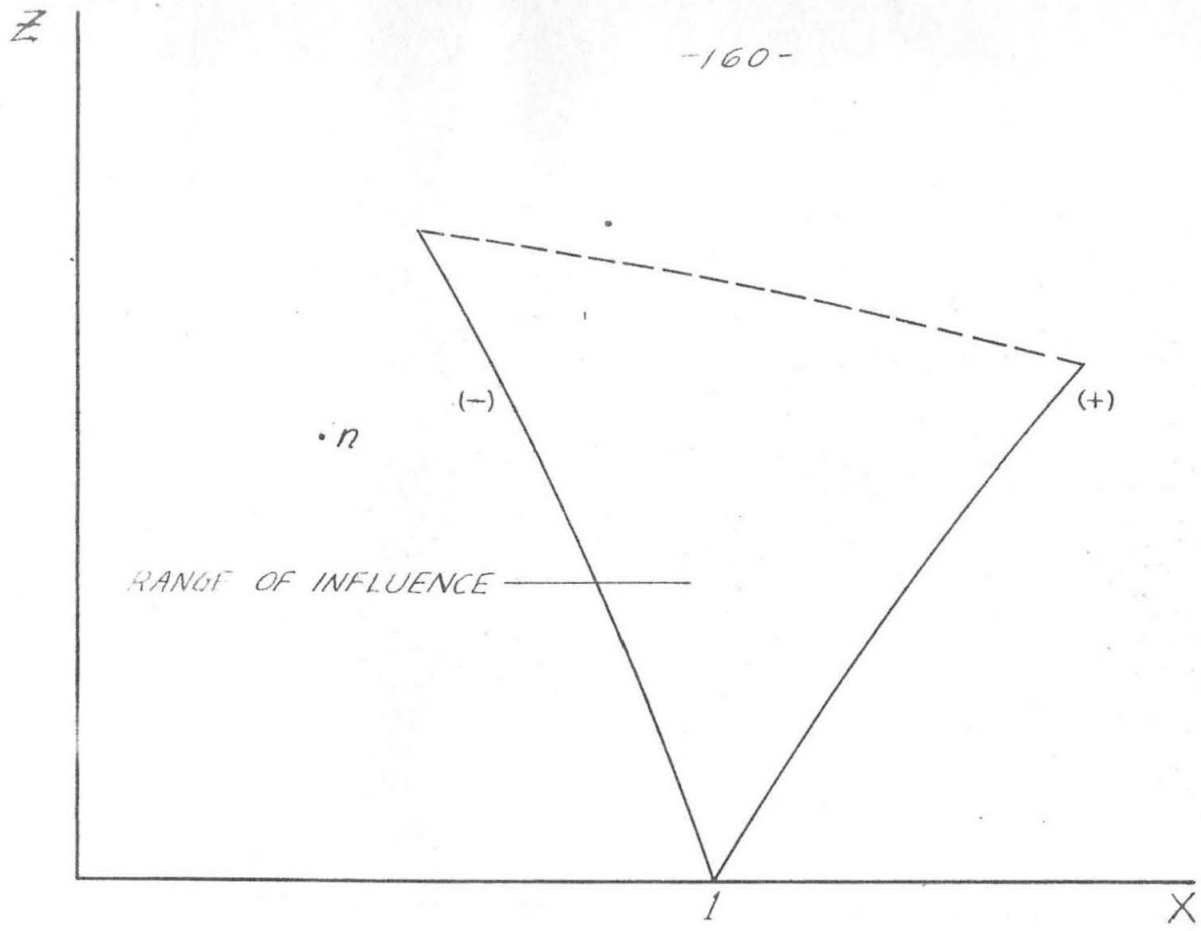

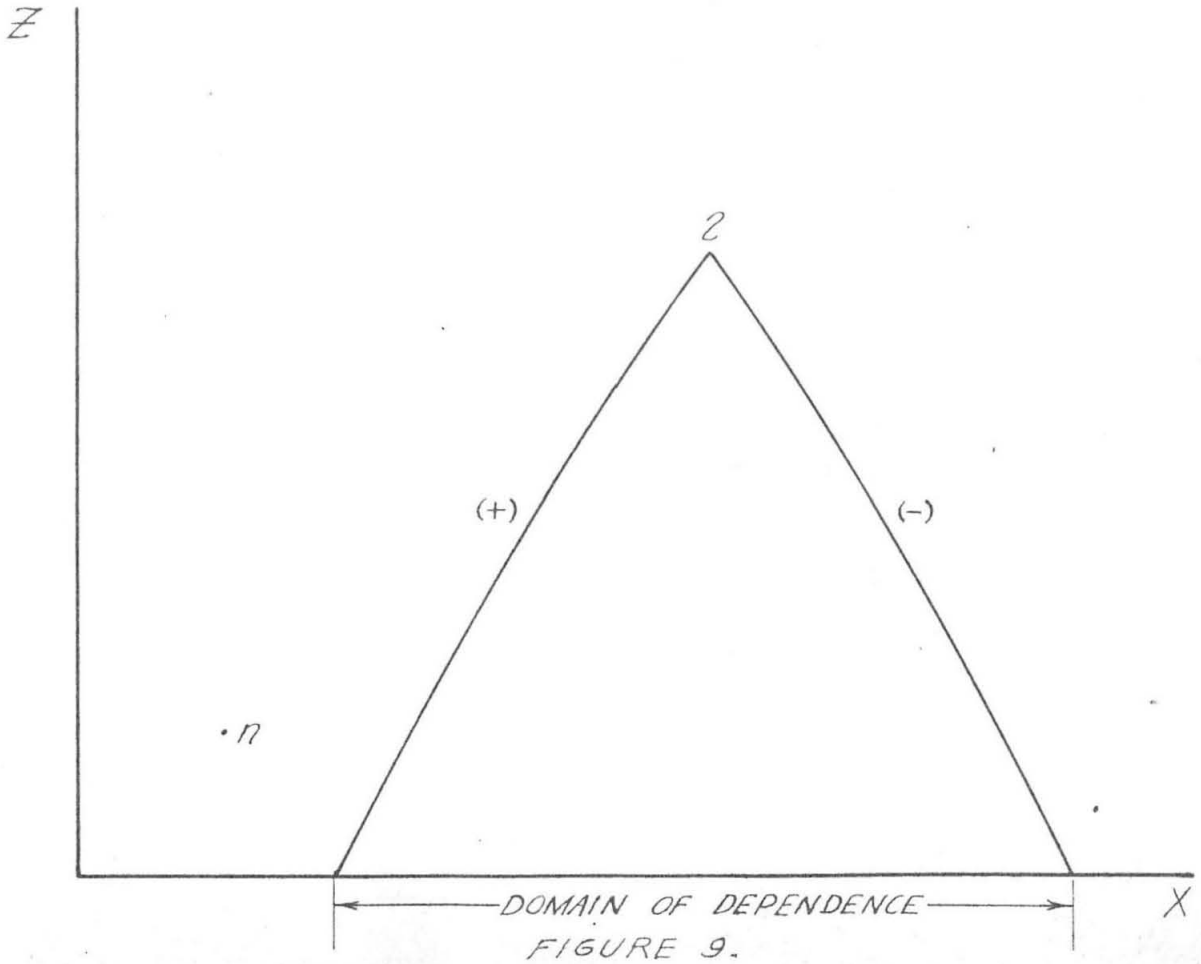

FIGURE 9.

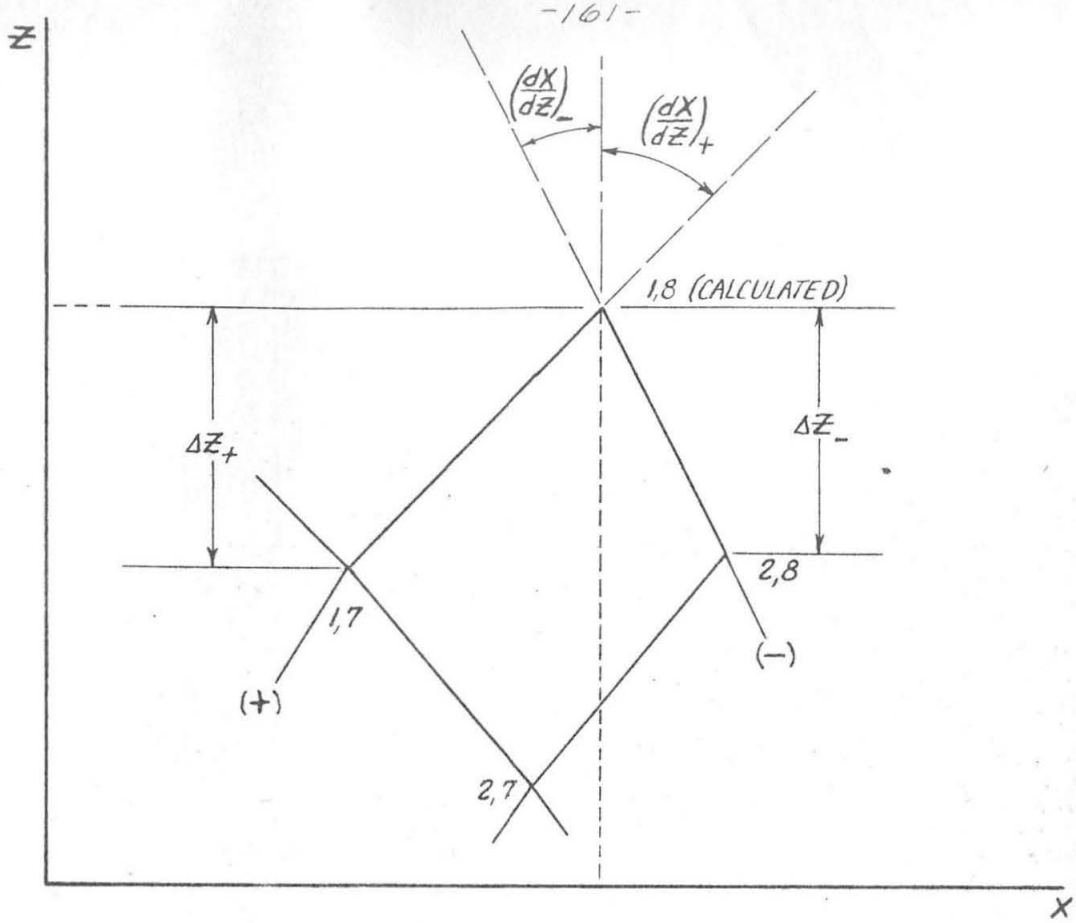

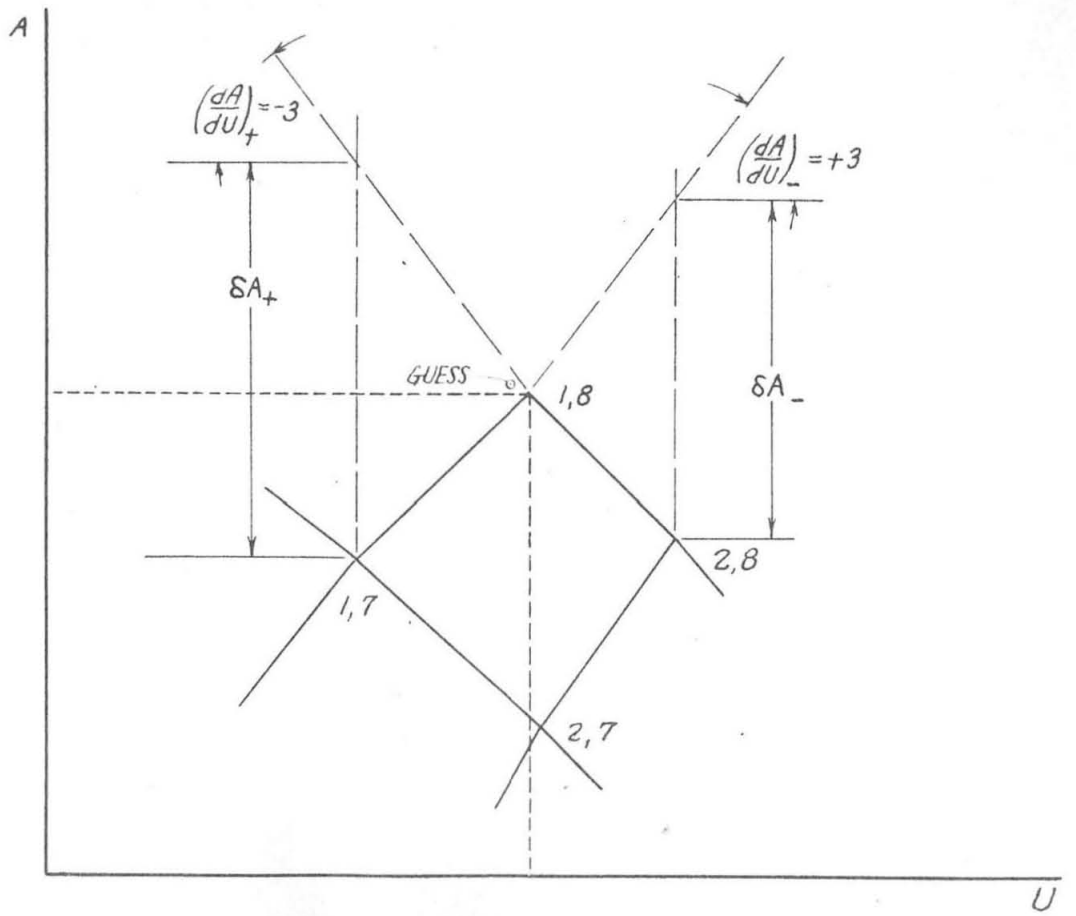

FIGURE 10 METHOD OF CALCULATION

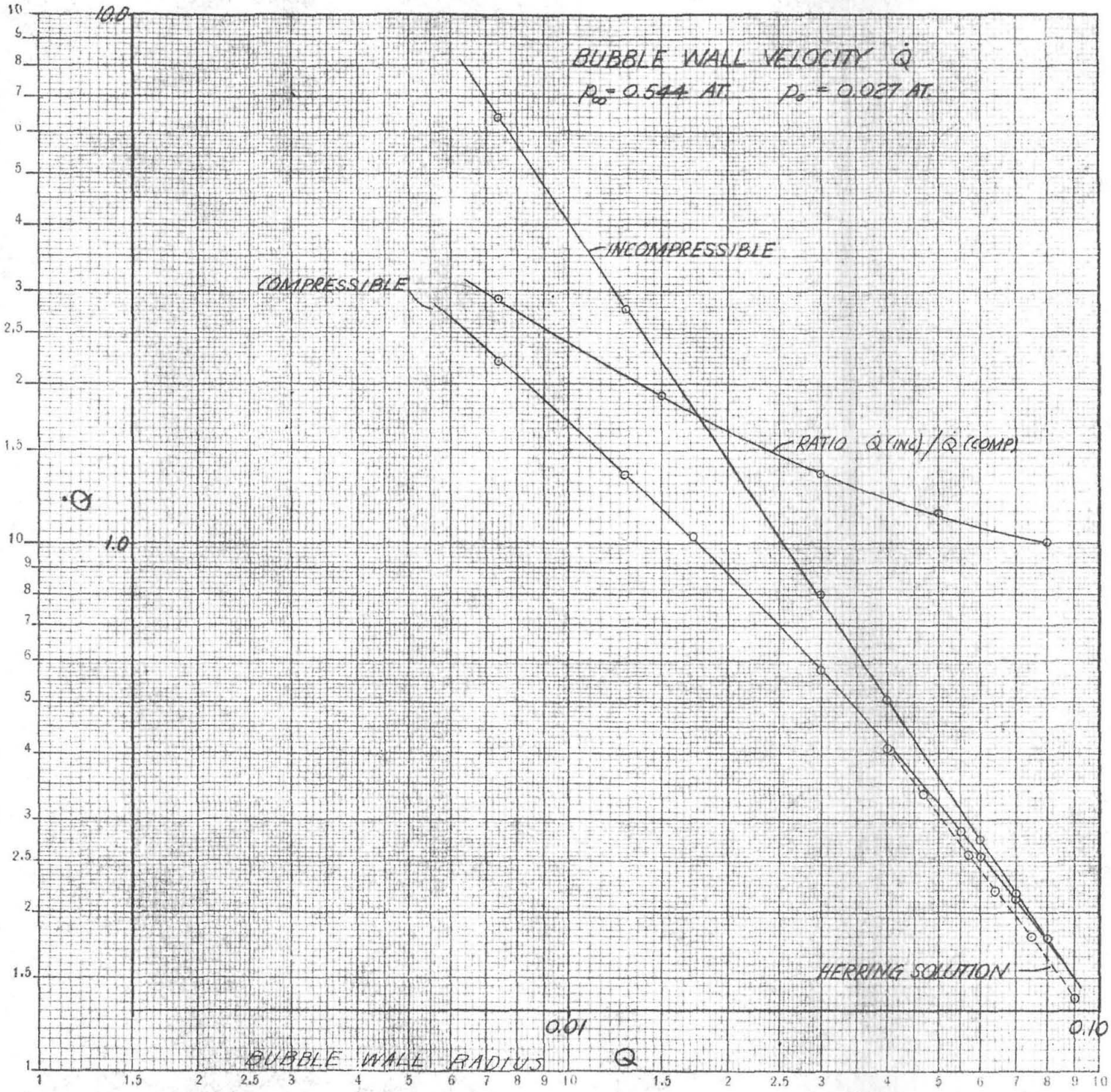
BUBBLE WALL VELOCITY $\dot{Q}$
P_∞ = 0.544 AT. p_v = 0.027 AT.
INCOMPRESSIBLE
COMPRESSIBLE
RATIO $\dot{Q}$(INC) / $\dot{Q}$ (COMP)
HERRING SOLUTION
$\dot{Q}$
10.0
1.0
0.01
0.10
BUBBLE WALL RADIUS Q
KEUFFEL & ESSER CO. N. Y. NO. 359-110
Logarithmic, 2 X 2 Cycles.
MADE IN U.S.A.

FIGURE 12

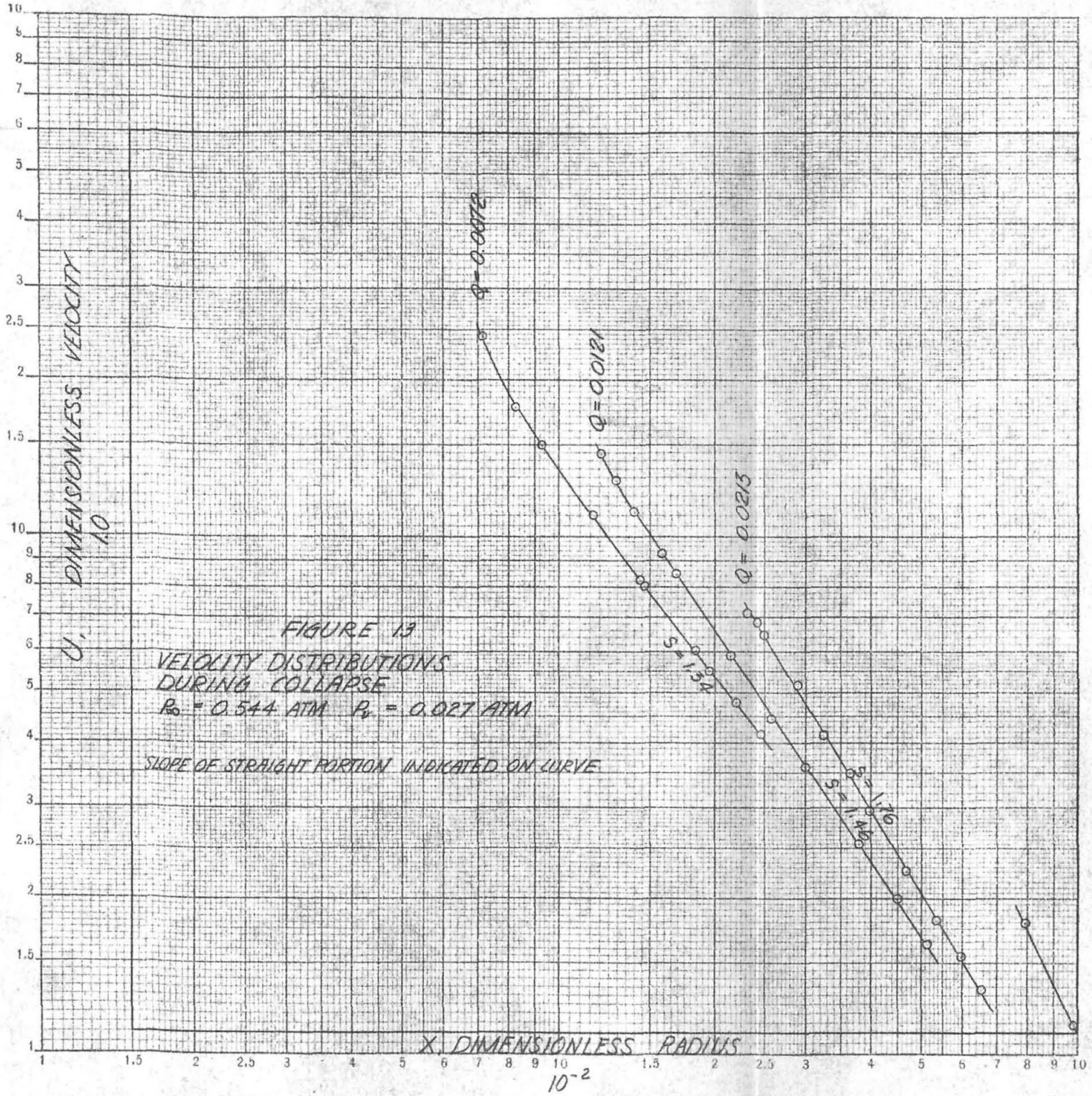

FIGURE 13
VELOCITY DISTRIBUTIONS
DURING COLLAPSE
P_∞ = 0.544 ATM P_v = 0.027 ATM

SLOPE OF STRAIGHT PORTION INDICATED ON CURVE

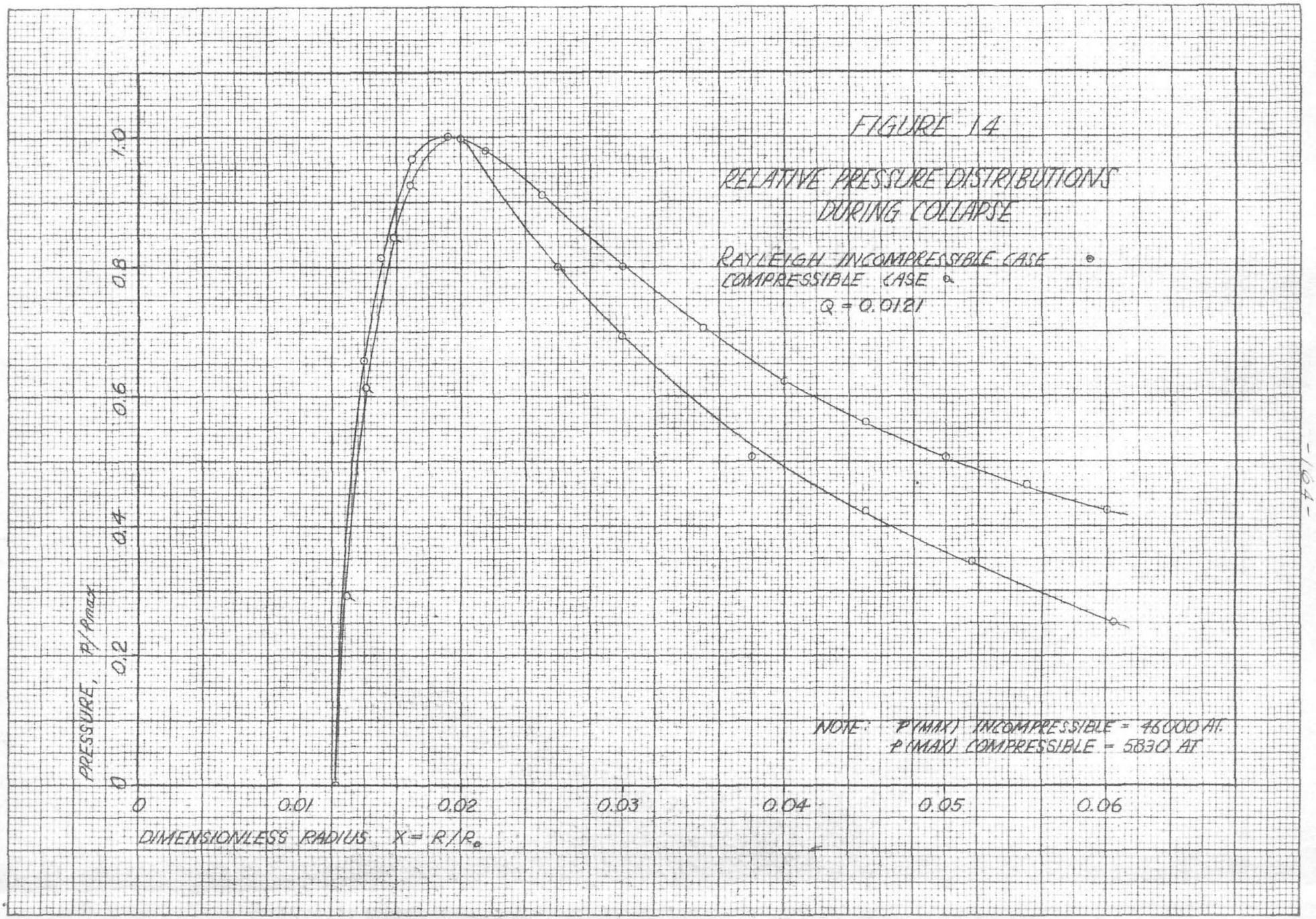
FIGURE 14
RELATIVE PRESSURE DISTRIBUTIONS DURING COLLAPSE
RAYLEIGH INCOMPRESSIBLE CASE
COMPRESSIBLE CASE
Q = 0.0121
NOTE: P(MAX) INCOMPRESSIBLE = 46000 AT.
P(MAX) COMPRESSIBLE = 5830 AT
PRESSURE, P/Pmax
1.0
0.8
0.6
0.4
0.2
0
0
0.01
0.02
0.03
0.04
0.05
0.06
DIMENSIONLESS RADIUS X = R/R0

FIGURE 15

MAXIMUM PRESSURE VS WALL RADIUS

BUBBLE COLLAPSE

P_o = 0.544 ATM ϵ = 0.027 ATM

INCOMPRESSIBLE

COMPRESSIBLE

MAXIMUM PRESSURE, ATM

BUBBLE WALL RADIUS, CM

10^5

10^4

1000

0.001

0.010

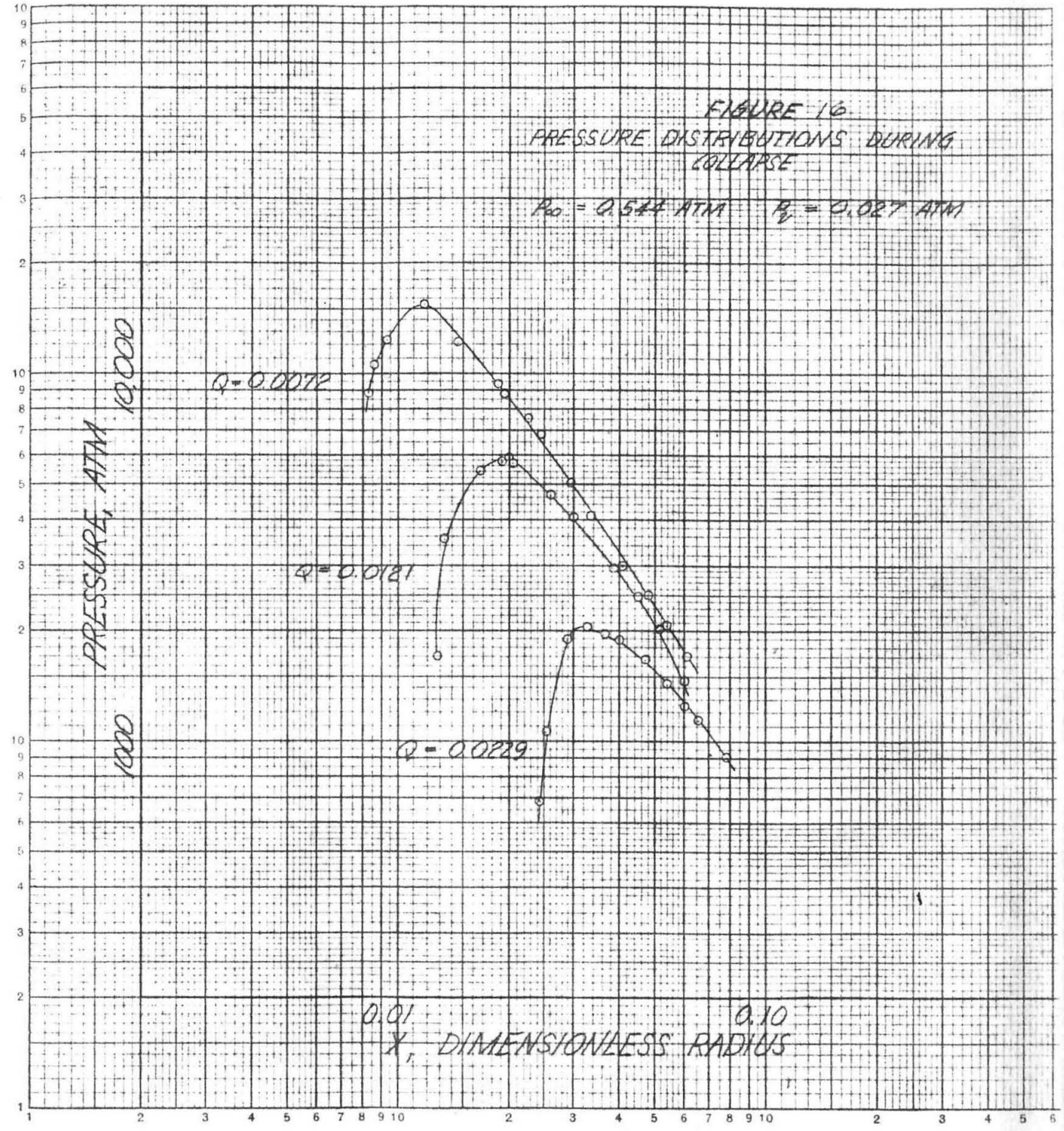
FIGURE 16
PRESSURE DISTRIBUTIONS DURING COLLAPSE
P_{∞} = 0.544 ATM
P_v = 0.027 ATM
Q = 0.0072
Q = 0.0121
Q = 0.0229
PRESSURE, ATM
1000
10000
0.01
0.10
X_r DIMENSIONLESS RADIUS

FIGURE 17
ENERGY DISTRIBUTIONS DURING COLLAPSE

BUBBLE WALL POSITIONS Q = 0.080, 0.023, 0.0074

NOTE: DOTTED LINE SHOWS RADIUS INSIDE WHICH 40% OF AVAILABLE ENERGY IS CONCENTRATED

$$\text{TOTAL ENERGY} = \int_{Q}^{\infty} (e\rho)_{\text{TOTAL}}\, 4\pi X^2\, dX$$

= AREA UNDER CURVE

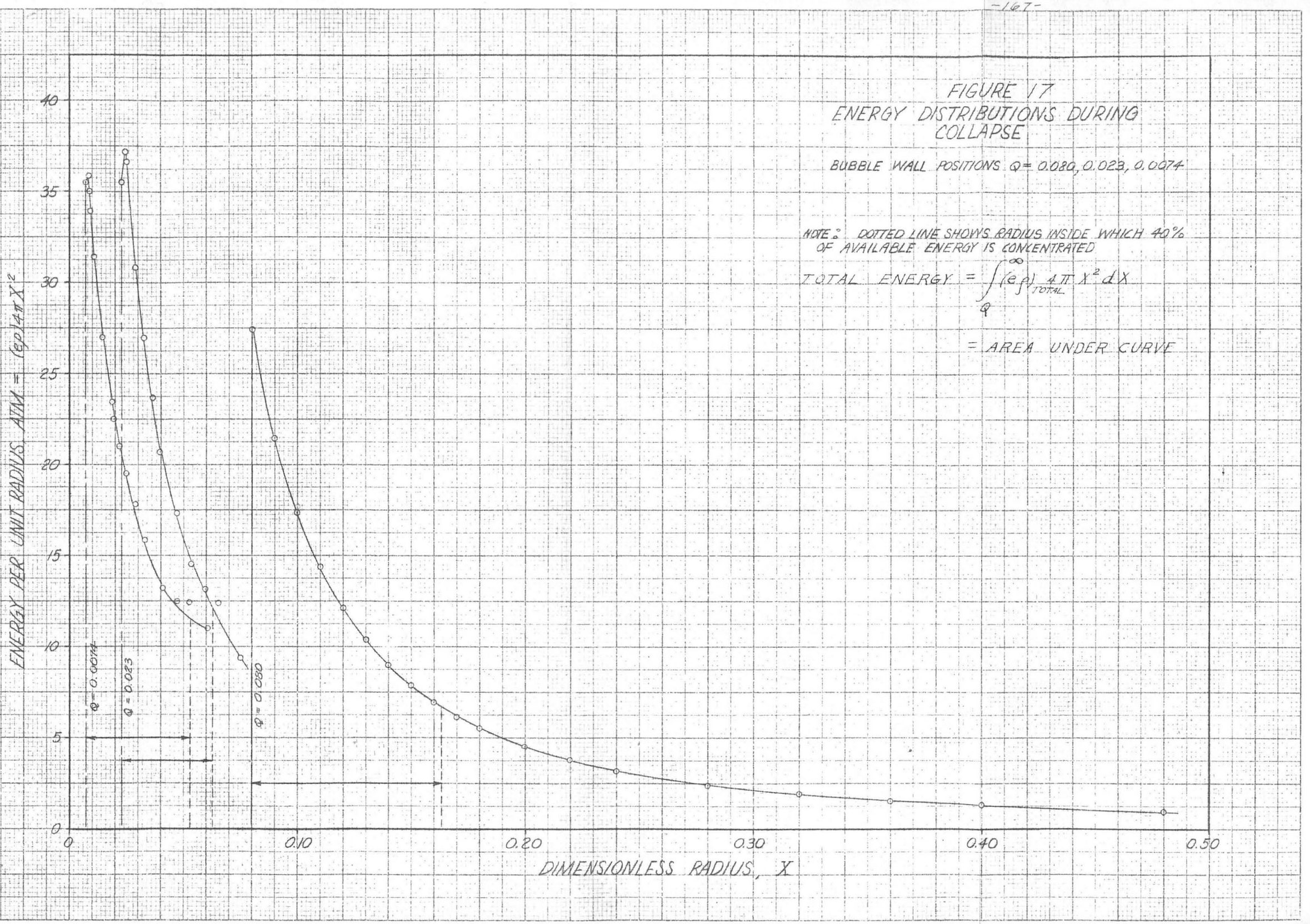

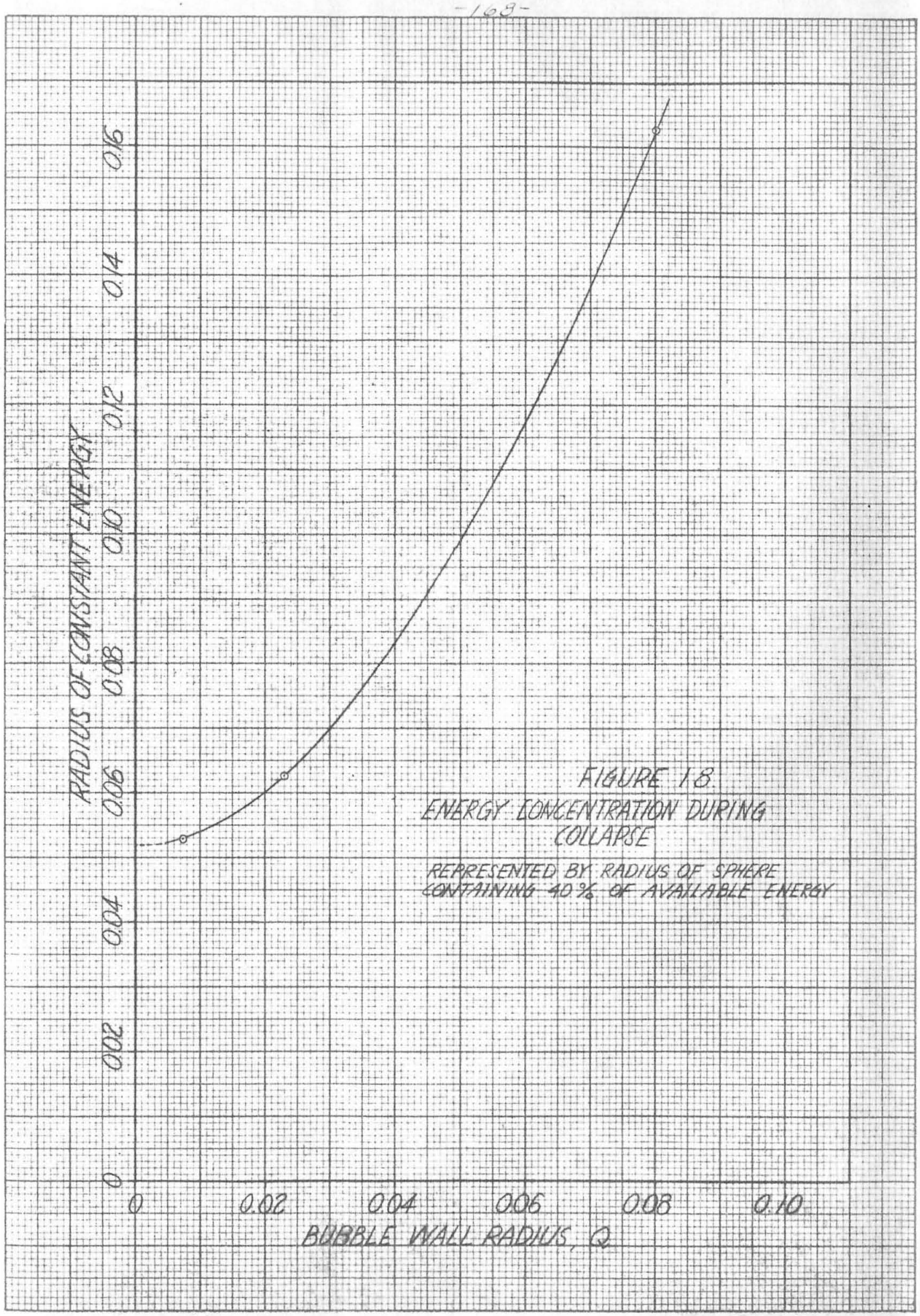

FIGURE 18.
ENERGY CONCENTRATION DURING COLLAPSE

REPRESENTED BY RADIUS OF SPHERE CONTAINING 40% OF AVAILABLE ENERGY

FIGURE 19
PRESSURE DUE TO SUDDEN IMPACT
EXACT SOLUTION BY METHOD OF CHARACTERISTICS
ACOUSTIC APPROXIMATION

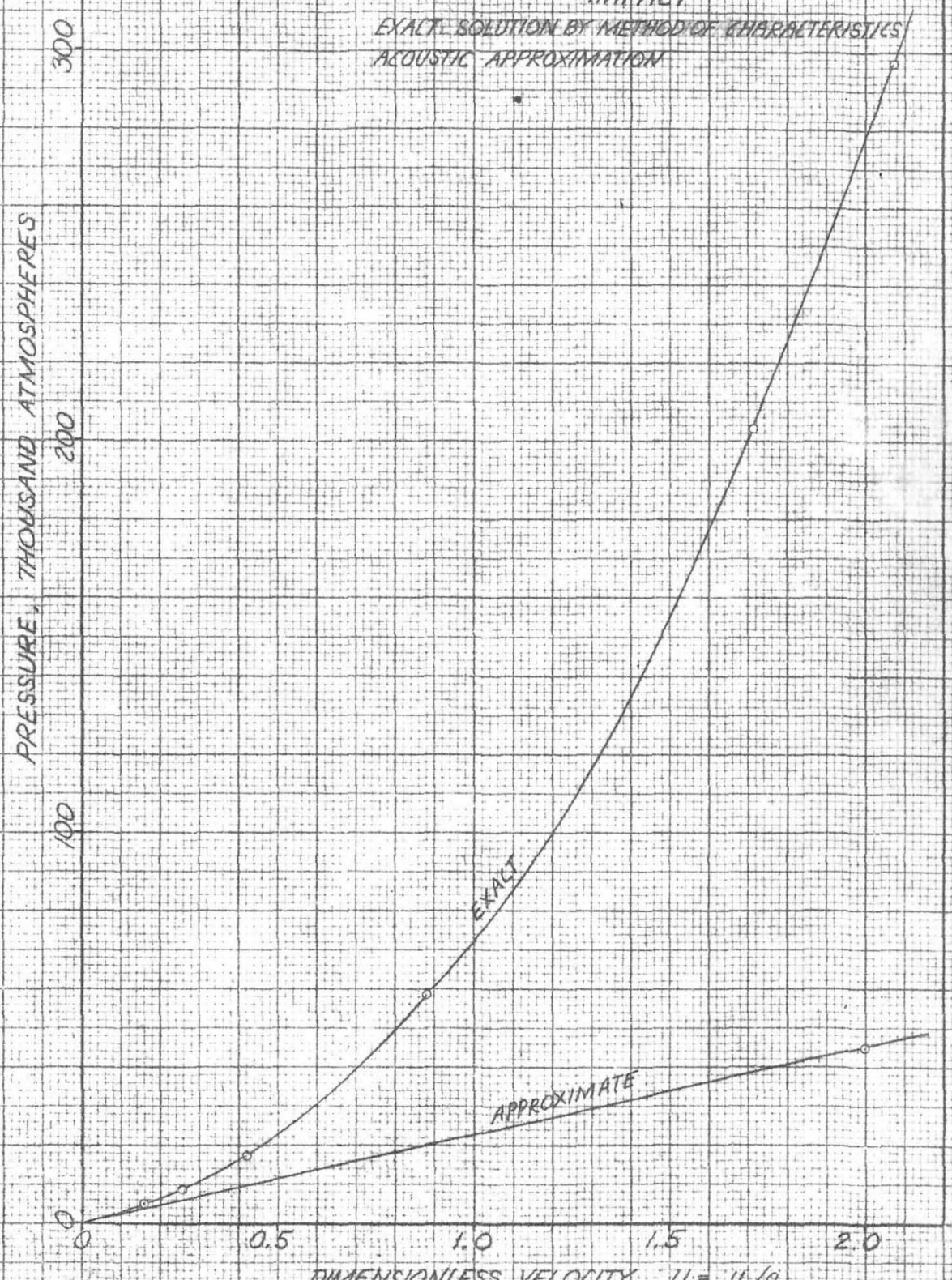

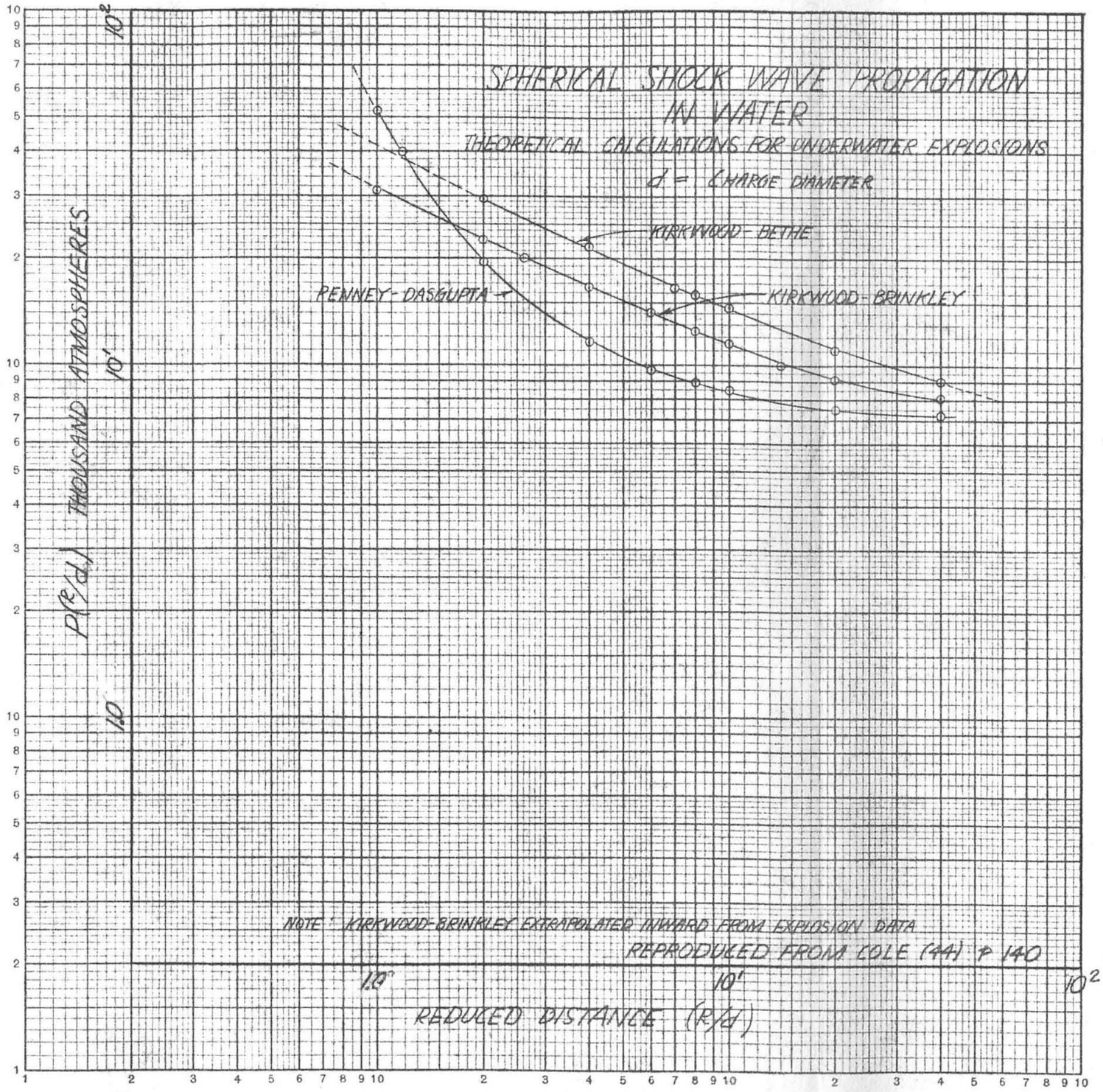

KEUFFEL & ESSER CO., N. Y. NO. 359-120
Logarithmic, 3 X 3 Cycles.
MADE IN U.S.A.

FIG. 20

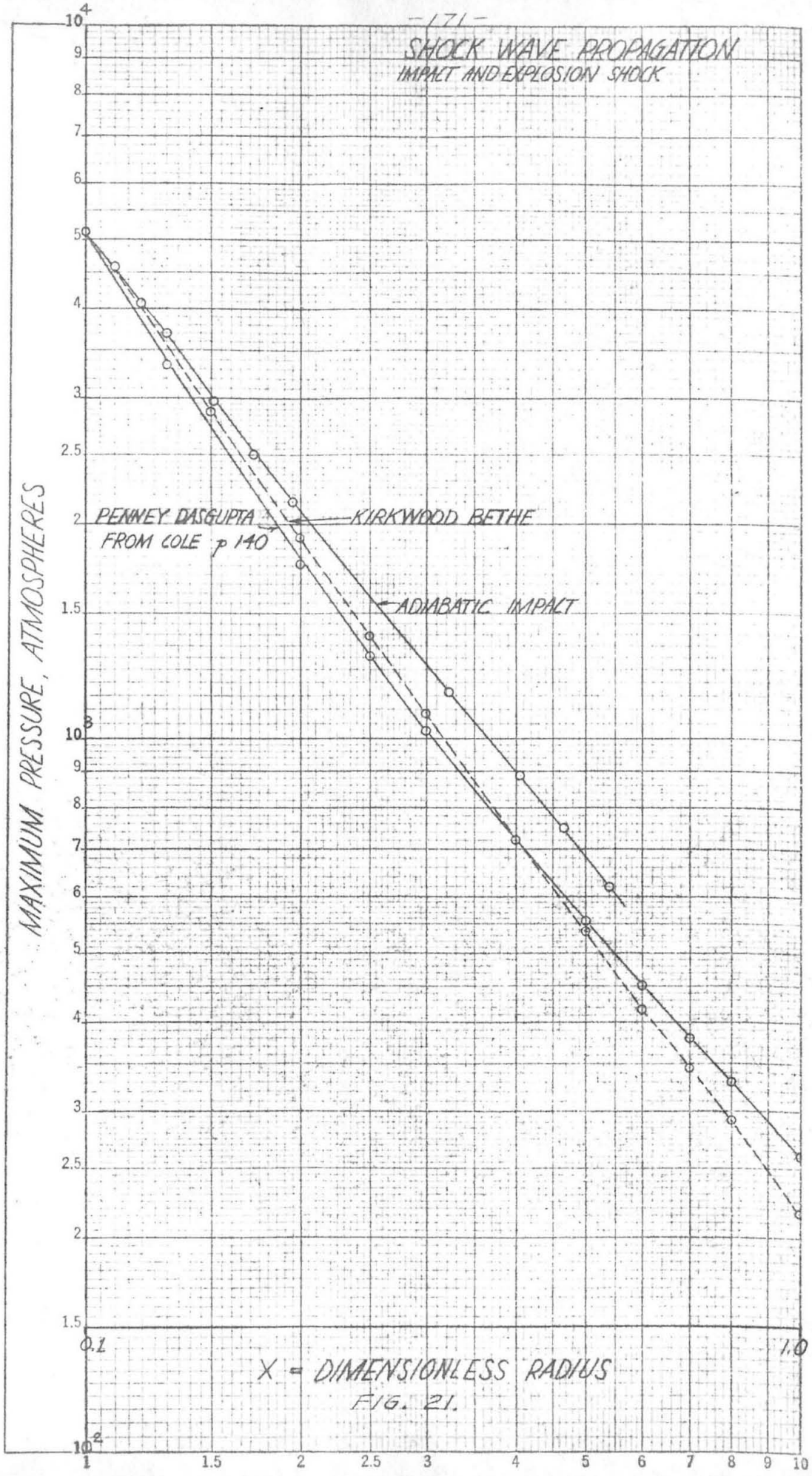
SHOCK WAVE PROPAGATION
IMPACT AND EXPLOSION SHOCK
MAXIMUM PRESSURE, ATMOSPHERES
PENNEY DASGUPTA
FROM COLE p 140
KIRKWOOD BETHE
ADIABATIC IMPACT
X = DIMENSIONLESS RADIUS

FIG. 21.

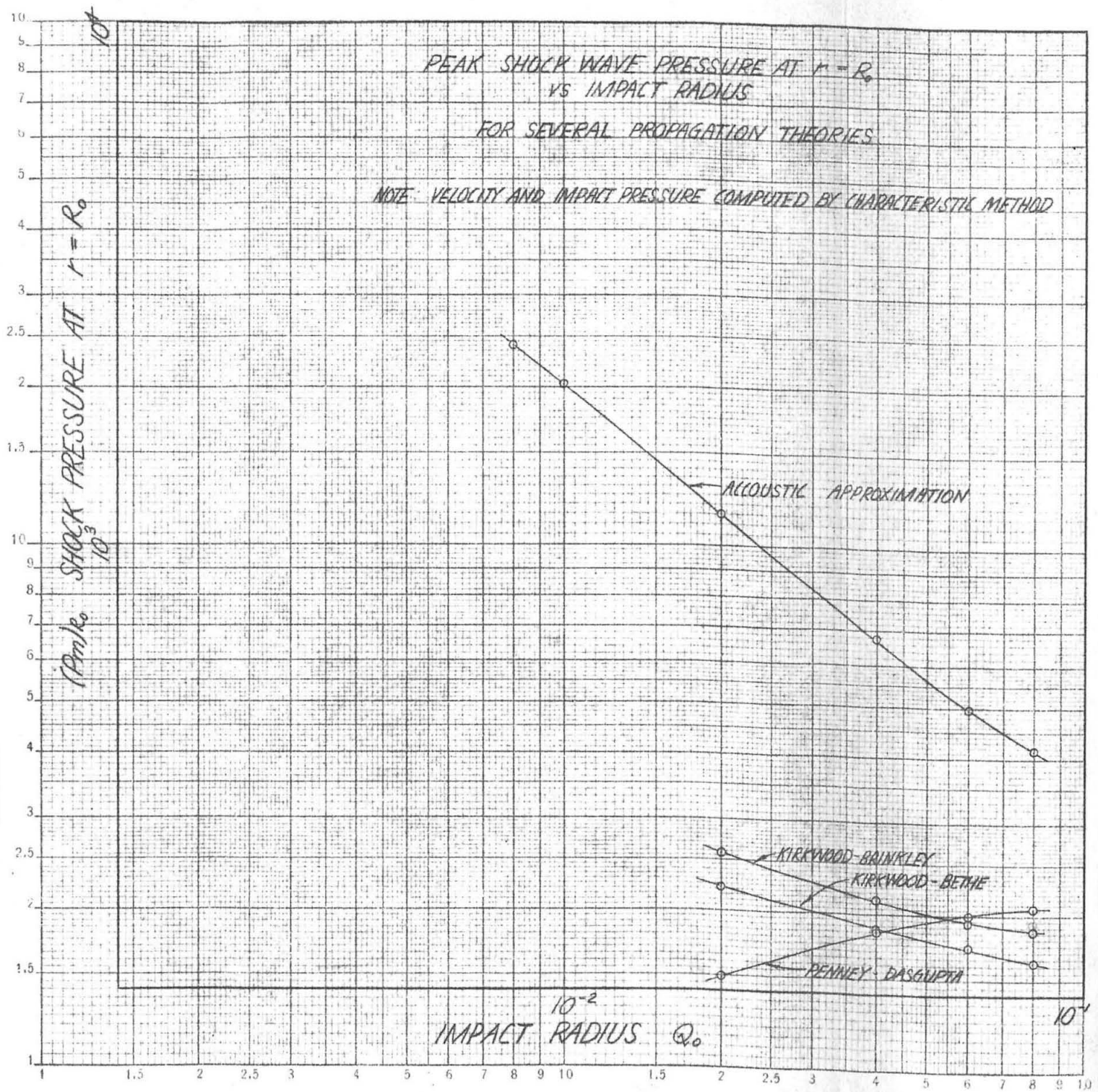
PEAK SHOCK WAVE PRESSURE AT r = R₀
VS IMPACT RADIUS
FOR SEVERAL PROPAGATION THEORIES
NOTE VELOCITY AND IMPACT PRESSURE COMPUTED BY CHARACTERISTIC METHOD
(Pm)/k₀ SHOCK PRESSURE AT r = R₀
10⁴
10³
ACCOUSTIC APPROXIMATION
KIRKWOOD-BRINKLEY
KIRKWOOD-BETHE
PENNEY-DASGUPTA
10⁻²
10⁻¹
IMPACT RADIUS Q₀
KEUFFEL & ESSER CO., N. Y. NO. 355-110
Logarithmic, 2 X 2 Cycles.
MADE IN U.S.A.

FIG 22

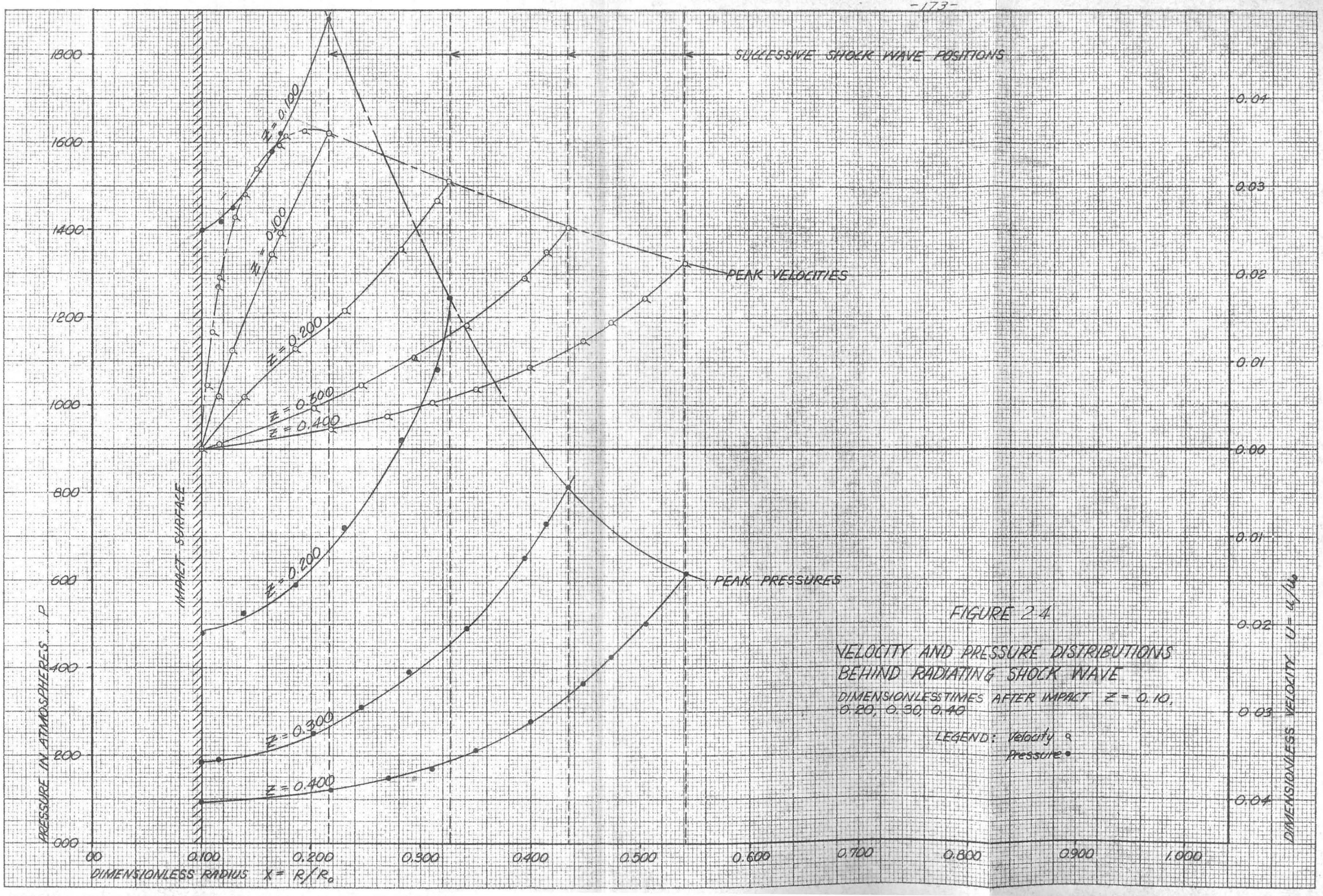

FIGURE 2.4

VELOCITY AND PRESSURE DISTRIBUTIONS BEHIND RADIATING SHOCK WAVE

DIMENSIONLESS TIMES AFTER IMPACT $Z = 0.10, 0.20, 0.30, 0.40$

LEGEND: Velocity ○ Pressure ●

FIGURE 2.5
PRESSURE ON IMPACT SURFACE
vs DIMENSIONLESS TIME

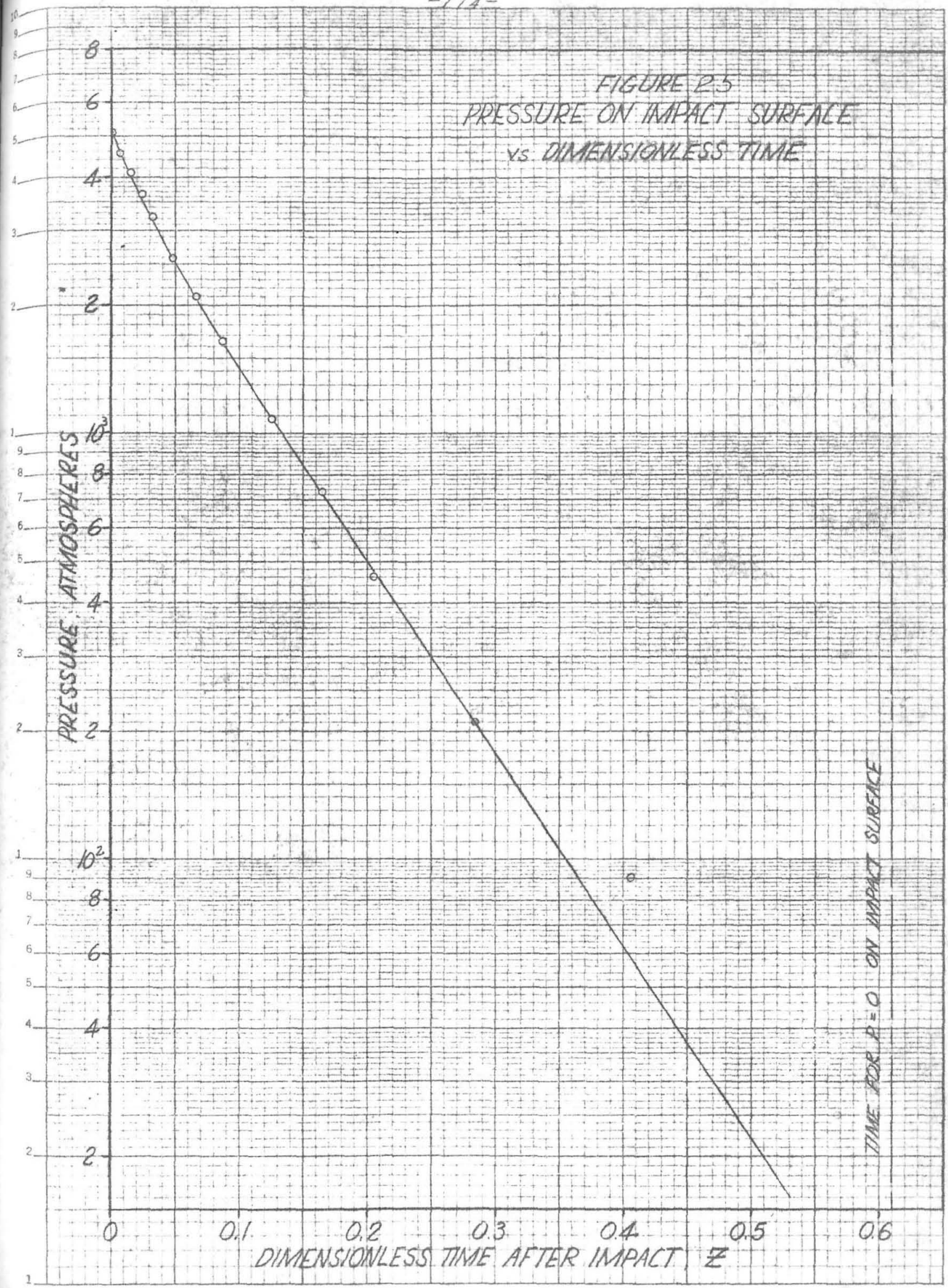

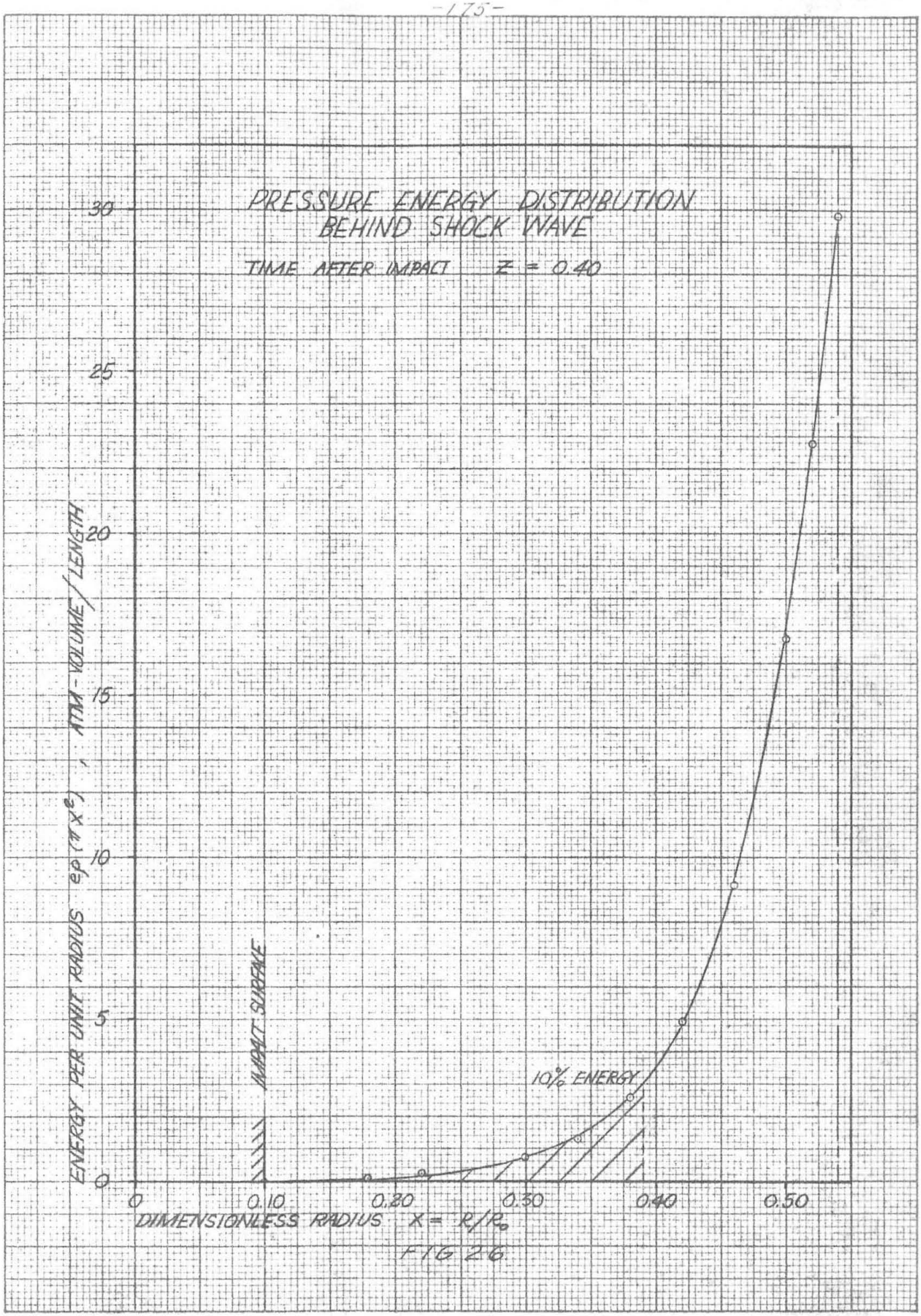
PRESSURE ENERGY DISTRIBUTION
BEHIND SHOCK WAVE
TIME AFTER IMPACT Z = 0.40
ENERGY PER UNIT RADIUS ep (m x e) , ATM - VOLUME / LENGTH
30
25
20
15
10
5
0
IMPACT SURFACE
10% ENERGY
0
0.10
0.20
0.30
0.40
0.50
DIMENSIONLESS RADIUS X = R/R0

FIG 26

TABLE 1. INVESTIGATIONS EMPLOYING VENTURIS OR WATER TUNNELS.

NAME	DATE	NOTES ON TESTS AND EQUIPMENT	REMARKS
PARSONS AND COOK(6)	1917	2 DIM. VENTURI WITH GLASS WALLS TEST SPECIMEN IN CENTER.	STUDIED MECHANISM OF DESTRUCTION. COLLAPSE IMPACT BLAMED.
FOTTINGER & SPANNHAKE(9)	1914–1925	2 DIM. WATER TUNNEL WITH TEST BLADE BETWEEN GLASS WALLS.	SHOWED DAMAGE OCCURRED IN COLLAPSE AREA. ATTACK ON GLASS SHOWED MECHANICAL ACTION TO BE PRIMARY.
ACKERET(E)	1926–1930	2 DIM. VENTURI WITH GLASS WALLS AND PRESSURE TAPS.	SHOWED MIN. PRESSURE EQUALS VAPOR PRESS. MEASURED PRESSURE DISTRIBUTION AND SHOWED ANALOGY WITH SHOCK FRONTS IN LAVAL NOZZLE.
DE HALLER(16)	1933	2 DIM. VENTURI WITH PIEZO – ELECTRIC PRESSURE PICK-UP.	MEASURED PEAK PRESSURES OF ONLY 3000 PSI.
SCHROTER(13)(14)(15)	1934	2 DIM. VENTURI WITH SPECIAL IMPINGEMENT SURFACE.	STUDIED MECHANISM OF ATTACK AND RESISTANCE OF MATERIALS.
HUNSAKER(17)18)	1935	2 DIM. VENTURI WITH VARIED PROFILE. FLASH PHOTOS. AT 3000/SEC.	SHOWED EFFECT OF AIR DIFFUSION IN LONG THROATED VENTURI. FOUND MAX. DAMAGE IN 21^{0} DIFFUSOR. FOUND PERIODICITY IN MASS CAVITATION.

TABLE I. (CONTINUED) INVESTIGATIONS EMPLOYING VENTURIS OR WATER TUNNELS.

NAME	DATE	NOTES ON TESTS AND EQUIPMENT	REMARKS
VAN ITERSON(28)	1936	CIRCULAR VENTURI WITH SHAPR APPROACH	OBSERVED CAVITATION AT HIGH CALC. PRESSURE, AND CONCUDED THAT BUBBLES CONTAINED AIR. DOUBTFUL VALIDITY.
VATER(11)	1937	2 DIM. VENTURI	MICROSCOPIC ANALYSIS OF METALLIC DAMAGE.
MOUSSON(12)	1937	2 DIM. VENTURI LIKE SCHROTER'S.	MICROSCOPIC ANALYSIS OF METALLIC DAMAGE.
BOTTOMLEY(36)	1948	2 DIM. VENTURI WITH SHARP APPROACH PRESSURE TAPS ON CENTER LINE.	CORROBORATED OBSERVATIONS OF VAN ITERSON. DOUBTFUL VALIDITY.
ROUSE(37)	1948	RECTANGULAR WATER TUNNEL WITH CYLINDRICAL MODEL.	OBSERVED PRESSURE DISTRIBUTIONS ON MODELS OF DIFFERENT SHAPES FOR SEVERAL INTENSITIES OF CAVITATION.
KNAPP AND HOLLANDER (19)	1948	WATER TUNNEL WITH CYLINDRICAL WORKING SECTION, CYL. MODELS. FLASH PHOTOS OF CAVITATION AT 30,000 FRAMES/SEC.	OBSERVED PRESSURE DISTRIBUTIONS DURING VARYING INTENSITIES OF CAVITATION. RECORDED INDIVIDUAL BUBBLE COLLAPSE AND REBOUND.

TABLE 2. INVESTIGATIONS EMPLOYING IMPACT WHEELS OR WASSERSCHLAG TESTERS.

NAME	DATE	NOTES ON TESTS AND EQUIPMENT	REMARKS
HONEGGER (20)	1927	FIRST APPLICATION. PASSED SPECIMEN THROUGH WATER STREAM.	DISCOVERY OF RAPID METHOD OF TESTING COMPARATIVE EROSION RESISTANCE OF MATERIALS.
COOK (48)	1923	SPECIMEN PASSED THROUGH MIST OF FINE DROPLETS.	DAMAGE PRODUCED WAS OF SAME NATURE AS CAVITATION. SPECULATED THAT ACTION WAS DUE TO LOCAL CAVITATION.
GARDNER, O. (40)	1932	OBSERVED EROSION IN STEAM TURB.	SPECULATED THAT DAMAGE WAS DUE TO PRESSURE AND STRESS CONC. IN FINE CRACKS AND FISSURES.
DE HALLER(16)	1933	RECORDED PRESSURE IMPACT AND CORRELATED WITH EROSION BY PIEZO ELECTIC PRESSURE PICK-UP.	RECORDED 4500 PSI CAUSING DAMAGE; 60% LESS THAN CALCULATED.
SODERBERG(23)	1935	PASSED HARDENED OR COATED SPECIMEN THROUGH WATER STREAM.	FOUND VERY HARD SURFACES, ESPCIALLY STELLITE TO HAVE GREAT RESISTANCE.
SCHWARTZ AND MANTEL(22)	1937	PASSED SPEC. THROUGH STREAM.	RATED LARGE NUMBER OF METALS ON EROSION RESISTANCE. ESTIMATED SPEED FOR THRESHALD OF DAMAGE.

TABLE 3. INVESTIGATIONS EMPLOYING VIBRATING SPECIMEN TESTERS.

NAME	DATE	NOTES ON TESTS AND EQUIPMENT	REMARKS
GAINES (25)	1932	NICKEL TUBE INSERTED THRU BOTTOM OF VESSEL CONTAINING WATER	DEVELOPED FIRST HIGH AMPLITUDE MAGNETOSTRICTION OSCILLATOR.
HUNSAKER(18)	1935	SIMILAR TO GAINES.	CHECKED SIMILARITY OF DAMAGE WITH CAVITATION DAMAGE.
SCHUMB, PETERS, & MILLIGAN(24)	1937	SIMILAR TO GAINES.	DESCRIBE TESTS OF EROSION DAMAGE.
KERR(32)	1937	HOLD SPECIMEN FACE DOWN 1/4 IN. BELOW LIQUID SURFACE.	RATED 80 METALS ON EROSION RESISTANCE IN FRESH AND SEA WATER
RIGHTMIRE(26)	194L	PLACED SPECIME IN BOTTOM SURFACE OF CLOSED VESSEL.	PHOTOGRAPHED BUBBLE HISTORY DURING CYCLE OF MOTION. CALC. PRESSURES. OF 5000 PSI.
POULTER(30)	1942	VIBRATED SPECIMENS PERPENDICULAR TO AND PARALLEL TO SURFACE CONTACTING LIQUID.	DEMONSTRATED PENETRATION-EXPANSION DAMAGE. PRODUCED PROTECTIVE COATINGS BY PENETRATION PROCESS WITH OILS.
BEECHING	1942	SIMILAR TO GAINES	RATED BRONZES USED IN PROPELLER WORK ON RLATIVE RESISTANCE.
KORNFELD AND SUVAROV(27)	1944	SIMILAR TO GAINES	PHOTOGRAPHED BUBBLE HISTORIES AND STUDIED CONFIGURATIONS AND SHAPES.
BRIGGS, MASON, AND JOHNSON.(33)	1947	CRYSTAL OSCILLATOR	ESTIMATED TENSIONS REQUIRED TO CAUSE CAVITATION WITH SOUND WAVES

Table IV. Rayleigh Collapse Time Integral, $f(R/R_o)$

R/R_o	$f(R/R_o)$	R/R_o	$f(R/R_o)$
0.000	0.7468	0.600	0.6292
0.040	0.7467	0.640	0.6067
0.080	0.7461	0.680	0.5813
0.120	0.7448	0.720	0.5524
0.160	0.7427	0.760	0.5194
0.200	0.7400	0.800	0.4813
0.240	0.7355	0.840	0.4370
0.280	0.7302	0.860	0.4116
0.320	0.7235	0.880	0.3840
0.360	0.7154	0.900	0.3529
0.400	0.7058	0.920	0.3178
0.440	0.6944	0.940	0.2772
0.480	0.6813	0.960	0.2279
0.520	0.6662	0.980	0.1622
0.560	0.6489	1.000	0.0000

Bubble Collapse Data

P 0.544 Atm. P 0.027 Atm. Z 0 at Q 0.080

(0)		(0, 1)		(0, 2)		(0, 3)	
U	0.1789	U	0.1600	U	0.1440	U	0.1297
A	0.9998	A	1.0079	A	1.0147	A	1.0183
X	0.0800	X	0.0842	X	0.0885	X	0.0928
Z	0.0000	Z	0.0050	Z	0.0101	Z	0.0151

(0, 4)		(0, 5)		(0, 6)		(0, 8)	
U	0.1173	U	0.1060	U	0.0960	U	0.0800
A	1.0213	A	1.0223	A	1.0224	A	1.0237
X	0.0975	X	0.1020	X	0.1067	X	0.1161
Z	0.0201	Z	0.0252	Z	0.0302	Z	0.0404

(0, 9)		(0, 10)		(0, 11)		(0, 12)	
U	0.0673	U	0.0570	U	0.0498	U	0.0429
A	1.0243	A	1.0238	A	1.0243	A	1.0239
X	0.1257	X	0.1354	X	0.1452	X	0.1550
Z	0.0505	Z	0.606	Z	0.707	Z	0.0807

(0, 13)		(0, 15)	
U	0.0375	U	0.0289
A	1.0247	A	1.0228
X	0.1649	X	0.1846
Z	0.0908	Z	0.1108

Bubble Collapse Data

P 0.544 Atm. P 0.027 Atm. Z 0 at Q 0.080

(1)	(1, 2)	(1, 3)	(1, 4)
U 0.1414	U 0.1305	U 0.1160	U 0.1056
A 1.0125	A 1.0158	A 1.0185	A 1.0209
X 0.0900	X 0.0944	X 0.0988	X 0.1034
Z 0.0000	Z 0.0049	Z 0.0099	Z 0.0149

(1, 5)	(1, 6)
U 0.0961	U 0.0877
A 1.0221	A 1.0219
X 0.1080	X 0.1121
Z 0.0199	Z 0.0249

(2)	(2, 3)	(2, 4)	(2, 5)
U 0.1146	U 0.1050	U 0.0952	U 0.0875
A 1.0185	A 1.0202	A 1.0211	A 1.0221
X 0.1000	X 0.1045	X 0.1090	X 0.1136
Z 0.0000	Z 0.0049	Z 0.0099	Z 0.0148

(2, 6)	(2, 8)	(2, 10)	(2, 11)
U 0.0800	U 0.0680	U 0.0498	U 0.0435
A 1.0223	A 1.0234	A 1.0211	A 1.0210
X 0.1184	X 0.1278	X 0.1472	X 0.1568
Z 0.0198	Z 0.0298	Z 0.0498	Z 0.0598

Bubble Collapse Data

P 0.544 Atm. P 0.027 Atm. Z 0 at Q 0.080

(4, 13)	(4., 15)
U 0.0305	U 0.0242
A 1.0201	A 1.0185
X 0.1875	X 0.2072
Z 0.6695	Z 0.0894

(5)	(5, 6)	(5, 7)	(5, 8)
U 0.0678	U 0.0628	U 0.0585	U 0.0545
A 1.0223	A 1.0222	A 1.0219	A 1.0218
X 0.1300	X 0.1348	X 0.1395	X 0.1442
Z 0.0000	Z 0.0049	Z 0.0098	Z 0.0147

(6)	(6, 7)	(6, 8)	(6, 9)
U 0.0584	U 0.0545	U 0.0507	U 0.0440
A 1.0219	A 1.0217	A 1.0213	A 1.0213
X 0.1400	X 0.1448	X 0.1496	X 0.1591
Z 0.0000	Z 0.0049	Z 0.0098	Z 0.0197

(6, 10)	(6, 11)
U 0.0385	U 0.0340
A 1.0201	A 1.0195
X 0.1688	X 0.1785
Z 0.0296	Z 0.0395

Bubble Collapse Data

P 0.544 Atm. P 0.027 Atm. Z 0 at Q 0.080

(10)	(10, 11)	(10, 12)	(10, 13)
U 0.0286	U 0.0257	U 0.0233	U 0.0212
A 1.0178	A 1.0172	A 1.0169	A 1.0158
X 0.2000	X 0.2097	X 0,2195	X 0.2293
Z 0.0000	Z 0.0098	Z 0.0196	Z 0.0295

(10, 15)
U 0.0179)
A 1.0155
X 0,2490
Z 0.0493

(11)	(11, 12)	(11, 13)	(11, 14)
U 0.0237	U 0.0215	U 0.0195	U 0.0178
A 1.0165	A 1.0160	A 1.0154	A 1.0147
X 0.2200	X 0.2298	X 0.2396	X 0.2494
Z 0.0000	Z 0.0098	Z 0.0197	Z 0.0295

(12)	(12, 13)	(12, 14)	(12, 15)
U 0.0199	U 0.0182	U 0.0165	U 0.0151
A 1.0153	A 1.0148	A 1.0145	A 1.0141
X 0.2400	X 0.2498	X 0.2597	X 0.2694
Z 0.0000	Z 0.0098	Z 0.0197	Z 0.0295

Bubble Collapse Data

P 0.544 Atm. P 0.027 Atm. Z 0 at Q 0.080

(3)	(3, 4)	(3, 5)	(3, 6)
U 0.0947	U 0.0866	U 0.0797	U 0.0734
A 1.0211	A 1.0220	A 1.0226	A 1.0230
X 0.1100	X 0.1146	X 0.1192	X 0.1239
Z 0.0000	Z 0.0049	Z 0.0098	Z 0.0148

(3, 7)
U 0.0677
A 1.0229
X 0.1287
Z 0.0197

(4)	(4, 5)	(4, 6)	(4, 7)
U 0.0795	U 0.0734	U 0.0678	U 0.0628
A 1.0222	A 1.0226	A 1.0223	A 1.0226
X 0.1200	X 0.1247	X 0.1294	X 0.1340
Z 0.0000	Z 0.0049	Z 0.0098	Z 0.0148

(4, 8)	(4, 9)	(4, 10)	(4, 11)
U 0.0583	U 0.0502	U 0.0436	U 0.0382
A 1.0225	A 1.0214	A 1.0205	A 1.0196
X 0.1388	X 0.1484	X 0.1582	X 0.1678
Z 0.0197	Z 0.0296	Z 0.0396	Z 0.0494

Bubble Collapse Data

P 0.544 Atm. P 0.027 Atm. Z 0 at Q 0.080

(7)	(7, 8)		
U 0.0509	U 0.0475		
A 1.0214	A 1.0210		
X 0.1500	X 0.1548		
Z 0.0000	Z 0.0049		
(8)	(8, 9)	(8, 10)	(8, 11)
U 0.0448	U 0.0394	U 0.0347	U 0.0308
A 1.0217	A 1.0199	A 1.0186	A 1.0183
X 0.1600	X 0.1696	X 0.0173	X 0.1890
Z 0.0000	Z 0.0098	Z 0.0196	Z 0.0295
(8, 13)	(8, 15)		
U 0.0252	U 0.0205		
A 1.0187	A 1.0175		
X 0.2087	X 0.2283		
Z 0.0494	Z 0.0692		
(9)	(9, 10)	(9, 11)	(9, 12)
U 0.0354	U 0.0315	U 0.0280	U 0.0258
A 1.0192	A 1.0183	A 1.0176	A 1.0163
X 0.1800	X 0.1897	X 0.1994	X 0.2092
Z 0.0000	Z 0.0098	Z 0.0196	Z 0.0295

Bubble Collapse Data

P 0.544 Atm. P 0.027 Atm. Z 0 at Q 0.080

(13)		(13, 14)		(13, 15)	
U	0.0170	U	0.0146	U	0.0143
A	1.0142	A	1.0137	A	1.0132
X	0.2600	X	0.2699	X	0.2707
Z	0.0000	Z	0.0098	Z	0.0197

(14)		(14, 15)		(14, 16)	
U	0.0146	U	0.0134	U	0.0127
A	1.0133	A	1.0129	A	1.0126
X	0.2800	X	0.2899	X	0.2997
Z	0.0000	Z	0.0098	Z	0.0197

(15)		(15, 16)	
U	0.0127	U	0.0118
A	1.0125	A	1.0122
X	0.3000	X	0.3099
Z	0.0000	Z	0.0098

(16)	
U	0.0112
A	1.0118
X	0.3200
Z	0.0000

Bubble Collapse Data

P 0.544 Atm. P 0.027 Atm. Z 0 at Q 0.080

(A, 1)		(A, 2)		(a, 3)		(A,4)	
U	0.1848	U	0.1610	U	0.1475	U	0.1325
A	0.9999	A	1.0078	A	1.0133	A	1.0187
X	0.0782	X	0.0825	X	0.0868	X	0.0914
Z	0.0101	Z	0.0152	Z	0.0203	Z	0.0254

(A, 5)	
U	0.1190
A	1.0202
X	0.0959
Z	0.0305

(B, 2)		(B, 3)		(B, 4)		(B, 6)	
U	0.1910	U	0.1696	U	0.1515	U	0.1210
A	0.9999	A	1.0077	A	1.0147	A	1.0200
X	0.0763	X	0.0806	X	0.0851	X	0.0942
Z	0.0204	Z	0.0256	Z	0.0308	Z	0.0412

(B, 7)		(B, 8)		(B, 9)		(B, 10)	
U	0.1095	U	0.0982	U	0.0815	U	0.0680
A	1.0231	A	1.0240	A	1.0243	A	1.0244
X	0.0989	X	0.1037	X	0.1133	X	0.1230
Z	0.0464	Z	0.0516	Z	0.0618	Z	0.0721

Bubble Collapse Data

P 0.544 Atm. P 0.027 Atm. Z 0 at Q 0.080

(B, 11)	(B, 12)	(B, 13)	
U 0.0580	U 0.0498	U 0.0434	
A 1.0250	A 1.0245	A 1.0254	
X 0.1327	X 0.1425	X 0.1524	
Z 0.0822	Z 0.0923	Z 0.1025	
(C, 3)	(C, 5)	(C, 6)	(C, 7)
U 0.1962	U 0.1550	U 0.1378	U 0.1253
A 0.9999	A 1.0142	A 1.0180	A 1.0207
X 0.0742	X 0.0831	X 0.0876	X 0.0903
Z 0.0309	Z 0.0416	Z 0.0469	Z 0.0522
(C, 8)	(C, 8 1/2)	(C, 9)	
U 0.1100	U 0.0999	U 0.0902	
A 1.0232	A 1.0267	A 1.0258	
X 0.0971	X 0.1019	X 0.1067	
Z 0.0574	Z 0.0627	Z 0.0677	
(D, 4)	(D, 5)	(D, 6)	(D, 7)
U 0.2063	U 0.1803	U 0.1590	U 0.1412
A 0.9999	A 1.0083	A 1.0145	A 1.0204
X 0.0720	X 0.0763	X 0.0809	X 0.0856
Z 0.0418	Z 0.0473	Z 0.0526	Z 0.0580

Bubble Collapse Data

P 0.544 Atm. P 0.027 Atm. Z 0 at Q 0.080

(D, 8)	(D, 8-k/2)	(D, 9)	(D, 9-1/2)
U 0.1244	U 0.1120	U 0.1004	U 0.0908
A 1.0253	A 1.0295	A 1.0295	A 1.0302
X 0.0903	X 0.0952	X 0.0998	X 0.1048
Z 0.0634	Z 0.0687	Z 0.0738	Z 0.0790

(D, 10)	(D, 11)	(D, 12)	(D, 13)
U 0.0820	U 0.0687	U 0.0578	U 0.0496
A 1.0292	A 1.0309	A 1.0307	A 1.0311
X 0.1097	X 0.1194	X 0.1292	X 0.1390
Z 0,0841	Z 0.0944	Z 0.1047	Z 0.1148

(D, 14)	(D, 15)
U 0.0430	U 0.0368
A 1.0317	A 1.0276
X 0.1491	X 0.1589
Z 0.1250	Z 0.1350

(E, 5)	(E, 6)	(E, 7)	(E, 8)
U 0.2134	U 0,1861	U 0.1636	U 0.1443
A 0.9999	A 1.0103	A 1.0202	A 1.0218
X 0.0697	X 0.0742	X 0.0787	X 0.0834
Z 0.0529	Z 0.0584	Z 0.0640	Z 0.0694

Bubble Collapse Data

P 0.544 Atm. P 0.027 Atm. % O as Q 0.080

(E, 8-1/2)		(E, 9)		(E, 9-1/2)		(E, 10)	
U	0.1290	U	0.1148	U	0.1030	U	0.0928
A	1.0270	A	1.0273	A	1.0288	A	1.0285
X	0.0882	X	0.0928	X	0.0978	X	0.1026
Z	0.0747	Z	0.0799	Z	0.0852	Z	0.0903

(F, 6)		(F, 7)		(F, 8)		(F, 8-1/2)	
U	0.2237	U	0.1937	U	0.1691	U	0.1492
A	0.9999	A	1.0097	A	1.0190	A	1.0278
X	0.0672	X	0.0716	X	0.0763	X	0.0810
Z	0.0643	Z	0.0698	Z	0.0754	Z	0.0809

(F, 9)		(F, 9-1/2)		(F, 10)		(F, 10-1/2)	
U	0.1316	U	0.1175	U	0.1050	U	0.0948
A	1.0288	A	1.0301	A	1.0305	A	1.0348
X	0.0857	X	0.0906	X	0.0954	X	0.1003
Z	0.0861	Z	0.0915	Z	0.0967	Z	0.1019

(F, 11)		(F, 12)		(F, 13)		(F, 14)	
U	0.0850	U	0.0700	U	0.0590	U	0.0503
A	1.0343	A	1.0345	A	1.0357	A	1.0361
X	0.1052	X	0.1151	X	0.1250	X	0.1350
Z	0.1072	Z	0.1175	Z	0.1277	Z	0.1380

Bubble Collapse Data

P 0.544 Atm. P 0.027 Atm. Z 0 at Q 0.080

(G, 7)	(G, 8)	(G, 8-1/2)	(G, 9)
U 0.2325	U 0.2005	U 0.1750	U 0.1530
A 0.9999	A 1.0152	A 1.0278	A 1.0320
X 0.0645	X 0.0691	X 0.0738	X 0.0784
Z 0.0757	Z 0.0814	Z 0.0870	Z 0.0923

(G, 9-1/2)	(G, 10)	(G, 10-1/2)	(G, 11)
U 0.1330	U 0.1186	U 0.1082	U 0.0948
A 1.0329	X 0.1369	A 1.0401	A 1.0400
X 0.0833	X 0.0882	X 0.0930	X 0.0980
Z 0.0978	Z 0.1031	Z 0.1083	Z 0.1136

(H, 8)	(H, 8-1/2)	(H, 9)	(H, 9-1/2)
U 0.2470	U 0.2120	U 0.1830	U 0.1567
A 0.9999	A 1.0183	A 1.0290	A 1.0319
X 0.0617	X 0.0662	X 0.0707	X 0.0756
Z 0.0875	Z 0.0932	Z 0.0987	Z 0.1044

(H, 10)	(H, 10-1/2)	(H, 11)	(H, 11-1/2)
U 0.1380	U 0.1224	U 0.1080	U 0.0962
A 1.0401	A 1.0452	A 1.0463	A 1.0482
X 0.0803	X 0.0852	X 0.0902	X 0.0952
Z 0.1098	Z 0.1151	Z 0.1205	Z 0.1259

Bubble Collapse Data

P 0.544 Atm. P 0.027 Atm. Z 0.81 9 0.080

(H, 12)		(H, 13)		(H, 14)	
U	0.0862	U	0.0710	U	0.0588
A	1.0472	A	1.0475	A	1.0482
X	0.1000	X	0.1100	X	0.1201
Z	0.1309	Z	0.1413	Z	0.1515

(J, 8-1/2)		(J, 9)		(J, 9-1/2)		(J, 10)	
U	0.2650	U	0.2240	U	0.1897	U	0.1648
A	0.9999	A	1.0160	A	1.0272	A	1.0400
X	0.0587	X	0.0631	X	0.0678	X	0.0725
Z	0.9993	Z	0.1050	Z	0.1108	Z	0.1164

(J, 10-1/2)		(J, 11)		(J, 11-1/2)		(J, 12)	
U	0.1448	U	0.1260	U	0.1097	U	0.0988
A	1.0490	A	1.0480	A	1.0500	A	1.0527
X	0.0773	X	0.0823	X	0.0873	X	0.0922
Z	0.1218	Z	0.1272	Z	0.1327	Z	0.1378

(K, 9)		(K, 9-1/2)		(K, 10)		(K, 10-1/2)	
U	0.2837	U	0.2355	U	0.2008	U	0.1736
A	0.9999	A	1.0200	A	1.0408	A	1.0518
X	0.0552	X	0.0598	X	0.0644	X	0.0692
Z	0.1112	Z	0.1172	Z	0.1230	Z	0.1285

Bubble Collapse Data

P 0.544 Atm. P 0.027 Atm. Z 0 at Q 0.080

(K, 11)	(K, 11-1/2)	(K, 12)	(K, 12-1/2)
U 0.1453	U 0.1268	U 0.1122	U 0.0990
A 1.0540	A 1.0612	A 1.0645	A 1.0652
X 0.0742	X 0.0792	X 0.0841	X 0.0891
Z 0.1340	Z 0.1396	Z 0.1448	Z 0.1500

(K, 13)	(K, 14)
U 0.0875	U 0.0703
A 1.0670	A 1.0685
X 0.0942	X 0.1044
Z 0.1550	Z 0.1655

(L, 9-1/2)	(L, 10)	(L, 10-1/2)	(L, 11)
U 0.3059	U 0.2540	U 0.2103	U 0.1775
A 0.9999	A 1.0323	A 1.0508	A 1.0628
X 0.0515	X 0.0560	X 0.0607	X 0.0655
Z 0.1237	Z 0.1297	Z 0.1355	Z 0.1412

(L, 11-1/2)	(L, 12)	(L, 12-1/2)	(L, 13)
U 0.1518	U 0.1320	U 0.1146	U 0.1000
A 1.0692	A 1.0757	A 1.0763	A 1.0773
X 0.0706	X 0.0755	X 0.0805	X 0.0857
Z 0.1467	Z 0.1520	Z 0.1572	Z 0.1625

Bubble Collapse Data

P 0.544 Atm. P 0.027 Atm. Z 0 at Q 0.080

(L, 13-1/2)		(L, 14)	
U	0.0889	U	0.0788
A	1.0795	A	1.0778
X	0.0908	X	0.0959
Z	0.1676	Z	0.1726

(L,1/2, 11-1/4)		(L 1/2, 11-1/2)	
U	0.1835	U	0.1690
A	1.0677	A	1.0726
X	0.0636	X	0.0661
Z	0.1476	Z	0.1504

(M, 10)		(M, 10-1/2)		(M, 11)		(M, 11-3/4)	
U	0.3341	U	0.2730	U	0.2240	U	0.2047
A	0.9999	A	1.0430	A	1.0658	A	1.0752
X	0.0476	X	0.0519	X	0.0567	X	0.0592
Z	0.1361	Z	0.1422	Z	0.1488	Z	0.1511

(M, 11-1/2)		(M, 11-3/4)		(M, 12)		(M, 12-1/2)	
U	0.1876	U	0.1720	U	0.1595	U	0.1360
A	1.0805	A	1.0832	A	1.0884	A	1.0913
X	0.0616	X	0.0641	X	0.0665	X	0.0716
Z	0.1539	Z	0.1567	Z	0.1593	Z	0.1646

Bubble Collapse Data

P 0.544 Atm. P 0.027 Atm. Z 0 at Q 0.080

(M, 13)		(M, 13-1/2)		(M, 14)	
U	0.1155	U	0.1005	U	0.0872
A	1.0960	A	1.0990	A	1.0978
X	0.0767	X	0.0819	X	0.0870
Z	0.1700	Z	0.1752	Z	0.1803

(M 1/2, 10-3/4)		(M 1/2, 11)		(M 1/2, 11-1/4)		(M 1/2, 11½)	
U	0.2886	U	0.2595	U	0.2357	U	0.2140
A	1.0417	A	0.0557	A	1.0703	A	1.0783
X	0.0598	X	0.0522	X	0.0546	X	0.0571
Z	0.1486	Z	0.1517	Z	0.1546	Z	0.1575

(M 1/2, 11-3/4)		(M 1/2, 12)	
U	0.1950	U	0.1802
A	1.0828	A	1.0913
X	0.1595	X	0.0619
Z	0.1602	Z	0.1629

(N, 10-1/2)		(N, 10-3/4)		(N, 11)		(N, 11 3/4)	
U	0.3775	U	0.3552	U	0.2987	U	0.2682
A	0.9999	A	1.0365	A	1.0596	A	1.0803
X	0.0431	X	0.0452	X	0.0476	X	0.0499
Z	0.1487	Z	0.1520	Z	0.1551	Z	0.1581

Bubble Collapse Data

P 0.544 Atm. P 0.027 Atm. Z 0 as Q 0.080

(N, 11-1/2)	(N, 11-3/4)	(N, 12)	(N, 12-1/4)
U 0.2410	U 0.2180	U 0.1998	U 0.1880
A 1.0925	A 1.0988	A 1.1092	A 1.1126
X 0.0524	X 0.0548	X 0.0572	X 0.0597
Z 0.1610	Z 0.1639	Z 0.1665	Z 0.1693

(N, 12-1/2)	(N, 13)	(N, 13-1/2)	(N, 14)
U 0.1644	U 0.1378	U 0.1168	U 0.0995
A 1.1145	A 1.1190	A 1.1205	A 1.1180
X 0.0623	X 0.0675	X 0.0727	X 0.0779
Z 0.1720	Z 0.1774	Z 0.1826	Z 0.1877

(o, 10-3/4)	(o, 11)	(o, 11-1/4)	(o, 11-1/2)
U 0.4072	U 0.3593	U 0.3185	U 0.2830
A 0.9999	A 1.0452	X 1.0708	A 1.0932
X 0.0405	X 0.0426	X 0.0449	X 0.0473
Z 0.1554	Z 0.1587	Z 0.1617	Z 0.1648

(o, 11-3/4)	(o, 12)	(o, 12-1/4)	(o, 12-1/2)
U 0.2528	U 0.2290	U 0.2055	U 0.1848
A 1.1078	A 1.1211	A 1.1272	A 1.1290
X 0.0497	X 0.0521	X 0.0546	X 0.0572
Z 0.1677	Z 0.1704	Z 0.1732	Z 0.1759

Bubble Collapse Data

P 0.544 Atm. P 0.027 Atm. Z 0 at Q 0.080

(P, 11)	(P, 11-1/4)	(P, 11-1/2)	(P, 11-3/4)
U 0.4472	U 0.3918	U 0.3438	U 0.3038
A 0.9999	A 1.0503	A 1.0860	A 1.1095
X 0.0376	X 0.0396	X 0.0418	X 0.0442
Z 0.1622	Z 0.1655	Z 0.1686	Z 0.1716

(P, 12)	(P, 12-1/4)	(P, 12-1/2)	(P, 12-3/4)
U 0.2710	U 0.2402	U 0.2138	U 0.1910
A 1.1311	A 1.1428	A 1.1536	A 1.1565
X 0.0465	X 0.0490	X 0.0516	X 0.0542
Z 0.1744	Z 0.1772	Z 0.1801	Z 0.1828

(P, 13)	(P, 13-1/2)	(P, 14)
U 0.1705	U 0.1400	U 0.1145
A 1.1560	A 1.1605	A 1.1570
X 0.0569	X 0.0622	X 0.0676
Z 0.1855	Z 0.1908	Z 0.1960

(Q,

(Q, 11-1/4)	(Q, 11-1/2)	(Q, 11-3/4)	(Q, 12)
U 0.4959	U 0.4288	U 0.3712	U 0.3260
A 0.9999	A 1.0713	A 1.1193	A 1.1538
X 0.3435	X 0.0363	X 0.0388	X 0.0407
Z 0.1690	Z 0.1724	Z 0.1756	Z 0.1784

Bubble Collapse Data

P 0.544 Atm. P 0.027 Atm. Z 0 at Q 0.000

(Q_0 12-1/4)		(Q_0 12-1/2)		(Q_0 12-3/4)		(Q_0 13)	
U	0.2838	U	0.2480	U	0.2172	U	0.1900
A	1.1737	A	1.1900	A	1.1945	A	1.1945
X	0.0432	X	0.0485	X	0.0542	X	0.0611
Z	0.1813	Z	0.1842	Z	0.1869	Z	0.1896

(Q_0 13-1/2)		(Q_0 14)	
U	0.1510	U	0.1200
A	1.2025	A	1.1980
X	0.0566	X	0.0622
Z	0.1949	Z	0.2001

(R_0 11-1/2)		(R_0 11-3/4)		(r_0 12)		(R_0 12-1/4)	
U	0.5674	U	0.4830	U	0.4147	U	0.3520
A	0.9999	A	1.0988	A	1.1713	A	1.2080
X	0.0306	X	0.0324	X	0.0344	X	0.0368
Z	0.1762	Z	0.1795	Z	0.1826	Z	0.1855

(R_0 12-1/2)		(R_0 12-3/4)		(R_0 13)		(R_0 13-1/4)	
U	0.2993	U	0.2550	U	0.2175	U	0.1900
A	1.2350	S	1.2470	A	1.2490	A	1.2548
X	0.0394	X	0.0422	X	0.0450	X	0.0471
Z	0.1883	Z	0.1912	Z	0.9940	Z	0.1967

Bubble Collapse Data

P 0.544 Atm. P 0.027 Atm. Z 0 at Q 0.080

(R, 13-1/2)		(R, 14)	
U	0.1660	U	0.1265
A	1.2535	A	1.2460
X	0.0506	X	0.0563
Z	0.1992	Z	0.2044

(S, 11-3/4)		(S, 12)		(S, 12-1/4)		(S, 12-3/8)	
U	0.6451	U	0.5530	U	0.4558	U	0.4095
A	0.9999	A	1.1920	A	1.2770	A	1.3000
X	0.0262	X	0.0277	X	0.0299	X	0.0313
Z	0.1833	Z	0.1866	Z	0.1896	Z	0.1911

(S, 12-1/2)		(S, 12-3/4)		(S, 13)		(S, 13-1/4)	
U	0.3765	U	0.3090	U	0.2535	U	0.2135
A	1.2970	A	1.3260	A	1.3330	A	1.3385
X	0.0325	X	0.0354	X	0.0383	X	0.0412
Z	0.1926	Z	0.1955	Z	0.1983	Z	0.2010

(T, 11-7/8)		(T, 12)		(T, 12-1/8)		(T, 12-1/4)	
U	0.7381	U	0.6740	U	0.6074	U	0.5460
A	0.9999	A	1.1200	A	1.2250	A	1.2820
X	0.0239	X	0.0245	X	0.0253	X	0.0264
Z	0.1868	Z	0.1884	Z	0.1902	Z	0.1916

Bubble Collapse Data

P 0.544 Atm. P 0.027 Atm. Z 0 at Q 0.080

(T, 12-3/8)		(T, 12-1/2)		(T, 12-5/8)		(T, 12-3/4)	
U	0.4770	U	0.4300	U	0.3835	U	0.3415
A	1.3090	A	1.3573	A	1.3855	A	1.3985
X	0.0276	X	0.0289	X	0.0303	X	0.0318
Z	0.1932	Z	0.1947	Z	0.1962	Z	0.1976

(T, 13)		(T, 13-1/4)	
U	0.2705	U	0.2220
A	1.4050	A	1.4110
X	0.0348	X	0.0379
Z	0.2004	Z	0.2031

(U, 12)		(U, 12-1/8)		(U, 12-1/4)		(U, 12-3/8)	
U	0.8443	U	0.7550	U	0.6720	U	0.5840
A	0.9999	A	1.1770	A	1.2920	A	1.3740
X	0.0211	X	0.0216	X	0.0224	X	0.0236
Z	0.1903	Z	0.1921	Z	0.1936	Z	0.1954

(U, 12-1/2)		)U, 12-5/8)		(U, 12-3/4)		(U, 13)	
U	0.5090	U	0.4425	U	0.3840	U	0.2890
A	1.4370	A	1.4780	A	1.5000	A	1.5080
X	0.0249	X	0.0263	X	0.0278	X	0.0311
Z	0.1969	Z	0.1983	Z	0.1998	Z	0.2026

Bubble Collapse Data

P 0.544 Atm. P 0.027 Atm. Z 0 at Q 0.080

(V, 12-1/8)		(V, 12-1/4)		(V, 12-3/8)		(V, 12-1/2)	
U	1.0334	U	0.9140	U	0.7625	U	0.6318
A	0.9999	A	1.2750	A	1.5130	A	1.6490
X	0.0173	X	0.0176	X	0.0185	X	0.0198
Z	0.1943	Z	0.1960	Z	0.1978	Z	0.1994

(V, 12-5/8)		(V, 12-3/4)		(V, 12-7/8)	
U	0.5245	U	0.4293	U	0.3545
A	1.6890	A	1.7350	A	1.7439
X	0.0213	X	0.0230	X	0.0249
Z	0.2006	Z	0.2021	Z	0.2034

(W, 12-3/16)		(W, 12-1/4)		(W, 12-5/16)		(W, 12-3/8)	
U	1.1660	U	1.0940	U	0.9975	U	0.8945
A	0.9999	A	1.2190	A	1.4065	A	1.5915
X	0.1523	X	0.0152	X	0.0155	X	0.0160
Z	0.1962	Z	0.1970	Z	0.1980	Z	0.1989

(W, 12-7/16)		(W, 12-1/2)		(W, 12-5/8)	
U	0.7965	U	0.7070	U	0.5680
A	1.7050	A	1.7870	A	1.8570
X	0.0166	X	0.0174	X	0.0189
Z	0.1997	Z	0.2004	Z	0.2017

Bubble Collapse Data

P 0.544 Atm. P 0.027 Atm. Z 0 at Q 0.080

(X, 12-1/4)	(X, 12-5/16)	(X, 12-3/8)	(X, 12-7/16)
U 1.3400	U 1.2275	U 1.0900	U 0.9470
A 0.9999	A 1.3900	A 1.6770	A 1.8850
X 0.0130	X 0.0128	X 0.0133	X 0.0139
Z 0.1980	Z 0.1990	Z 0.1999	Z 0.2007

(X, 12-1/2)	(
U 0.8130	
A 2.0070	
X 0.0147	
Z 0.2014	

(Y, 12-5/16)	(Y, 12-11/32)	(Y, 12-3/8)	(Y½, 12-11/32)
U 1.7500	U 1.6880	U 1.5600	U 1.9200
A 0.9999	A 1.4950	A 1.8900	A 1.4000
X 0.0094	X 0.0092	X 0.0092	X 0.0084
Z 0.2003	Z 0.2007	Z 0.2011	Z 0.2010

(Z, 12-11/32)	(Y½, 12-3/8)
U 2.2180	U 1.7500
A 0.9999	A 1.9200
X 0.0074	X 0.0083
Z 0.2014	Z 0.2015